ESTCP

FINAL REPORT

PFAS Leaching at AFFF-Impacted Sites: Insights into Soil-to-Groundwater Ratios

Charles Schaefer
Maxwell Hire
CDM Smith Inc.

Christopher Higgins
Stephanie Shea
Colorado School of Mines

April 2025

ESTCP Project ER20-5088

REPORT DOCUMENTATION PAGE

Form Approved
OMB No. 0704-0188

1. REPORT DATE *(DD-MM-YYYY)*	**2. REPORT TYPE**	**3. DATES COVERED** *(From - To)*
25-04-2025	ESTCP Final Report	2/4/2021 - 2/3/2025

4. TITLE AND SUBTITLE

PFAS Leaching at AFFF-Impacted Sites: Insights into Soil-to-Groundwater Ratios

5a. CONTRACT NUMBER
21-C-0012

5b. GRANT NUMBER
N/A

5c. PROGRAM ELEMENT NUMBER
N/A

6. AUTHOR(S)
Schaefer, Charles E., Ph.D. (CDM Smith)
Hire, Maxwell, P.G. (CDM Smith)
Higgins, Christopher P., Ph.D. (Colorado School of Mines)
Shea, Stephanie, Ph.D. (Colorado School of Mines)

5d. PROJECT NUMBER
ER20-5088

5e. TASK NUMBER
N/A

5f. WORK UNIT NUMBER
N/A

7. PERFORMING ORGANIZATION NAME(S) AND ADDRESS(ES)

CDM FEDERAL PROGRAMS
CORPORATION 9200 WARD PKWY
STE 320 KANSAS CITY MO 64114-
3372

8. PERFORMING ORGANIZATION REPORT NUMBER

ER20-5088

9. SPONSORING / MONITORING AGENCY NAME(S) AND ADDRESS(ES)

Office of the Deputy Assistant Secretary of Defense (Energy Resilience & Optimization)
3500 Defense Pentagon, RM 5C646
Washington, DC 20301-3500

10. SPONSOR/MONITOR'S ACRONYM(S)
ESTCP

11. SPONSOR/MONITOR'S REPORT NUMBER(S)
ER20-5088

12. DISTRIBUTION / AVAILABILITY STATEMENT

Distribution Statement A: Approved for Public Release, Distribution is Unlimited

13. SUPPLEMENTARY NOTES
None

14. ABSTRACT

The overall goal of this project was to demonstrate improved insight into PFAS leaching through the unsaturated zone to serve as a basis for developing soil cleanup criteria and facilitating site management. At each demonstration site, an initial high-resolution characterization of site soil, equilibrium (i.e., static) porewater sampling of the collected soil cores, and, *in situ* measurements of PFAS concentrations using porous cup suction lysimeters was performed. At a majority of the historically AFFF-impacted demonstration sites, soil and porewater results showed that potential perfluoroalkyl acid precursors persisted. Bench-scale measurements of PFAS concentrations in soil porewater were typically consistent with field measurements, suggesting that apparent local equilibrium assumptions for PFAS phase behavior were appropriate. PFAS accumulation at the air-water interface was also shown to be an important factor at some sites, and was dependent upon the moisture content, soil grain size, and the PFAS surface activity.

15. SUBJECT TERMS
PFAS, AFFF, leaching, interface

16. SECURITY CLASSIFICATION OF:			**17. LIMITATION OF ABSTRACT**	**18. NUMBER OF PAGES**	**19a. NAME OF RESPONSIBLE PERSON**
a. REPORT	**b. ABSTRACT**	**c. THIS PAGE**			Dr. Charles Schaefer
U	U	U	UU	104	**19b. TELEPHONE NUMBER** *(include area code)* 732-590-4633

Standard Form 298 (Rev. 8-98)
Prescribed by ANSI Std. Z39.18

FINAL REPORT
Project: ER20-5088

TABLE OF CONTENTS

Page

TABLE OF CONTENTS (Continued)

Page

LIST OF FIGURES

Page

LIST OF TABLES

Page

ACRONYMS AND ABBREVIATIONS

°C	degrees Celsius
µg/kg	micrograms per kilogram
µg/L	micrograms per liter
µL	microliter
AFCEC	Air Force Civil Engineer Center
AFFF	aqueous film-forming foam
BAA	Project Broad Agency Announcement
bgs	below ground surface
CA	California
CAD	collisionally activated dissociation
CEC	cation exchange capacity
CERCLA	Comprehensive Environmental Response, Compensation, and Liability Act
cm	centimeter
d	diameter
Da	Dalton
DF	dilution factor
DoD	Department of Defense
EPA	U.S. Environmental Protection Agency
ESI-	negative electrospray ionization
ESI+	positive electrospray ionization
ESTCP	Environmental Security Technology Certification Program
FECA	fluorinated ether carboxylates
ft	feet
FTS	fluorotelomer sulfonate
g	grams
GPR	ground penetrating radar
HPLC	high-pressure liquid chromatography
HRMS	high resolution mass spectrometry
ID	Idaho
IS	internal standard
kg	kilogram
L	liter
LC	liquid chromatography

LC/MS or LC-MS	liquid chromatography-mass spectrometry
LC-HRMS	liquid chromatography high resolution mass spectrometry
LOQ	limit of quantification
m	meter
m/z	mass-to-charge ratio
MA	Massachusetts
ME	Maine
mEq/g	milliequivalents per gram
mg/g	milligram per gram
mg/kg	milligrams per kilogram
mg/L	milligrams per liter
min	minutes
mL	milliliter
mL/min	milliters per minute
mm	millimeter
mM	millimolar
ms	millisecond
MS/MS	tandem mass spectrometry
NaBr	Sodium bromide
NaCl	Sodium chloride
ng/L	nanograms per liter
ng·L-1	nanograms per liter
NH	New Hampshire
PCSL	porous cup suction lysimeter
PFAA	perfluoroalkyl acid
PFAS	poly- and perfluoroalkyl substances
PFBS	perfluorobutanesulfonate,
PFHpS	perfluoroheptanesulfonate
PFHxA	perfluorohexanoic acid
PFHxS	perfluorohexanesulfonate,
PFOA	perfluorooctanoic acid
PFOS	perfluorooctanesulfonate
PFPeA	perfluoropentanoic acid
PFPeS	perfluoropentanesulfonate
pg	picogram
pg/mL	picograms per milliliter
ppm	parts per million
psi	pounds per square inch
QSPR	quantitative structure-property relationships
RCRA	Resource Conservation and Recovery Act

SERDP	Strategic Environmental Research and Development Program
TOC	total organic carbon
USEPA	United States Environmental Protection Agency
UST	underground storage tank
V	volt
XIC	extracted ion chromatogram
µm	micrometer

ACKNOWLEDGEMENTS

We are grateful to the contributions from Yida Fang, Nathan Smith, Nicholas Gonda, Chuhui Zhang, and Joseph Miller in performing this research. We are also appreciative of the many beneficial comments received from the ESTCP technical committee during this project, as well as for the ESTCP financial support of this work. Finally, we are grateful to the many DoD site managers for working with us to provide the necessary site access required to perform this project.

ABSTRACT

INTRODUCTION AND OBJECTIVES

As DoD efforts to characterize AFFF-impacted source areas and attain insights into the mechanisms controlling PFAS fate and transport in unsaturated soils are ongoing, field-based in situ characterization of PFAS leaching (via unsaturated zone pore-water measurements) coupled with soil characterization represent a practical dataset that is largely absent. Such practical information and field-based data, coupled with DoD's ongoing mechanistic studies, have potential to provide unique insights into developing/validating meaningful predictive models of PFAS soil-to-groundwater ratios (or, mass discharge from AFFF-impacted soils in the vadose zone), and ultimately guidance for determining soil concentrations protective of groundwater. ***The overall goal of this project is to demonstrate improved insight into PFAS leaching through the unsaturated zone to serve as a basis for developing soil cleanup criteria and facilitating site management.*** Obtaining a field-based dataset relating PFAS soil levels, soil characteristics, and porewater leaching to underlying groundwater impacts provide the DoD with much needed information to validate conceptual site models and develop soil management guidelines.

TECHNOLOGY DESCRIPTION

A multi-phased approach was employed to attain insight into soil-to-groundwater PFAS leaching, and ultimately guidance for determining soil concentrations protective of groundwater. This approach was utilized at five primary sites selected for this technology demonstration. At each demonstration site, an initial high-resolution characterization of site soil, equilibrium (i.e., static) porewater sampling of the collected soil cores, and, finally, *in situ* measurements of PFAS concentrations using porous cup suction lysimeters was performed.

PERFORMANCE AND COST ASSESSMENT

At a majority of the demonstration sites, where it had been several years since the last know AFFF release, soil and porewater results showed that potential perfluoroalkyl acid (PFAA) precursors persisted. Bench-scale measurements of PFAS concentrations in soil porewater via microlysimeter sampling were typically consistent with field lysimeter measurements, suggesting that apparent local equilibrium assumptions for PFAS phase behavior were appropriate. PFAS accumulation at the air-water interface was also shown to be an important factor at some sites, and was dependent upon the moisture content, soil grain size, and the PFAS surface activity. For the micro-lysimeter sampling, the estimated cost for evaluation within a typical fire-training area is $7,750.

IMPLEMENTATION ISSUES

Field lysimeter sampling was challenging, and occasionally ineffective, at sites where moisture contents were low and/or where there was substantial silt or clay present. Low permeability materials also inhibited collection of porewater at the bench-scale via microlysimeter sampling. In addition, poor agreement between field lysimeter and bench-scale PFAS porewater data was obtained at a site that consisted of back-filled materials.

PUBLICATIONS

Schaefer, C.E., Nguyen, D., Fang, Y., Gonda, N., Zhang, C., Shea, S. and Higgins, C.P., 2024. PFAS Porewater concentrations in unsaturated soil: Field and laboratory comparisons inform on PFAS accumulation at air-water interfaces. *J. Contam. Hydrol. 264*, 104359.

EXECUTIVE SUMMARY

INTRODUCTION

Use of aqueous film-forming foams (AFFFs) at Department of Defense (DoD) facilities has resulted in persistent subsurface contamination of poly- and perfluoroalkyl substances (PFAS). At many of these locations, the retention and slow release of PFAS from the unsaturated zone to underlying groundwater is the suspected (or known) cause of PFAS groundwater contamination. However, due to the unique complexities associated with PFAS phase behavior (e.g., sorption at air-water interfaces, retention of cationic species) and migration (e.g., rate-limited desorption), the relationship between PFAS levels measured in unsaturated soils and PFAS levels in percolating porewater (and, ultimately the underlying groundwater) is poorly understood. As a result, guidance is lacking regarding determination of soil screening criteria that are protective of underlying groundwater, as scientifically- or empirically-based data are generally lacking; this has proven to be a challenge with respect to site management. Thus, improved insights into the relationship between unsaturated zone PFAS composition and concentration, soil physical and chemical properties, and PFAS levels in percolating porewater/underlying groundwater are urgently needed.

As DoD efforts to characterize AFFF-impacted source areas and attain insights into the mechanisms controlling PFAS fate and transport in unsaturated soils are ongoing, ***field-based in situ characterization of PFAS leaching (via unsaturated zone pore-water measurements) coupled with soil characterization and underlying groundwater impacts represent a practical dataset that is largely absent***. Such practical information and field-based data, coupled with DoD's ongoing mechanistic studies, have potential to provide unique insights into developing/validating meaningful predictive models of PFAS soil-to-groundwater ratios (or, mass discharge from AFFF-impacted soils in the vadose zone), and ultimately guidance for determining soil concentrations protective of groundwater. Furthermore, traditional approaches for soil screening to estimate impact-to-groundwater values may be inappropriate due to PFAS sorption at air-water interfaces and perfluoroalkyl acid precursor transformation.

OBJECTIVES

The overall goal of this project is to demonstrate improved insight into PFAS leaching through the unsaturated zone to serve as a basis for developing soil cleanup criteria and facilitating site management. Obtaining a field-based dataset relating PFAS soil levels, soil characteristics, and porewater leaching to underlying groundwater impacts provide the DoD with much needed information to validate conceptual site models and develop soil management guidelines. Specific objectives are to:

- Assess the factors controlling PFAS leaching in the vadose zone
- Determine how soil properties impact PFAS porewater migration and overall source longevity
- Identify unsaturated zone characteristics that impact PFAS migration to groundwater
- Attain insight into the role of PFAS air-water interfacial retention on vadose zone migration
- Develop a screening-level basis for PFAS soil concentrations protective of underlying groundwater that can be used for improved site management

TECHNOLOGY DESCRIPTION

Please note that portions of the Technology Description and Performance Assessment have been reprinted (adapted) with permission from the pre-print of {Schaefer, C.E., Nguyen, D., Fang, Y., Gonda, N., Zhang, C., Shea, S. and Higgins, C.P., 2024. PFAS Porewater concentrations in unsaturated soil: Field and laboratory comparisons inform on PFAS accumulation at air-water interfaces. Journal of Contaminant Hydrology, 264, p.104359.}. Copyright 2024. Elsevier

A multi-phased approach was employed to attain insight into soil-to-groundwater PFAS leaching, and ultimately guidance for determining soil concentrations protective of groundwater. This approach was utilized at five primary sites selected for this technology demonstration. At each demonstration site, an initial high-resolution characterization of site soil, equilibrium (i.e., static) porewater sampling of the collected soil cores, and, finally, *in situ* measurements of PFAS concentrations using porous cup suction lysimeters was performed.

A 5.4-cm soil core was collected at each site Sites A through E) using a gas-powered core sampling kit (AMS, Inc., American Falls, ID). PFAS in the collected soil core were analyzed every 0.1 to 0.2 m for a total depth (depending on the site) of up to 2.4 m. Soil samples were also collected for total organic carbon (TOC), cation exchange capacity, and moisture content. Three lysimeters were installed within a 0.8 m radius of the soil core for Sites A, B, C, and D; the borehole used for soil sampling was used for one of the installed lysimeters. For Site E, three lysimeters were initially installed to a depth of 1.7 m below ground surface, but failed to produce any water. Two lysimeters were then re-installed adjacent to the initial locations to depths of 0.76 m below ground surface.

Lysimeter installation and sampling were performed as described previously (Schaefer et al., 2022). Porous cup suction lysimeters (4.8 cm diameter), with 3.8 cm long ceramic heads and a 2 bar bubbling pressure, were purchased from Soil Moisture Equipment Corp. (Goleta, CA). A silica flour (200 mesh) slurry was poured into the lysimeter boreholes so that the slurry reached several centimeters above the porous cup; addition of this slurry was intended to maintain a saturated connection between the lysimeter and the native soil. A sand was layered above the silica flour, with bentonite chips used to fill the remaining annular space. A bromide tracer (500 mg/L bromide as NaBr) was included with the silica flour slurry to account for any potential dilution of the porewater by the slurry water.

A hand pump was used to apply vacuum (typically 65 centibar) and extract porewater, where several hours to overnight extraction was typically needed to collect water. When possible, the initial sample of porewater collected for each lysimeter (approximately 20 mL) was used for purging and discarded; up to 3 subsequent rounds of porewater collected for PFAS analysis were performed within a 2 to 6 day period. The first round of samples from one of the 3 lysimeters at Site C was excluded from the dataset because PFAS porewater concentrations were approximately two standard deviations less than that observed in the other seven porewater samples collected.

An additional intact soil core, collected during installation of the lysimeters, was collected for bench-scale porewater testing. The purpose of the bench-scale porewater testing was to serve as a comparison to the field-measured PFAS porewater concentrations, where the bench-scale system represented a static (or, equilibrated) sample compared to the dynamic (and potentially non-equilibrated) field sample. Bench-scale porewater samples were collected using micro-sampling lysimeters that have a 0.95 cm outside diameter, were 18 cm long, and have a porous ceramic head 3 cm in length (Soil Moisture Equipment Corp., Goleta, CA). Vacuum (approximately 55 centibar) was applied to collected soils using 10 mL disposable syringes, where the vacuum was typically applied overnight. Methanol used to rinse the micro-sampling lysimeters and syringes was collected and analyzed with the collected porewater to limit any PFAS sorptive losses to the porewater extraction system; prior testing showed that sorptive losses to the field lysimeters were negligible for PFOS (Schaefer et al. 2022). Ideally, porewater was extracted from an intact core at the same depth where the field lysimeter was placed, with 2 additional duplicates extracted within 15 cm of this depth (3 samples total). However, due to relatively dry soil conditions, only porewater from the Site D soil core could be collected in this manner. For the other sites, soil was homogenized in the 20-30 cm depth interval that overlapped the depth of the field lysimeter deployment; soil in this interval was visually homogeneous. This soil was then wetted using a 5 mM $CaCl_2$ solution, packed in polypropylene centrifuge tubes (approximately 80 g samples prepared in triplicate), and equilibrated for a minimum of three days before extracting the porewater with the micro-sampling lysimeters. **Figure ES-1** shows the bench-scale porewater sampling set-up. Even after wetting, porewater could not be extracted in the laboratory from the homogenized soil for Site E, thus no bench-scale porewater samples were collected from Site E soil.

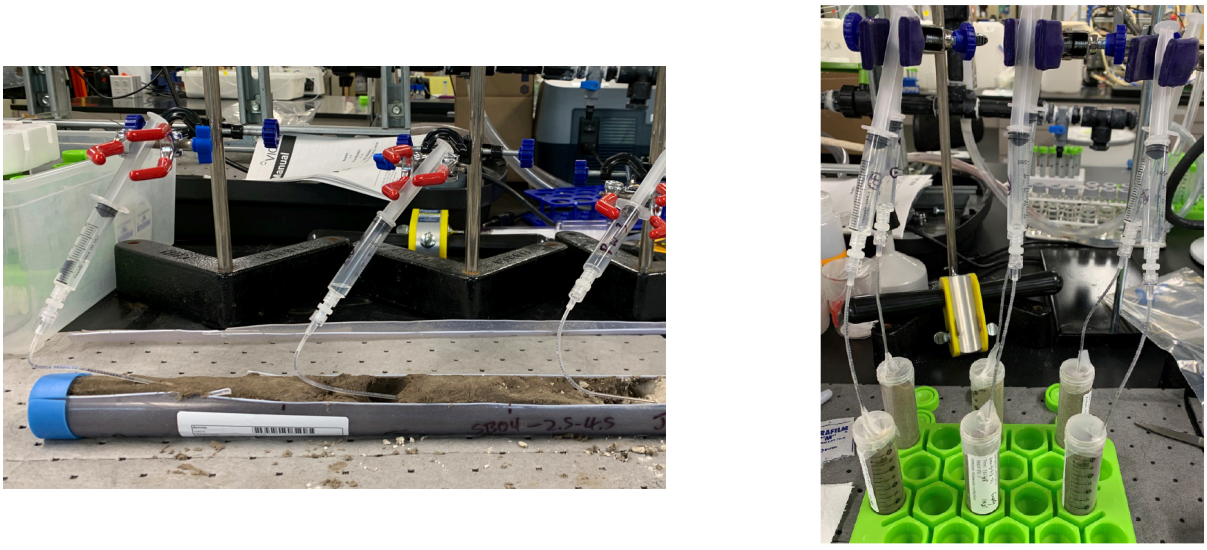

Figure ES-1. Bench-scale Porewater Sampling Using the Micro-sampling Lysimeters.

Sampling in an intact core is shown, and sampling from wetted and re-packed soil is shown.

PERFORMANCE ASSESSMENT

PFAS Soil Concentrations

In all cases, PFOS exhibited the most elevated PFAS concentration measured in the collected soil samples. The perfluorinated sulfonate relative concentration versus depth profiles for Sites A and B show clear chromatographic separation (**Figure ES-2**). The least hydrophobic compound (PFBS) has the deepest concentration maximum, while the PFOS concentration maximum is near the soil surface. In contrast, for Sites C and E, the relative concentration profiles are similar for each perfluorinated sulfonate, and no chromatographic separation was observed (**Figure ES-2**). Site D is omitted from Fig. ES-2 due to the large number of perfluorinated sulfonate results that were below the analytical detection limit. Similar results with respect to the vertical concentration profiles were observed for the perfluorinated carboxylates. The reason for the differences between Sites A and B, and Sites C and E, are unclear, as they could be due to the nature of AFFF releases, rainfall, and/or other soil properties.

PFAS Porewater Concentrations

Target (quantified) PFAS concentrations measured in the collected lysimeter porewater for each site, corrected for the appropriate bromide dilution factor (based on the bromide concentration in the sampled field lysimeter porewater relative to the bromide concentration used in the silica flour slurry), are summarized in **Figure ES-3**. At Site A, porewater PFAAs were largely dominated by shorter-chained (≤6 perfluorinated carbons) compounds. These porewater results are consistent with the corresponding soil data collected at the lysimeter installation depth of 1.5 m below ground surface. For Site B, 4:2 FTS accounted for the majority of the identified PFAS mass in the porewater, although 4:2 FTS was only observed in one of the two water-producing lysimeters and was not observed in any soil samples. Besides this detection of 4:2 FTS, similar to Site A, porewater at Site B also was dominated by shorter-chained PFAS.

PFOS and/or PFHxS were the predominant PFAAs for Sites D and E. These results for Sites D and E are consistent with the soil data, and may reflect the greater migration of PFOS and PFHxS at these sites due to increased rainfall and shallower lysimeter placement compared to Sites A and B. In contrast to Sites D and E, the porewater data for Site C was not indicative of the soil concentrations, as PFPeA and PFHxA were the predominant porewater PFAAs despite the fact that PFOS was by far the predominant PFAA in the soil. This apparent discrepancy is likely due to the elevated affinity of PFOS to the soil compared to PFPeA and PFHxA, and/or the relative affinity of PFOS to the air-water interface. It is also possible the predominance of PFPeA and PFHxA in Site C porewater was due to biotransformation of precursors present in Site C soil.

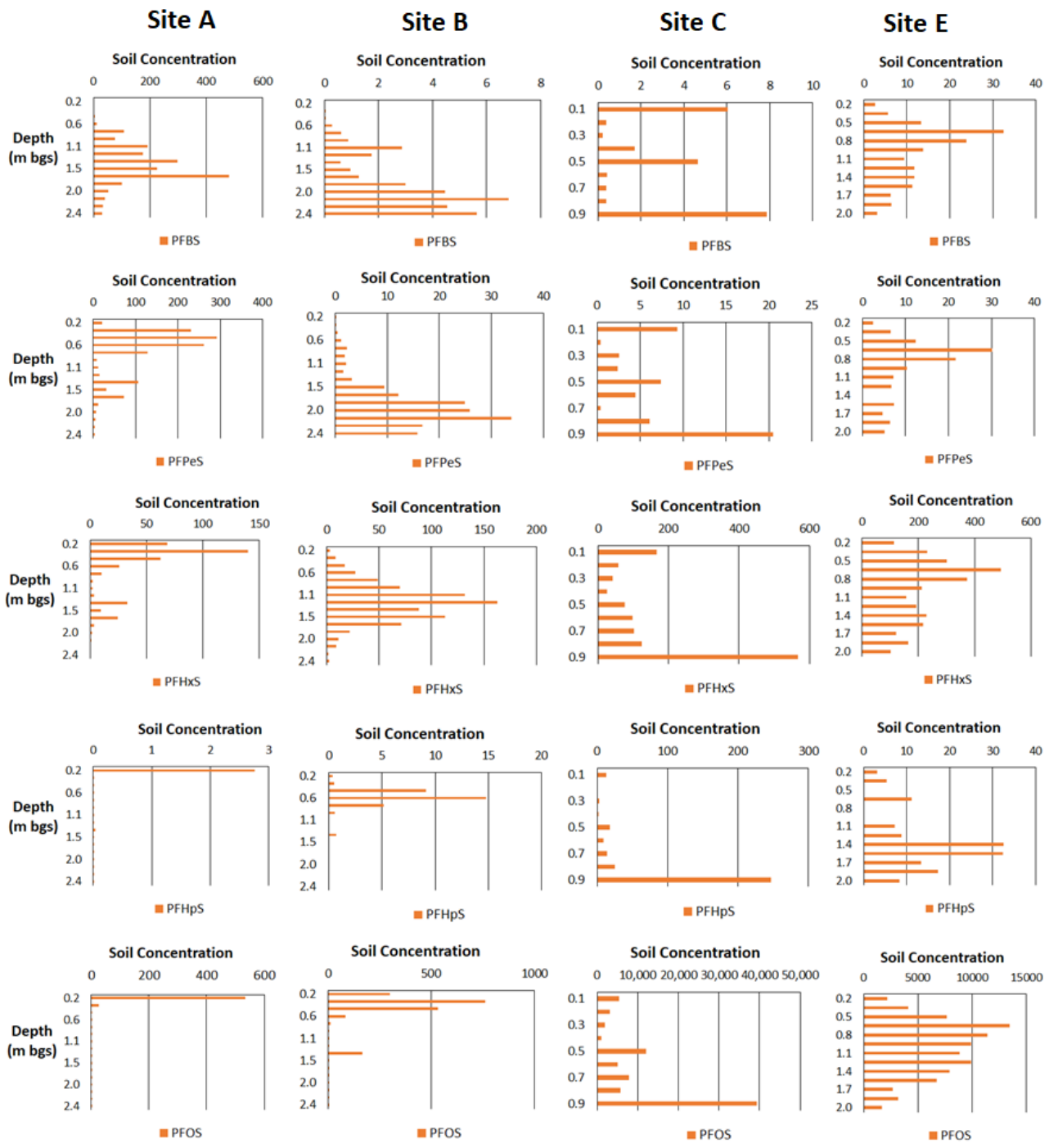

Figure ES-2. Perfluorinated sulfonate Soil Concentrations (µg/kg) Measured as a Function of depth in the Unsaturated Zone for Sites A. B, C, and E.

Non-detect results are plotted as 10% of the reporting limit. PFBS = perfluorobutanesulfonate, PFPeS = perfluoropentanesulfonate, PFHxS = perfluorohexanesulfonate, PFHpS = perfluoroheptanesulfonate, and PFOS = perfluorooctanesulfonate.

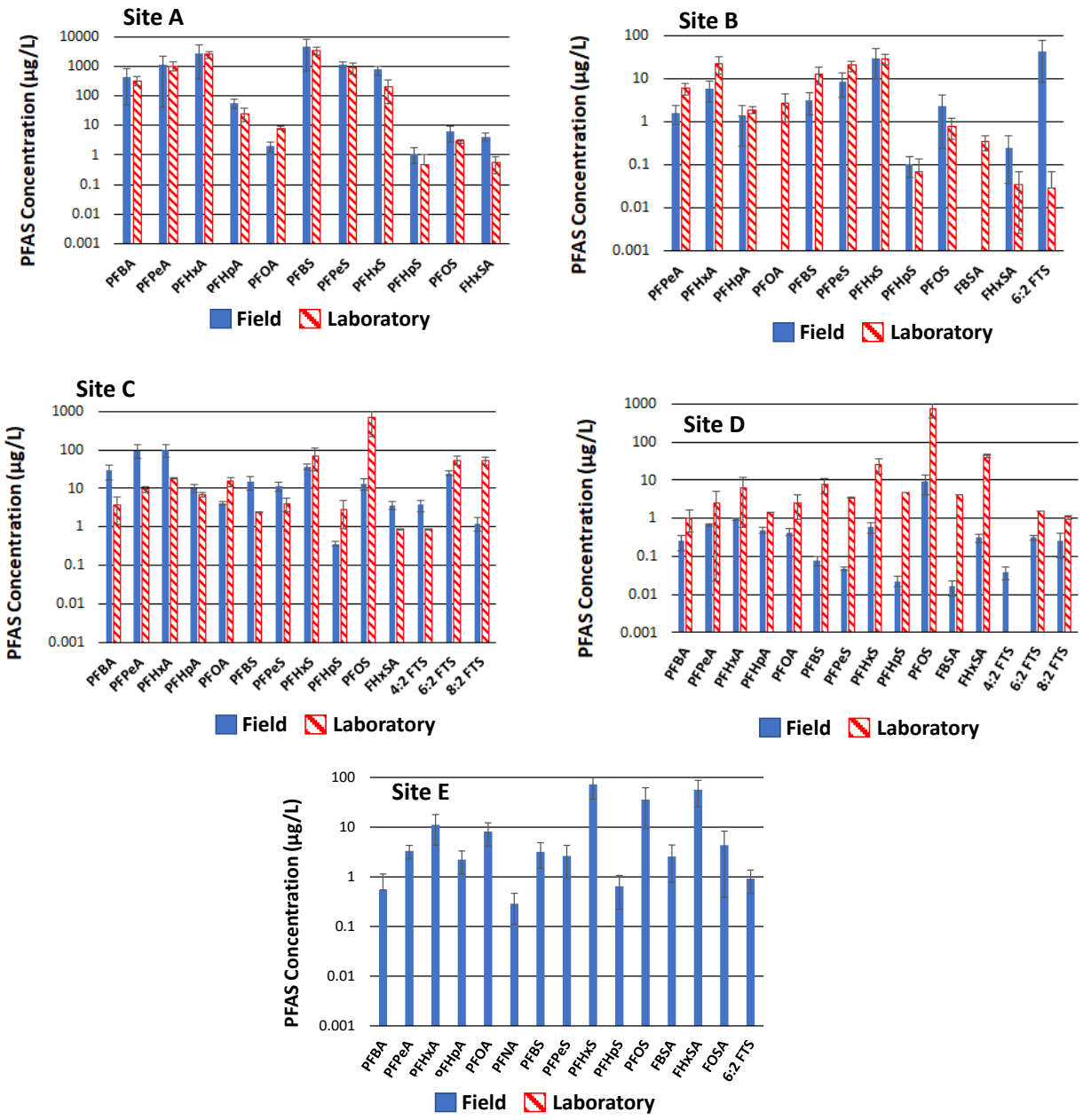

Figure ES-3. PFAS Porewater Concentrations for Quantifiable Analytes from Both the Field-deployed Lysimeters and in the Laboratory Using Porewater from the Collected Soil Cores.

Error bars represent 95% confidence intervals. For Site E, laboratory-based porewater samples could not be collected.

A comparison of the quantified PFAS porewater concentrations measured in the field lysimeters to those measured in the laboratory from the collected soil cores for each site, with the exception of Site E (field data only), is also provided in **Figure ES-3**. The small soil grain size for Site E precluded extraction of porewater in the laboratory from the collected soil core at the bench-scale.

For Sites A and B, PFAS concentrations measured in the field-collected porewater and in laboratory-collected porewater are typically within a factor of 2 to 5. Given the potential pore-scale variability among field-collected porewater and collected soil samples, such order of magnitude agreement is considered reasonable. Notable exceptions for Sites A and B are PFOA and 6:2 FTS. For PFOA, the limit of quantification (LOQ) for the field-collected porewater sample was 0.57 μg/L, which is just over 4-times less than that PFOA concentration measured in the laboratory-collected porewater. The large (3 orders of magnitude) discrepancy for 6:2 FTS in Soil B is not readily explained, but may be due to the variability of 6:2 FTS measured between lysimeters in the field (greater than 50 μg/L in one lysimeter, but below the limit of quantification of 0.11 μg/L at the other lysimeter).

For Site C, comparison between the field-collected porewater and laboratory-collected porewater are similar to that observed for Sites A and B. However, the concentrations for the long-chained compounds PFOS and 8:2 FTS are nearly 100-times greater in the laboratory-collected porewater sample than in the field-collected porewater sample. PFOS and 8:2 FTS are the most surface-active PFAS evaluated in this comparison (Lyu et al., 2018; Brusseau et al., 2019), and the wetting needed for the laboratory-collected porewater sample likely caused a substantial decrease in air-water interfacial area and subsequent release of PFAS into the aqueous phase.

Using a PFAS mass balance model similar to that previously developed (Schaefer et al., 2022), which is based on equilibrium relationship between soil, aqueous, and air-water interfacial phases, the impact of wetting and air-water interfacial area collapse on PFAS distribution and ultimately PFAS porewater concentrations was determined. Table ES-1 compares the measured versus precited PFAS porewater concentrations in the laboratory-measured (wetted soil core) samples. The generally reasonable (factor of 3) agreement between predicted and measured values suggests that the evaluation of PFAS concentrations in the collected soil cores can be used as a reasonable approximation for PFAS concentrations measured in situ using the porous cup suction lysimeters. These results also suggest that equilibrium relationship are generally appropriate for describing phase behavior. It is noted that, for Site D, PFAS concentrations measured in the field-collected porewater were generally 5- to 100-times less than those measured in the laboratory-collected porewater; Site D soils were not wetted prior to the laboratory-scale sampling (intact core was used). Thus, unlike Sites A, B, and C, the local equilibrium assumption does not appear to be valid for Site D. While a conclusive explanation for the discrepancy between the field-collected and laboratory-collected PFAS porewater concentrations for Site D is not resolved for this study, it is noted that the backfilled material in Site D was quite heterogeneous. Specifically, core logging noted what appeared to be polyethylene plastic sheeting and cm-sized pieces of concrete/rubble intermittently dispersed within the soil cores. In addition, ground penetrating radar (GPR) surveying performed prior to lysimeter installation showed several anomalies throughout, indicating discontinuities throughout the interrogated zone and suggesting the presence of voids or other debris. Such discontinuities could result in preferential or non-uniform flow that could bias PFAS concentrations in the lysimeters. The applicability of porous cup suction lysimeters in this type of media warrants further study.

Table ES-1. For Sites A, B, and C, Comparisons of PFAS Porewater Concentrations Measured in the Field Lysimeters (C_1) and in the Wetted Soil Cores (C_2) to the Model-Predicted Wetted Soil Core Values.

± values indicate 95% confidence intervals. 8:2 FTS and PFHpS comparison for Sites A and B are not provided because these compounds were not detected in the porewater and/or in the soil (at the depth of the lysimeters) at these two sites.

	Measured Porewater Concentration In Situ (C_1) (µg/L)	Measured Porewater Concentration in Wetted Laboratory Cores (C_2) (µg/L)	Predicted Porewater Concentration (C_2) (µg/L)
Site A			
PFOS	6.2 ± 3.4	3.0 ± 0.37	6.6 ± 3.3
Site B			
PFOS	2.2 ± 2.0	0.78 ± 0.38	2.8 ± 2.0
Site C			
PFOS	13 ± 4.1	680 ± 460	164 ± 75
8:2 FTS	1.2 ± 0.46	52 ± 13	16 ± 6.0
PFHpS	0.36 ± 0.051	2.9 ± 2.0	5.9 ± 3.4

COST ASSESSMENT

A cost assessment is presented to estimate the resources needed to provide bench-scale validation/ evaluation of PFAS concentrations measured in situ using porous cup suction lysimeters. Specifically, costs associated with the micro-lysimeter porewater sampling of collected soil sample (Fig. ES-1) is determined. For the micro-lysimeter sampling, the estimated cost (including PFAS analysis) for evaluation within a typical fire-training area is $7,750. This cost is largely driven by the PFAS analysis ($450/sample x 12 samples assumed).

IMPLEMENTATION ISSUES

The field-scale and bench-scale porewater sampling employed in this study were generally readily implementable. Specific challenges are noted as follows:

- Dry soil conditions. Sufficient soil moisture is needed to extract field porewater samples. Herein, porewater collection was challenging in the two driest soils (3.5% and 4.3% moisture content). Although a sufficient volume and number of porewater samples were collected for quantitative analyses, the targeted number of lysimeter samples was not obtained. Results of this study suggest that a soil moisture content of approximately 5% is needed for routine porewater collection use PCSLs (although this value also is dependent upon the soil grain size and texture). At many semi-arid or arid sites, this may necessitate timing lysimeter sampling events with rainfall events. Another option would be to apply vacuum for a longer period of time than what was used herein (typically 8 to 12 hours).

Such extended vacuum application would require additional labor efforts, or the use of a vacuum manifold system. For the microlysimeters, a soil moisture content of approximately 7% was needed to effectively extract porewater; this higher moisture content is due to the fact that the maximum vacuum that could be applied on the microlysimeters was less than that which could be applied to the field-deployed lysimeters.

- Low permeability soils. It is well-known that low permeability soils can prevent the effective collection of porewater when using PCSLs. Sites E and G had clay contents of 14% and 15%, respectively. Despite elevated moisture contents (9.6% and 13% for sites E and G, respectively), collecting porewater was challenging. For Site E, sufficient porewater was collected for quantitative analyses, but not all lysimeters produced water and no porewater was collected for some of the sampling rounds; site G yielded insufficient porewater to include in the study. Porewater collection results for site G, given the elevated moisture and average grain size of 0.2 mm, were particularly surprising. One possibility is that local heterogeneity in the clay distribution may have contributed to the difficulties in collecting porewater at site G. Overall, results of this study suggest that elevated clay levels could result in challenges when attempting to collect porewater using PCSLs.
- Applied vacuum. Another issue that occurred was that the lysimeters would occasionally not hold vacuum, and therefore porewater collection was limited. In most cases, this was due to improperly securing either the lysimeter cap, or improperly securing/crimping the vacuum tubing. Thus, proper attention should be given to these details. Another challenge (observed herein and in other lysimeter studies in which the project investigators are involved) the lysimeter caps appeared to be tampered with by wildlife. Thus, proper securing and protecting of the lysimeter caps is recommended.
- Site heterogeneity. For this project, lysimeters were installed at a single depth, and within a single stratigraphic zone. For sites where the soil data suggest that the geology and PFAS distribution are likely not uniform throughout the unsaturated zone, installing lysimeters at multiple depths should be considered to better inform on overall PFAS leaching and mass discharge to underlying groundwater. While such evaluation was beyond the scope of this current study, it is important to recognize that the spatially limited lysimeter investigation performed herein would need to be expanded to provide appropriate site characterization.
- Comparison of lab vs field Collected porewater. While reasonable agreement (typically within a factor of 3 and/or within the 95% confidence interval of the field measurements) was observed between field-collected porewater and porewater extracted in the laboratory from soil cores, two findings are noteworthy. First, in most cases, the soil needed to be wetted and re-packed to collected porewater in the laboratory. Second, if wetting caused a significant decrease in the air-water interfacial area, the impact on PFAS porewater concentrations due to release of PFAS at the air-water interface had to be accounted for (via mass balance) to properly compare the laboratory PFAS porewater concentrations to the field data.

1.0 INTRODUCTION

Environmental Security Technology Certification Program (ESTCP) Project ER20-5088 is intended to demonstrate the use of lysimetry at both the laboratory- and field-scale as a means to assess leachability of per- and polyfluoroalkyl substances (PFAS) through the unsaturated zone and to develop soil cleanup criteria protective of groundwater. This demonstration provides the U.S. Department of Defense (DoD) with practical information and field-based data that, coupled with ongoing mechanistic studies in the Strategic Environmental Research and Development Program (SERDP), have potential to provide unique insights into developing/validating meaningful predictive models of PFAS soil-to-groundwater mass discharge, and ultimately guidance for determining soil concentrations protective of groundwater. This unique dataset will also help the DoD prioritize aqueous film-forming foam (AFFF)-impacted sites with respect to risks to groundwater and receptors.

1.1 BACKGROUND

Use of AFFFs at DoD facilities has resulted in persistent subsurface contamination of PFAS. At many of these locations, the retention and slow release of PFAS from the unsaturated zone to underlying groundwater is the suspected (or known) cause of PFAS groundwater contamination. However, due to the unique complexities associated with PFAS phase behavior (e.g., sorption at air-water interfaces, retention of cationic species) and migration (e.g., colloidal transport), the relationship between PFAS levels measured in unsaturated soils and PFAS levels in percolating porewater (and, ultimately the underlying groundwater) is poorly understood. As a result, guidance is lacking regarding determination of soil screening criteria that are protective of underlying groundwater, as there is a general paucity of scientifically- or empirically-based data; this has proven to be a challenge with respect to site management. Thus, improved insights into the relationship between unsaturated zone PFAS composition and concentration, soil physical and chemical properties, and PFAS levels in percolating porewater/underlying groundwater are urgently needed.

As DoD efforts to characterize AFFF-impacted source areas and attain insights into the mechanisms controlling PFAS fate and transport in unsaturated soils are ongoing, field-based *in situ* characterization of PFAS leaching (via unsaturated zone porewater measurements) coupled with soil characterization and underlying groundwater impacts represent a practical dataset that is largely absent. Such practical information and field-based data, coupled with DoD's ongoing mechanistic studies, have potential to provide unique insights into developing/validating meaningful predictive models of PFAS soil-to-groundwater ratios (or, mass discharge from AFFF-impacted soils in the vadose zone), and, ultimately, guidance for determining soil concentrations protective of groundwater. Furthermore, traditional approaches (EPA 1996) for soil screening to estimate impact-to-groundwater values may be inappropriate because of PFAS sorption at air-water interfaces and perfluoroalkyl acid precursor transformation.

Our approach was to obtain detailed soil data (i.e., PFAS levels and physical/chemical properties) coupled with *in situ* porewater leaching/partitioning information at a wide range of AFFF impacted sites. This information provides the DoD with a unique dataset that will complement ongoing SERDP/ESTCP research efforts and develop meaningful empirical field data in support of developing soil cleanup criteria and estimates of source longevity.

Our effort is viewed as complementary to ongoing SERDP Project ER18-1204, where a detailed leaching/enhanced flushing study is being performed at a single site. By collecting soil and ambient leaching data at a large number of DoD sites, the study is intended provide insight into the dependence of *in situ* PFAS leaching on soil properties that might otherwise not be identified in ER18-1204 or other ongoing studies. In addition, the field leaching and soil data collected as part of this study serve as a field validation for developing conceptual and mathematical models, including those proposed in recent studies (EPA 1996 and Falta et al. 2005) of PFAS fate and transport through unsaturated soils. Together, such information will serve as a useful tool for DoD remedial project managers at many AFFF-impacted sites.

1.2 OBJECTIVE OF THE DEMONSTRATION

The overall objective of the demonstration is to establish improved insight into PFAS leaching through the unsaturated zone to serve as a basis for developing soil cleanup criteria and facilitating site management. Specific objectives are to:

- Assess the factors controlling PFAS leaching in the vadose zone;
- Determine how soil properties impact PFAS porewater migration and overall source longevity;
- Identify unsaturated zone characteristics that impact PFAS migration to groundwater;
- Attain insight into the role of air-water interfacial retention on PFAS vadose zone migration; and
- Develop a screening-level basis for PFAS soil concentrations protective of underlying groundwater.

1.3 REGULATORY DRIVERS

PFAS became contaminants of emerging concern in the early 2000s. In recent years, federal, state, and international authorities have established a number of health-based regulatory values and evaluation criteria. As with the case for most emerging contaminants, the regulatory process dealing with PFAS is in various stages of development, and the values and criteria being established vary between individual states, the U.S. government, and international agencies. The scientific community is rapidly recognizing and evolving its understanding of PFAS in the environment, causing an increased pace of development of guidance values and regulations. Human health protection is the primary focus of the PFAS regulations, guidance, and advisories developed to date. Regulations and guidance have focused on the perfluoroalkyl acids (PFAAs), precursor compounds, and fluorinated ether carboxylates (FECAs). Like many other emerging contaminants, the regulatory and guidance values for perfluorooctane sulfonic acid (PFOS) and perfluorooctanoic acid (PFOA) can vary across programs that govern PFAS, including the Resource Conservation and Recovery Act (RCRA); Comprehensive Environmental Response, Compensation, and Liability Act (CERCLA); Toxic Substances Control Act; Safe Drinking Water Act; Clean Air Act; Clean Water Act; and U.S. Food and Drug Administration. State regulatory agencies often have the delegated authority to regulate and enforce environmental and public health requirements, although the 50 states have different priorities, resources, and processes.

Internationally, including in the U.S., nonpolymer PFAS (primarily nonpolymer long-chain PFAAs) have been the regulatory focus. There are a number of draft toxicity evaluations available for different PFAS. This is an area of active research.

There are two types of soil screening levels: human health values protective of direct contact, and values protective of groundwater as a result of leaching through soils. As of November 2024, the U.S Environmental Protection Agency (EPA), has derived Regional Screening Levels (RSLs) for 37 PFAS, which include screening levels for human health values protective of direct contact, and values protective of groundwater as a result of leaching through soils. Generally speaking, screening levels protective of leachability to groundwater are orders of magnitude lower than values protective of direct contact with soils given the mobility of select PFAS. EPA has also finalized Maximum Contaminant Levels (MCLs) for six PFAS in drinking water. MCL-based screening levels protective of groundwater as a result of leaching through soils are also available.

2.0 TECHNOLOGY DESCRIPTION

This section provides a brief description of elements being evaluated as part of this demonstration project.

2.1 MASS DISCHARGE AND SOURCE LONGEVITY

Understanding the contaminant mass discharge through a source area in the vadose zone is critical for both determining the impacts to underlying groundwater, and for estimating the longevity of the source (based on a mass balance). Several studies have been performed examining this source behavior for chlorinated solvents or hydrocarbons (Falta et al. 2005, DiFilippo et al. 2008, Mobile et al. 2012), and such information has facilitated guidance regarding soil-based remediation standards, remedial design, and overall site management. However, field-based data measuring PFAS mass discharge relative to mass retained in the unsaturated soils is extremely sparse. As a result, data to support regulatory and/or remedial PFAS soil levels are lacking, as are data to support estimates of source zone longevity.

Stahl et al. (2013), using mesoscale (1 square meter by 1.5-meter depth) monolithic column experiments, showed that soil spiked with 25 milligrams per liter (mg/L) of both PFOA and PFOS yielded leachate concentrations of 58 and 0.5 mg/L, respectively. This large difference in leaching behavior, which cannot be explained considering only the K_{oc} values for PFOA and PFOS, highlights the complexities and current lack of understanding regarding PFAS leaching in unsaturated soils, and their associated impacts on mass discharge and underlying groundwater. Similar complexities were observed in a recent AFFF leaching study using applied foams and unsaturated soils (Høisæter et al. 2019).

2.2 USE OF POROUS CUP SUCTION LYSIMETERS FOR MEASURING LEACHATE

Porous cup suction lysimeters (PCSLs) have been used in many field and laboratory tests, with reviews related to their performance presented in multiple studies (e.g., Singh et al. 2018 and Weihermüller et al. 2007). PCSLs are often attractive due to their relatively low cost, ease of installation, minimal disturbance to *in situ* soil, and ability to be installed at depth. As shown in **Figure 2-1**, solute leaching using PCSLs compared reasonably well with both soil cores and subsurface drainage lysimeters (which are much more complex to install than PCLSs for *in situ* measurements but may overcome some limitations associated with PCSLs due to heterogeneous flow) for measuring nitrate leaching in sandy soils. Thus, PCSLs were shown to provide a reasonable prediction of solute migration. Wang et al. (2012) also showed that PCSLs results were within 50 percent of leaching values obtained using undisturbed monolithic core lysimeters.

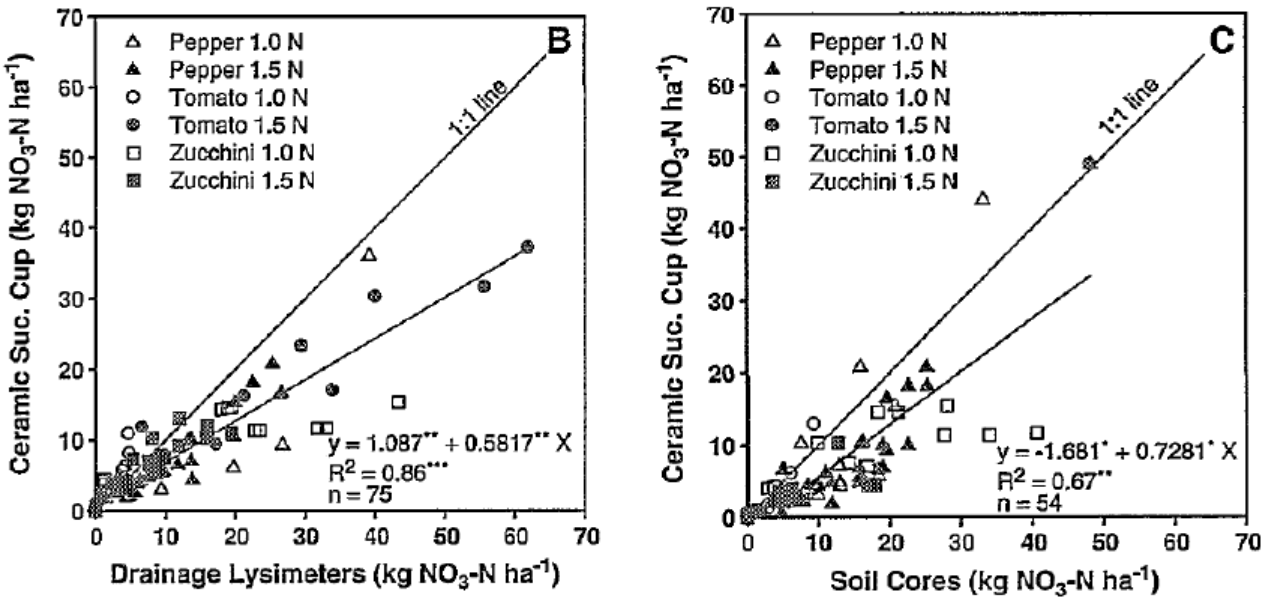

Figure 2-1. Nitrate Leaching Measured Using PCSLs Compared to Drainage Lysimeters (left) and Soils Cores (right) in a Nitrate Leaching Study Performed by Zotarelli et al. (2007).

Nitrate values measured using PCSLs were within a factor of two of estimates based on soil cores and drainage lysimeters.

While macropore or unstable flow in well-structured soils has been cited as a limitation for employing PCSLs (Singh et al. 2018, Weihermüller et al. 2007, and Flury et al. 1994), design considerations with respect to appropriate soil types, water infiltration volume and rate, and density of lysimeter placement can mitigate these concerns. Coarse (greater than 2 millimeter) and clayey soils typically provide the greatest challenges with respect to preferential flow, and therefore can be the most challenging to obtain representative samples using PCSLs (Flury et al. 1994 and Pampolino et al. 2000). Data from Fury et al. (1994) highlight the challenges with preferential flow in coarse soils, while finer-grained soils (fine sand range) facilitate more uniform unsaturated flow fields that are more conducive to PCSL sampling. Under moderate to low precipitation events, macropore flow in fine textured soils may be negligible (Hendrickx et al. 2001), resulting in improved PCSL sampling results. Simulation results for heterogeneous flow in unsaturated soil indicate that a single PCSL can predict solute breakthrough time within a factor of two of the actual solute breakthrough time, given a reasonably heterogeneous flow field (1 meter wide and 1 meter deep) (Weihermüller et al. 2006). Together, these studies suggest that use of PCSLs in soils consisting of fine sands to silts can provide a reasonable prediction of solute concentration in porewater, except perhaps under periods of heavy rainfall. Even under conditions where macropore flow through features such as fractures or earthworm channels may impact flow, PCSL samples are representative of the soil matrix and thus provide a reasonably conservative estimate of contaminant porewater concentrations that could discharge to underlying groundwater.

2.3 COMPLEX VADOSE ZONE PROCESSES

While PFAS sorption to organic carbon has been shown to play a significant role in the PFAS soil-to-groundwater ratio (**Figure 2-2**), other soil, hydraulic, and/or fluid properties also are clearly involved in understanding this pathway. Processes occurring in the vadose zone (e.g., unsaturated flow, formation of fluid-fluid interfaces, cycling of redox conditions) are complex compared to those typically observed in the saturated zone, and *in situ* testing using undisturbed soils may often be the most appropriate way to capture these processes. Field-scale approaches have been used to attain mechanistic insights of chlorinated solvent mass discharge that could not have been appropriately observed under laboratory conditions (Choi et al. 2002). We strongly believe that *in situ* measurements of PFAS behavior is a vital component needed to assess PFAS leaching behavior. Critical vadose zone processes that likely impact leaching include colloid-facilitated transport (particularly for zwitterionic and cationic species) and sorption at the air-water interface (described in the section below); both of these processes are highly dependent on the pore scale fluid configurations that are likely to be best preserved in field-scale studies. Thus, empirical field-scale measurements have substantial value, especially when coupled with the type of mechanistic bench-scale studies currently ongoing in several SERDP projects.

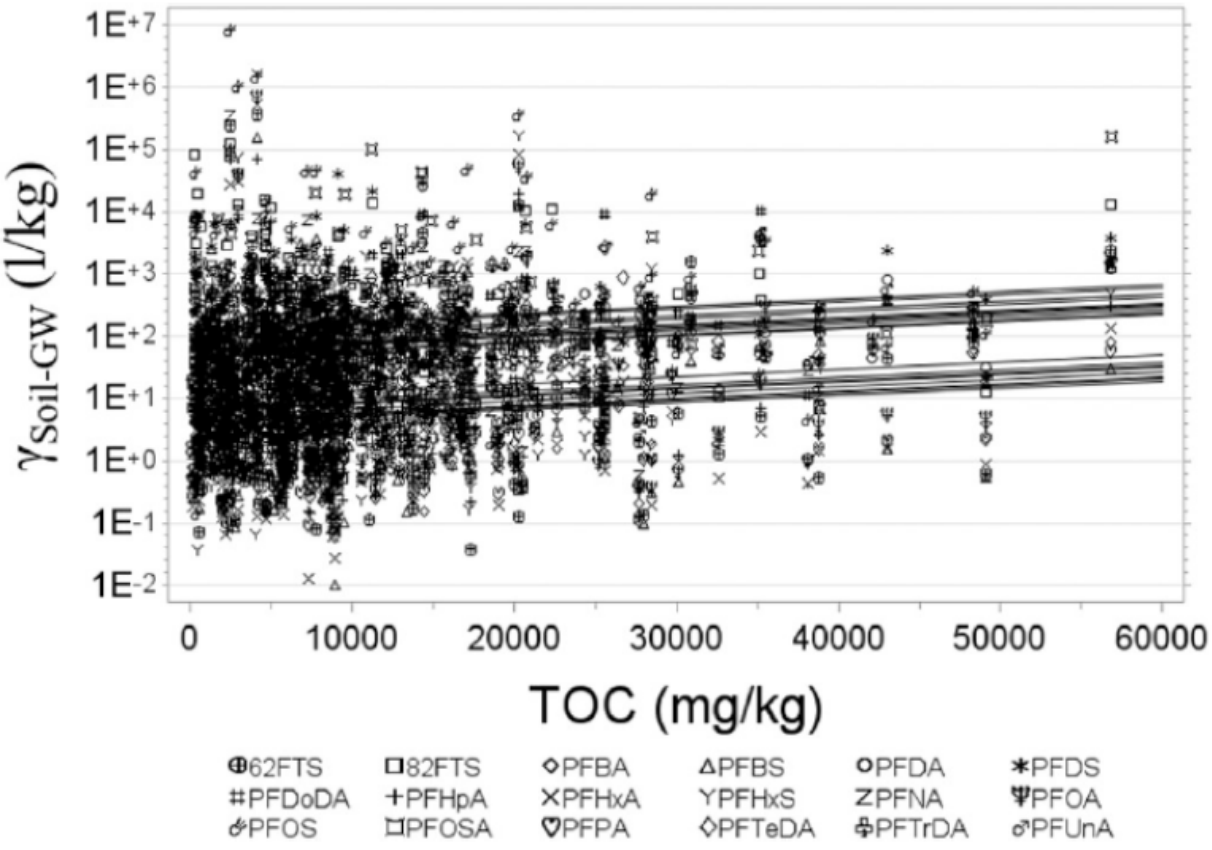

Figure 2-2. PFAS Soil-to-groundwater Ratios as a Function of soil TOC.

Figure from Anderson et al. (2019).

2.4 AIR-WATER INTERFACES

Recent studies (Psillakis et al. 2009, Enami et al. 2016, and Brusseau 2018) have verified that both perfluorinated carboxylates and sulfonates sorb at air-water interfaces in porous media. Given the large values of water-air interfacial areas (greater than 100 square centimeters per cubic centimeter) present in even coarse-grained vadose zone materials (Schaefer et al. 2000), PFAS sorption at water-air interfaces in the vadose zone likely will be significant; modeling performed by Brusseau (2018) (**Figure 2-3**) suggests such sorption may be important as a retention mechanism in the vadose zone.

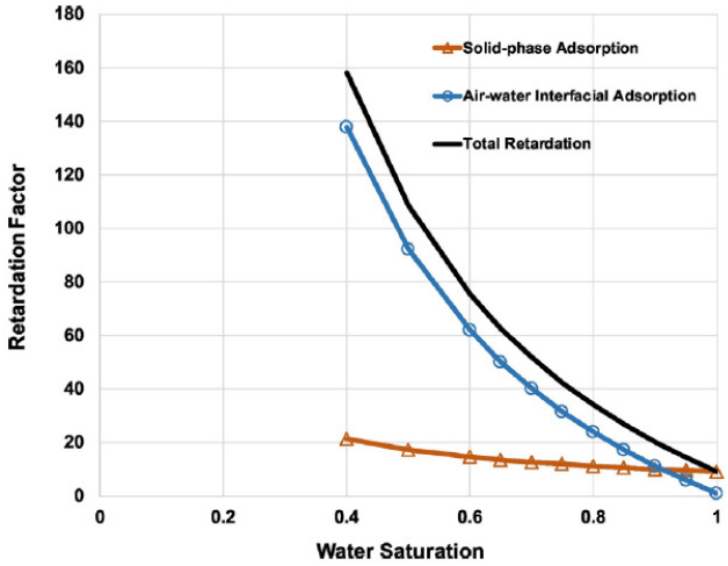

Figure 2-3. Retardation of PFOS in Unsaturated Sand Due to PFOS Retention at the air-Water Interface.

Figure from Brusseau (2018).

Our work as part of SERDP Project ER18-1259 showed that interfacial sorption at field-relevant PFAS concentrations can be predicted based on simple interfacial tension measurements, and that the extent of sorption may be substantially greater than previously predicted using the Langmuir sorption model. Furthermore, our work has shown that interfacial retention of PFOS is unaffected by the presence of PFAA precursors, further highlighting the importance of this mechanism in unsaturated soils (Schaefer et al. 2019).

Previous research has shown that species sorbed at the air-water interface are readily mobilized upon rewetting of the unsaturated media (e.g., during a rainfall event) (Sirivithayapakorn 2003), thus the water-air sorption of PFAS may enhance mass discharge to the underlying groundwater during episodic rain infiltration events that are prolonged and intense. In addition, analysis performed over a large number of sites by Anderson et al. (2019) suggest that air-water interfacial area may play a role in the PFAS soil-to-water ratio, and ultimately PFAS leaching in the vadose zone. This information, coupled with flow heterogeneity and transient wetting that typically occur in the vadose zone, point to the necessity for field-measured PFAS leaching to attain insight into soil concentrations that are protective of groundwater (i.e., soil-to-groundwater ratios).

Nonintuitive results, such as the observation that the clay fraction is inversely related to the PFAS soil-to-groundwater ratio (Anderson et al. 2019), further highlight the need for such field-based data.

2.5 VARIABLY SATURATED CONDITIONS

Vadose zone processes associated with precipitation-induced variably saturated conditions have been well studied. Many of these processes affect the pore water in the vadose zone and capillary fringe, and are likely to impact the release of PFAS from AFFF-impacted source areas. Specifically, naturally-present colloidal levels have been shown to increase during drainage, resulting in a significant enhancement of contaminant migration (Ryan et al. 1998 and Cheng et al. 2010). Investigations of this process for PFAS have been limited. Rádi et al. (2014) showed that cationic surfactants were substantially bound to colloidal humic materials. Other studies (Aherns et al. 2010 and Jia et al. 2010) suggest that natural colloidal and particulate materials increase the apparent solubility of some PFAS. Together, these findings point to the likelihood that the transport of zwitterionic/cationic PFAS may be significantly enhanced by natural colloids mobilized during transient wetting phases in the vadose zone.

2.6 SOIL SCREENING VALUES

The traditional approach for estimating nonvolatile contaminant soil concentrations in the vadose zone that are protective of underlying groundwater is based on equilibrium partitioning between the soil and aqueous phases (1):

$$C_T = C_p \left(K_d + \frac{\theta w}{\rho}\right) \quad \text{Eq. 1}$$

where C_T is the contaminant mass measured in a collected soil sample (which includes mass present in all phases), C_p is the contaminant aqueous concentration in the porewater, K_d is the contaminant linear soil-water partition coefficient, θ_w is the water-filled porosity, and ρ is the bulk density. Determination of a soil screening value for C_T is typically done by setting C_p equal to the contaminant regulatory goal in groundwater, and K_d is either determined based on batch soil-water sorption experiments, or estimated using the organic carbon content of the soil coupled with the contaminant K_{oc}.

Eq. 1 assumes the point of compliance is directly below the infiltrating porewater, and thus serves as a conservative soil screening value protective of groundwater. Often, a dilution factor is included in Eq. 1 that is proportional to the volume of infiltrating rainwater relative to volumetric groundwater flow to the compliance point (1). Since this dilution factor is based on sitewide and site-specific percolation and groundwater flow conditions, it is not included in our assessment performed as part of this proposed project, as our focus is on the localized soil-porewater relationship.

For PFAS, one challenge with respect to application of Eq. 1 is that C_T (which is what is measured when soil investigations are performed) also includes any PFAS mass retained at the air-water interface. To account for PFAS sorption at the air-water interface, Eq. 1 is modified as follows:

$$C_T = C_p \left(K_d + \frac{k_{aw} a_i}{\rho} + \frac{\theta_w}{\rho}\right) \quad \text{Eq. 2}$$

From Eq. 2, it can be seen that neglecting $K_{a\text{-}w}$ can result in an underestimation of C_T, leading to soil screening criteria that are too stringent. While some predictions of $K_{a\text{-}w}$ have been made using relatively simple bench-scale systems (Brusseau 2018 and Brusseau et al. 2019), actual field $K_{a\text{-}w}$ values for PFAS are unknown, and may be poorly predicted based on existing models. Our proposed approach will provide direct measures of both C_p and C_T, thus unambiguously determining if porewater concentrations for a given C_T exceed regulatory levels. The independent measurement of K_d under water saturated conditions also will allow for determination of $K_{a\text{-}w}$ values via mass balance, thereby providing a field evaluation of $K_{a\text{-}w}$ and the role of air-water interfaces during PFAS percolation in the vadose zone. It is also worth consideration that C_p measured in the porewater may be much lower than expected due to nonequilibrium conditions (e.g., the presence of slowly desorbing PFAS in soils and/or heterogeneous flow).

2.7 ADVANTAGES AND LIMITATIONS OF THE TECHNOLOGY

This project employs methods and techniques that have been demonstrated in previous laboratory and field projects; therefore, risks are minimal. The two greatest challenges will likely be (1) soil heterogeneity and (2) dry soil conditions that inhibit porewater collection with the lysimeters.

The issue of soil heterogeneity, which was raised during ESTCP's review of the preproposal, were discussed in Sections 2.1, 2.2, and 2.3. Avoidance of clayey soils (which are prone to heterogeneous macropore flow) and use of three replicate lysimeters per site mitigated these risks. With respect to potentially dry soil conditions that inhibit porewater collection in the lysimeters, lysimeter samples were collected during rainy seasons or shortly after a rainfall event. In addition, up to 2 days at high vacuum was allotted for porewater collection. Thus, even when soil moisture was low and porewater extraction rates were slow, this prolonged sampling time generally allowed for sufficient sample collection.

3.0 PERFORMANCE OBJECTIVES

The performance objectives of this demonstration project are presented in **Table 3-1**. A description of each performance objective, specific data requirements, success criteria, and results is provided in subsequent subsections.

Table 3-1. Performance Objectives

Performance Objective	Data Requirements	Success Criteria	Results
Quantitative Performance Objectives			
Determination of PFAS partitioning in porewater	• PFAS soil concentrations • PFAS concentrations in extracted porewater (using collected soil cores) • Soil moisture content	Repeatability (±30%) within replicates	Apparent PFAS soil-water partitioning, as determined based on microlysimeter porewater concentrations, were typically within a factor of 2
Determination of PFAS concentrations in vadose zone leachate	• PFAS concentrations measured via *in situ* lysimeters • PFAS soil concentrations • Soil moisture content	Repeatability (±30%) within replicates	PFAS field lysimeter porewater concentrations were typically within a factor of 2
Relate vadose zone characteristics with PFAS flux to groundwater (via prediction of PFAS porewater concentrations)	• PFAS concentrations measured in extracted porewater and via in situ lysimeters • Soil characteristics: pH, total organic carbon (TOC), cation exchange capacity (CEC), particle size distribution, and measured porewater saturations • Application of percolation model	Statistically significant correlation between vadose soil properties and porewater PFAS level ($R^2 \geq 0.8$, and P value <0.05)	Predictions of in situ PFAS porewater concentrations were possible for 4 out of the 5 primary sites. For 3 of these sites, PFAS predicted values (± 95% confidence interval of the predicted value) were within the 95% confidence interval of the measured value [with the exception of 8:2 FTS at one site]. For the fourth site (which had backfilled materials), field values could not be accurately predicted.
Qualitative Performance Objectives			
Ease of lysimeter sampling	Feedback from field and laboratory technicians	Minimal training requirements	Field staff were readily trained on lysimeter installation and sampling, although dry or low permeability soils presented a challenge.

3.1 PERFORMANCE OBJECTIVE #1

This objective is focused on determining the PFAS partitioning coefficients between soil and porewater extracted at different lengths of the soil cores collected at the five AFFF-impacted sites. The porewater collected in these samples is expected to be in local equilibrium with respect to the solid phase at each sample interval, and will provide insight into the PFAS levels associated with the porewater and air-water interfaces in absence of porewater flow.

3.1.1 Data Requirements

Soil concentrations in the collected cores, as well as PFAS concentrations in the extracted porewater (3 per soil core, all collected at the approximate depth of the field lysimeter), were used for this testing. With PFAS soil concentrations typically approximately constant in the small (15 cm) section of soil examined, variability in the measured porewater concentrations were used to assess the variability of the apparent PFAS partitioning between soil and air-water interfacial phases. The moisture content of the soil was also a key parameter that was measured.

3.1.2 Success Criteria

The success criterion for this objective was PFAS analytical and soil moisture content data collected from each soil core, and a 30 percent error between triplciate samples at a given core depth.

3.1.3 Results

As presented in Section 6.1.2, the variability in PFAS porewater concentrations for the microlysimeter sampling was approximately a factor of two. Such variability was likely due to a combination of factors, including inherent variability in the sampling method, PFAS analytical variability, and PFAS heterogeneity in the soil. While this error is greater than what was originally listed as the success criteria, we believe this testing provides critical insight into PFAS leaching behavior, and is on the same scale of variability observed in field lysimeter sampling.

3.2 PERFORMANCE OBJECTIVE #2

The goal of this objective is to evaluate the PFAS concentration in vadose zone leachate using *in situ* lysimeters. It was achieved through installation of three PCSLs at each AFFF-impacted site, at locations directly adjacent to the soil cores collected in Performance Objective 1. Each PCSL was sampled for porewater up to 3 times using constant applied vacuum and analyzed for PFAS. Results from this objective provide an estimation on the relationship between PFAS mass measured in soil and PFAS mass measured in porewater under dynamic conditions.

3.2.1 Data Requirements

Similar to Performance Objective 1, data required for this objective include the PFAS concentration in the porewater collected via *in situ* lysimeters and PFAS concentrations measured in the soil samples directly above each *in situ* lysimeter. In addition, soil moisture content was determined from soil samples to facilitate the modeling needed to calculate PFAS air-water interfacial area and ultimately PFAS accumulation at the air-water interface.

3.2.2 Success Criteria

The success criterion for this performance objective is identical to the previous objective, which is to have a less than 30 percent error in analytical results between the replicate lysimeter samples.

3.2.3 Results

As presented in Section 6.1.2, the variability in PFAS porewater concentrations was typically within a factor of 2 to 3. This is clearly greater than the 30% success greater originally listed. However, lysimeter data provide critical information needed to understand PFAS leaching, and the inherent error/variability associated with field lysimeter sampling must be considered when interpreting field results.

3.3 PERFORMANCE OBJECTIVE #3

The goal of this objective is to relate vadose zone characteristics with PFAS flux to groundwater via prediction of PFAS concentrations in porewater. This effort involved, as described in Section 6, involved relating soil and PFAS properties to ultimately predict the measured in situ PFAS porewater concentration.

3.3.1 Data Requirements

Data used to predict PFAS porewater concentrations included soil grain size distribution (to ultimately determine average soil particle diameter), in situ soil moisture content, PFAS soil concentrations, and PFAS aqueous concentrations as measured in both the bench-scale porewater samples using collected soil cores and the batch-slurry experiments; these bench-scale data enabled determination of a linear desorption partition coefficient (K_d) for the soils. An estimation of the air-water interfacial partition coefficient (K_i) was also required, which was calculated using a published empirical correlation that related PFAS properties (i.e., chain length and molar volume) and porewater properties (i.e., ionic strength) to K_i. Details of these data requirement and of the mass balance model used to predict PFAS porewater concentrations are provided in Section 6.

3.3.2 Success Criteria

While our initial intent for success criteria for this performance objective was based on deriving statistically significant correlation between vadose soil properties and porewater PFAS levels (specifically, $R^2 \geq 0.8$, and P value <0.05), it was discovered that determination of PFAS *desorption* behavior using readily obtainable soil parameters (e.g., TOC) was not possible. Thus, bench-scale testing, including batch soil-slurry desorption testing, was needed to determine appropriate desorption K_d values. Thus, results of this performance objective were ultimately based on the accuracy of the model predictions relative to the measured PFAS in situ porewater concentrations measured using the field-deployed lysimeters.

3.3.3 Results

Predictions of in situ PFAS porewater concentrations were possible for 4 out of the 5 primary sites evaluated in this study (inability to collect bench-scale porewater samples and ultimately determination of the desorption Kd inhibited this evaluation for one of the sites). For 3 of these sites, PFAS predicted values (± 95% confidence value of the predicted value) were within the 95% confidence interval of the measured value [with the exception of 8:2 FTS at one site]. For the fourth site (which had backfilled materials), field values could not be accurately predicted. Details of this evaluation are presented in Section 6.

3.4 PERFORMANCE OBJECTIVE #4

This objective is focused on evaluating the ease of lysimeter installation and application during field sampling.

3.4.1 Data Requirements

As the soil porewater collection is completed for each site, the data on the level of effort needed to install and sample using the lysimeter was collected via discussions with site personnel and review of field logbooks. These data include reporting of problems encountered in the field and the ability of field crews to resolve problems quickly. Issues related to both lysimeter installation and porewater collection were evaluated

3.4.2 Success Criteria

Success for this performance objective depends on documenting the issues related to the ease of use of the lysimeter, as well as technical review on the appropriateness of the data collected. Specifically, the extent of training needed to properly instruct field personnel on lysimeter installation and sampling was considered, as well as the extent to which the field crews were able to successfully implement installation and sampling. The extent of troubleshooting (including the extent to which any troubleshooting could be readily resolved by field personnel versus that which required input from senior technical staff) also was evaluated.

3.4.3 Results

The use of multiple test site locations for this project allowed for evaluation of multiple field crews with respect to the ease of lysimeter installation and sampling. Thus, use of multiple field crews and sites mitigated bias in this evaluation that could have been due to a particular field crew or site conditions. In general, field staff were readily trained on lysimeter installation and sampling, and extensive troubleshooting from senior technical staff was not needed to ensure proper sample collection. It is noted that careful planning and interaction with the field crew was needed to ensure that the lysimeters were installed at the most appropriate depths, especially for soils that exhibited notable changes in grain size with depth and/or sites with relative dry soils; such sites also required extended sample collection times, although it is recognized that more standard lysimeter sampling schemes would look to coordinate sampling efforts with rainfall events. Finally, in some cases, extra care had to be taken to ensure the caps/sample tubing on the lysimeters were secure so that the applied vacuums were maintained. Failure to maintain vacuum often resulted in negligible or less than desired porewater collection. Despite these considerations, overall field crews were able to install and sample lysimeters with relative ease.

4.0 FACILITY / SITE DESCRIPTION

Five primary DoD sites were evaluated in this study (denoted as Sites A through E). All studied sites were exposed to AFFF, and most of the sites were interrogated as part of this study at least a decade after the last known AFFF release. A summary of the testing for each site is provided in **Table 4-1**. Soil properties, lysimeter installation depths, porewater ionic strength, and average rainfall information are summarized for each test location in **Table 4-2**. Grain size distribution for each soil is provided in **Figures 4-1** through **4-5**.

Table 4-1. Summary of PFAS Testing and Evaluations Performed for Each Site.

	Site				
Test or Evaluation	**A**	**B**	**C**	**D**	**E**
Field PFAS Soil Concentrations (Figure 6-1 and Appendix C and D)	✓	✓	✓	✓	✓
Field PFAS Porewater Concentrations (Figure 6-2 and Appendix E)[1]	✓	✓	✓	✓	✓
Laboratory PFAS Porewater Concentrations (Figure 6-2)	✓	✓	✓	✓[2]	-[3]
Batch Desorption Testing (Appendix J)	✓	✓	✓	-	-
Detailed Mass Balance Evaluation[4]	✓	✓	✓	-	-

[1] Field porewater collection volumes and dilution factors are presented in Table 5-1 and Appendix F, respectively

[2] No additional wetting of the Soil D core was needed, as was the case for Sites A, B, and C, thus the laboratory-based porewater from Site D was extracted from an intact core at field moisture

[3] Porewater could not be extracted from the bench-scale micro-sampling lysimeter

[4] Presented in the Appendix G, along with PFAS interfacial sorption coefficients

Table 4-2. Site Information for Soils.

Lysimeters were in all cases placed above the current water table elevation. TOC = total organic carbon via combustion analysis. CEC = cation exchange capacity. NA =not analyzed

Parameter	Site A	Site B	Site C	Site D	Site E
Avg. Grain Size (mm)	0.30	0.20	0.28	0.11	0.039
Approx. % Clay	0	0	7	2	15
Moisture (%)[1]	3.5	4.3	4.8	13	13
TOC (mg/g)	0.85	4.2	51	8.3	32
pH	7.5	7.8	5.8	8.1	9.2
CEC (mEq/100g)	7.5	9.2	32	8.0	52
AEC (µmol/kg)	<0.4	<0.4	NA	NA	<0.4
Rainfall[2] (cm)	37	37	130	131	82
Porewater Ionic Strength[3] (mM)	16	13	45	8.0	9.9
Depth to water (m)	~20	~3.0	0.91	1.4	~6.1
Lysimeter Depth[4] (m)	1.5	1.5	0.74	1.0	0.76
Moisture content after wetting (%) [5]	7	8	15	-	-

[1] based on collected soil during lysimeter installation at the depth of the lysimeter

[2] based on data from weather-and-climate.com. Average annual rainfall is listed.

[3] corrected to account for any bromide present in the porewater. Ionic strength estimated based on measured electrical conductivity

[4] lysimeters have a 3.8 cm long porous ceramic cup for porewater sampling

[5] for lysimeter micro-sampling on the collected soil core for laboratory porewater sampling. This wetting was not performed for soils D and E. For soil E, the moisture content was already elevated, but the small grain size prohibited collection of any water. For soil D, micro-sampling lysimeters were employed using the intact soil core.

Site A: Site A is located in the western US, and is a DoD site used as a fire training area. The climate for this region is defined as semi-arid (25 to 50 cm annual precipitation). The vadose zone is described as a silty sand, and the depth to water is approximately 20 m. The last reported release of AFFF at this site was in 2017. Grain size distribution for soil at Site A is shown in **Figure 4-1**.

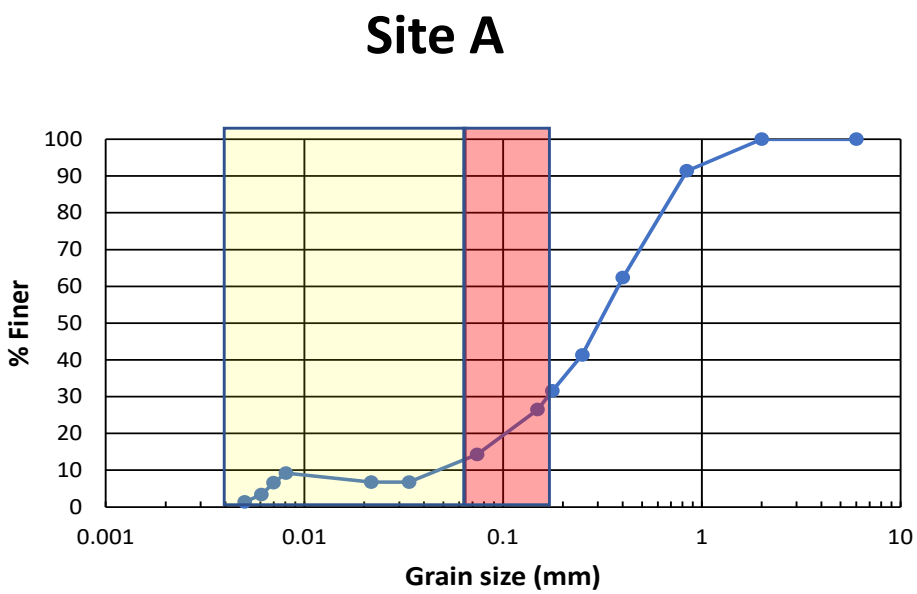

Figure 4-1. Grain Size Distribution for Soils from Site A.

The light yellow shading shows the wetted region in the field (assuming fine pores/grains are preferentially wetted). The pink shading shows the wetted region after wetting for the soil core porewater sampling.

Site B: Site B is located in the western US, and is a DoD site used as a flashover fire training area. The climate for this region is defined as semi-arid. The vadose zone is described as a gravelly sand with trace fines, and the depth to water is approximately 3 m. The last reported release of AFFF at this site was in the early 1990s. Grain size distribution for soil at Site B is shown in **Figure 4-2**.

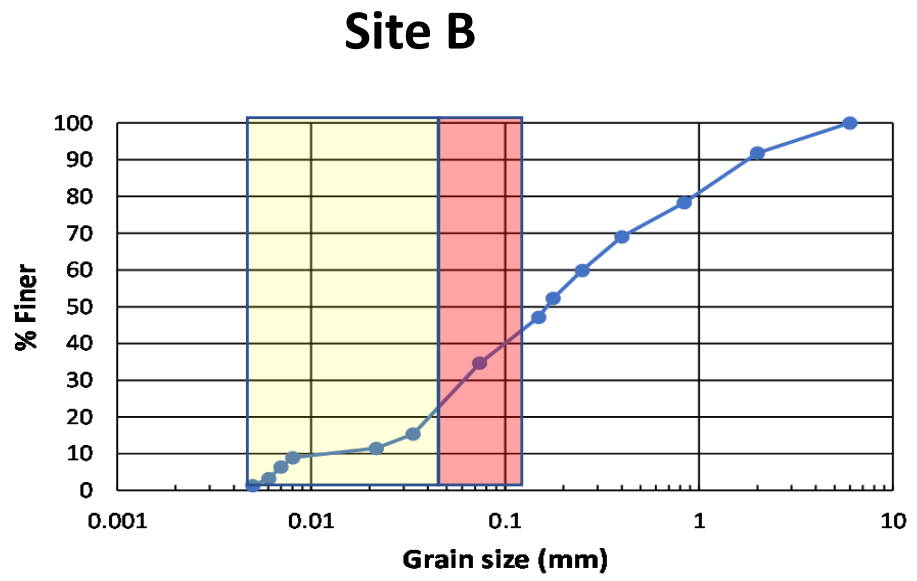

Figure 4-2. Grain Size Distribution for Soils from Site B.

The light yellow shading shows the wetted region in the field (assuming fine pores/grains are preferentially wetted). The pink shading shows the wetted region after wetting for the soil core porewater sampling.

Site C: Site C is located in the eastern US, and is a DoD site where fire training activities occurred from the 1960s to the 1980s. Reported AFFF handling in the vicinity of this area has occurred as recently as 2018. The vadose zone consists of sands and silts, with some clay, and the depth to water is approximately 0.9 m. Grain size distribution for soil at Site C is shown in **Figure 4-3**.

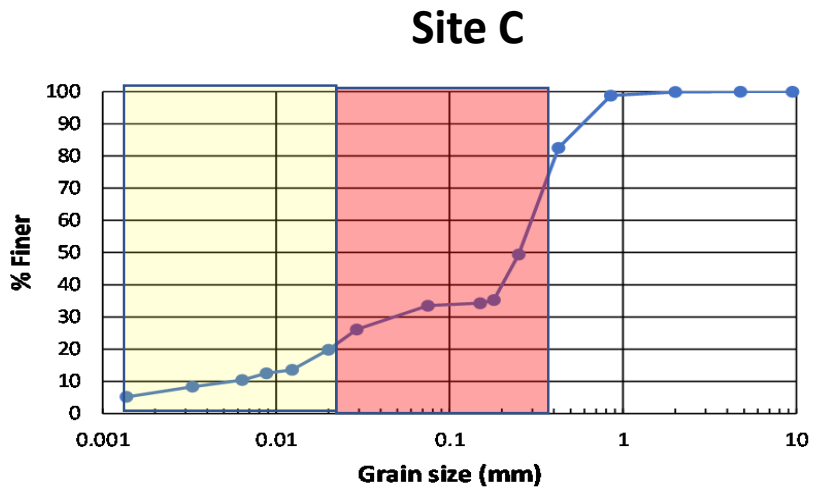

Figure 4-3. Grain Size Distribution for Soils from Site C.

The light yellow shading shows the wetted region in the field (assuming fine pores/grains are preferentially wetted). The pink shading shows the wetted region after wetting for the soil core porewater sampling.

Site D: Site D is located in the southeastern US, and is a DoD site used as a fire training area. The vadose zone consists of sandy soil, and the depth to water is approximately 1.4 m. The last reported release of AFFF at this site was in 1991. Soils within the AFFF source area were excavated in 1994 (down to approximately 1 to 1.5 m) and thermally treated to address petroleum hydrocarbon contamination. These treated soils were then backfilled within the excavated area. Grain size distribution for soil at Site D is shown in **Figure 4-4**.

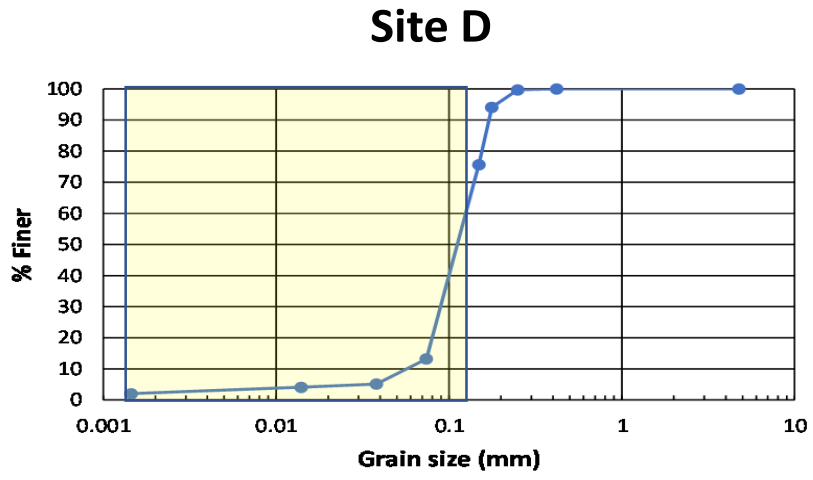

Figure 4-4. Grain Size Distribution for Soils from Site D.

The light yellow shading shows the wetted region in the field (assuming fine pores/grains are preferentially wetted).

Site E: Site E is located in the southwestern US, and is a DoD site. Site E is located adjacent to a fire station. The vadose zone is described as silty sand to a sandy silt, and the depth to water is approximately 6 m. An approximately 5 gallon accidental release of AFFF concentrate was reported at this site in 2008. Grain size distribution for soil at Site E is shown in **Figure 4-5**.

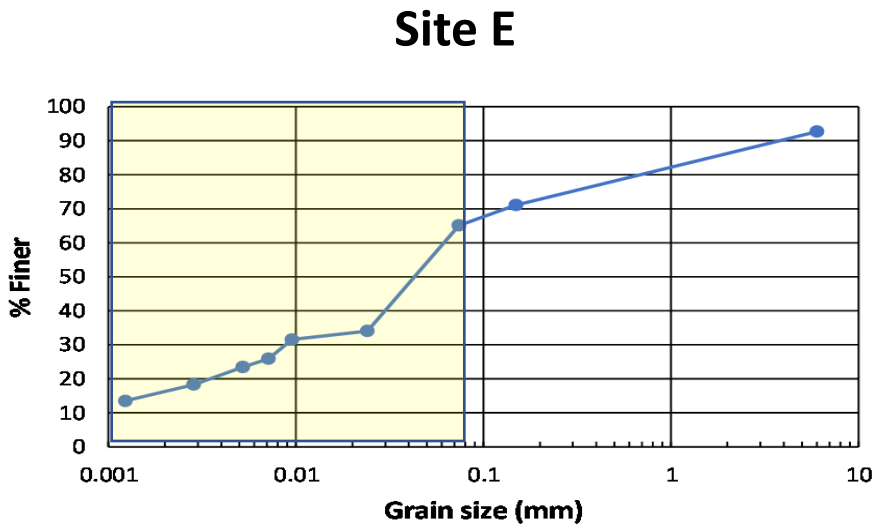

Figure 4-5. Grain Size Distribution for Soils from Site E.

The light yellow shading shows the wetted region in the field (assuming fine pores/grains are preferentially wetted).

In addition to Sites A through E, two additional DoD sites (Sites F and G) were also used to supplement this demonstration. Sites F and G were also historically exposed to AFFF. Soil and porewater properties, lysimeter installation depths, and average rainfall information are summarized for these two additional sites in **Table 4-3**.

Site F is a former underground storage tank (UST) DoD site located in the eastern coastal US. The site was used for the storage and transfer of AFFF. Site lithology within the vadose zone (0 to approximately 1.5 m bgs) consists primarily of a sandy lean clay, with a clear transition to clay near the water table.

Site G is Joint Base Charleston Air (JBCA) located in Charleston, South Carolina. Soil and porewater at this site are also being investigated under Air Force Civil Engineer Center (AFCEC) Broad Agency (BAA) Project 2108, and data collected under this AFCEC project were used to supplement this ESTCP project (AFCEC project also led by PI Schaefer). As part of this ESTCP project, additional rounds of lysimeter sampling at select lysimeters was performed to evaluate variability in PFAS porewater concentrations over time, and with changes in soil moisture content. Site G is a former fire training area that operated from 1971 to 1983. Site lithology within the vadose zone at Site G consists primarily of sand with interbedded clays.

Table 4-3. Site Information for Supplemental Site Soils.

Lysimeters were in all cases placed above the current water table elevation. TOC = total organic carbon via combustion analysis. CEC = cation exchange capacity.

Parameter	Site F	Site G
Avg. Grain Size (mm)	0.2	0.15
Approx. % Clay	14	10
Moisture (%)	9.6	NA[3]
TOC (mg/g)	13	6.2
pH	6.7	6.8 to 8.2
CEC (mEq/100g)	19	NM
Rainfall[1] (cm)	130	130
Porewater Ionic Strength (mM)	NM	12
Depth to water (m)	~1.5	~1.8
Lysimeter Depth[2] (m)	0.6	1.4

[1] based on data from weather-and-climate.com. Average annual rainfall is listed.

[2] lysimeters have a 3.8 cm long porous ceramic cup for porewater sampling

[3] soil moisture varied over time, as shown in Figure 6-5.

NM – not measured

5.0 TEST DESIGN

5.1 FIELD SOIL AND POREWATER COLLECTION

Sites A through E

A 5.4-cm soil core was collected at each site using a gas-powered core sampling kit (AMS, Inc., American Falls, ID). PFAS in the collected soil core were analyzed every 0.1 to 0.2 m for a total depth (depending on the site) of up to 2.4 m. Soil samples were also collected for total organic carbon (TOC), cation exchange capacity, and moisture content. Three lysimeters were installed within a 0.8 m radius of the soil core for Sites A, B, C, and D; the borehole used for soil sampling was used for one of the installed lysimeters. For Site E, three lysimeters were initially installed to a depth of 1.7 m below ground surface, but failed to produce any water. Two lysimeters were then re-installed adjacent to the initial locations to depths of 0.76 m below ground surface.

Site F

Three lysimeters were installed at Site F using the methods described for Sites A through E. The lysimeters were installed at a depth of approximately 0.7 m, which is slightly above a clayey zone located at approximately 0.8 m below ground surface. However, porewater recovery was minimal (less than approximately 50 mL) across 4 attempted rounds of sampling, and the bromide tracer in the collected porewater showed minimal (<10%) dissipation, indicating that very little actual soil porewater was collected. Two additional lysimeters were installed at a later date. However, only one of the lysimeters produced water that was sufficient for sample collection. Thus, given the lack of in situ porewater data and absence of replicate lysimeters for this site, Site F was omitted from further evaluation.

Site G

For Site G, the project utilized a network of three lysimeters (L24, L27, and L29) installed as part of AFCEC Project 2108 to depths of 1.4 m below ground surface The Site G lysimeters were located within the former fire training area approximately 12 m from each other.

Lysimeter Installation and Sampling

Lysimeter installation and sampling were performed as described previously (Schaefer et al., 2022). Porous cup suction lysimeters (4.8 cm diameter), with 3.8 cm long ceramic heads and a 2 bar bubbling pressure, were purchased from Soil Moisture Equipment Corp. (Goleta, CA). A silica flour (200 mesh) slurry was poured into the lysimeter boreholes so that the slurry reached several centimeters above the porous cup; addition of this slurry was intended to maintain a saturated connection between the lysimeter and the native soil. A sand was layered above the silica flour, with bentonite chips used to fill the remaining annular space. A bromide tracer (500 mg/L bromide as NaBr) was included with the silica flour slurry to account for any potential dilution of the porewater by the slurry water.

A hand pump was used to apply vacuum (typically 65 centibar) and extract porewater, where several hours to overnight extraction was typically needed to collect water. When possible, the initial sample of porewater collected for each lysimeter (approximately 20 mL) was used for purging and discarded; up to 3 subsequent rounds of porewater collected for PFAS analysis were

performed within a 2 to 6 day period for Sites A, B, D and E. The first round of samples from one of the 3 lysimeters at Site C was excluded from the dataset because PFAS porewater concentrations were approximately two standard deviations less than that observed in the other seven porewater samples collected. **Table 5-1** summarizes the porewater samples collected from the lysimeters installed at Sites A though E. **Table 5-2** summarizes the sampling performed at Site G, which occurred over a 13-month timeframe in which 4 rounds of porewater sampling were conducted.

Table 5-1. Approximate Purge and Sample Volumes (in mL) from Each of the Three Lysimeters (L1 through L3) at Sites A through E.

Grayed boxes represent samples that were NOT used for subsequent PFAS evaluation. Grayed boxes in Round 1 were typically due to low initial purge volumes. Boxes without values indicate that no porewater was available for collection.

Site A	**L1**	**L2**	**L3**
Initial purge	5	20	20
Round 1	4	23	23
Round 2	23	48	20
Round 3	-	-	42
Site B			
Initial purge	-	-	-
Round 1	14	-	43
Round 2	-	-	-
Round 3	14	-	26
Site C			
Initial purge	10	13	20
Round 1	150	10	75
Round 2	100	70	37
Round 3	45	17	18
Site D			
Initial purge	18	8	160
Round 1	380	410	31
Round 2	250	110	-
Round 3	575	525	-
Site E			
Initial purge	-	-	-
Round 1	-	70	70
Round 2	-	60	60
Round 3	-	-	5

Table 5-2. Lysimeter Porewater Sampling at Site G.

The July 2023 and October 2023 sampling events were performed as part of AFCEC BAA 2108.

Lysimeter	Vacuum Application Date	Collection Date	Vacuum Applied (cb)	Sample Vacuum (cb)	Sample Volume (mL)
L24	July 12, 2023	July 13, 2023	64	48	450
L27	July 13, 2023	July 14, 2023	64	38	900
L29	July 12, 2023	July 13, 2023	60	30	1225
L24	October 16, 2023	October 17, 2023	62	50	489
L27	October 16, 2023	October 17, 2023	62	40	1339
L29	October 16, 2023	October 17, 2023	61	25	1014
L24	December 7, 2023	December 7, 2023	58	0	15*
L27	December 7, 2023	December 7, 2023	54	54	15*
L29	December 7, 2023	December 7, 2023	54	0	15*
L24	July 2, 2024	July 2, 2024	70	70	15
L27	July 2, 2024	July 2, 2024	70	70	15
L29	July 2, 2024	July 2, 2024	70	0	4

Notes:
cb – centibars
mL – milliliters
* – volume estimated

5.2 BENCH-SCALE POREWATER SAMPLES (SITES A THORUGH E)

An additional intact soil core, collected during installation of the lysimeters, was collected for bench-scale porewater testing. The purpose of the bench-scale porewater testing was to serve as a comparison to the field-measured PFAS porewater concentrations, where the bench-scale system represented a static (or, equilibrated) sample compared to the dynamic (and potentially non-equilibrated) field sample. Bench-scale porewater samples were collected using micro-sampling lysimeters that have a 0.95 cm outside diameter, were 18 cm long, and have a porous ceramic head 3 cm in length (Soil Moisture Equipment Corp., Goleta, CA). Vacuum (approximately 55 centibar) was applied to collected soils using 10 mL disposable syringes, where the vacuum was typically applied overnight. Methanol used to rinse the micro-sampling lysimeters and syringes was collected and analyzed with the collected porewater to limit any PFAS sorptive losses to the porewater extraction system; prior testing showed that sorptive losses to the field lysimeters were negligible for PFOS (Schaefer et al. 2022). Ideally, porewater was extracted from an intact core at the same depth where the field lysimeter was placed, with 2 additional duplicates extracted within 15 cm of this depth (3 samples total). However, due to relatively dry soil conditions, only porewater from the Site D soil core could be collected in this manner. For the other sites, soil was homogenized in the 20-30 cm depth interval that overlapped the depth of the field lysimeter deployment; soil in this interval was visually homogeneous. This soil was then wetted using a 5 mM CaCl2 solution, packed in polypropylene centrifuge tubes (approximately 80 g samples prepared in triplicate), and equilibrated for a minimum of three days before extracting the porewater with the micro-sampling lysimeters.

Figure 5-1 shows the bench-scale porewater sampling set-up. **Table 4-2** shows the soil moisture contents before and after wetting for Sites A through E, where appropriate. Even after wetting, porewater could not be extracted in the laboratory from the homogenized soil for Site E, ***thus no bench-scale porewater samples were collected from Site E soil.***

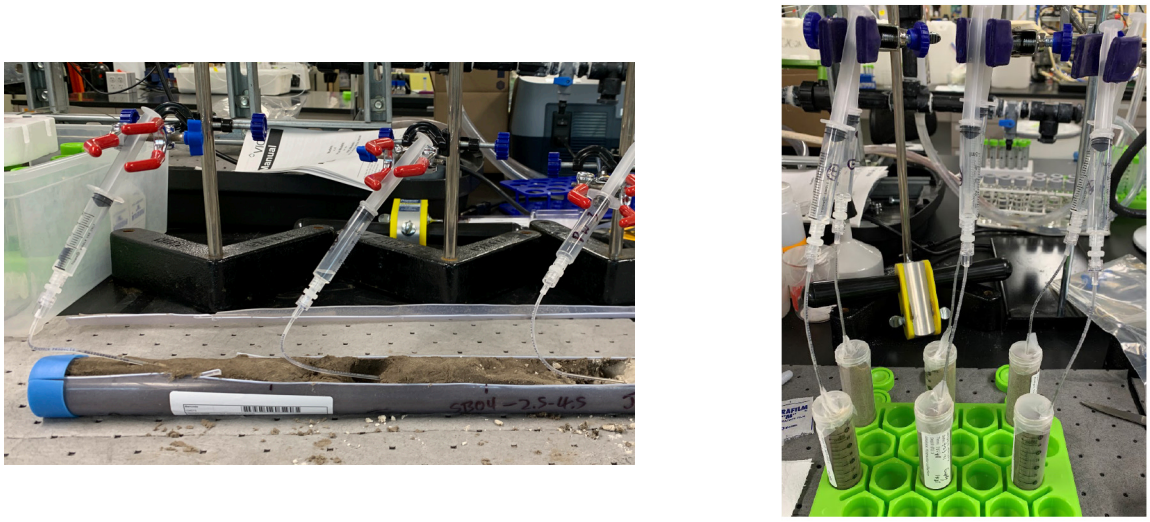

Figure 5-1. Bench-scale Porewater Sampling Using the Micro-sampling Lysimeters.

Sampling in an intact core is shown, and sampling from wetted and re-packed soil is shown.

5.3 BATCH SLURRY DESORPTION TESTING (SITE A THROUGH E)

Using soil collected over the depth interval of the field-lysimeter porewater sampling, batch slurry desorption tests were performed for Sites A, B, and C under saturated conditions to further assess PFAS desorption equilibrium and interrogate the impacts of air-water interfacial area collapse on PFAS release. Batch desorption testing was performed using previously developed methodology (Schaefer et al. 2021). The soil desorption reactors were prepared by mixing 30 g of soil with 100 mL of 5 mM $CaCl_2$ solution. Duplicate reactors were prepared for each soil. Aliquots of aqueous samples from each reactor were collected over a 14- to 56-day period for target PFAS analysis (quantifiable analytes) to ensure equilibrium was attained.

5.4 ANALYTICAL

Soil TOC was analyzed via combustion analysis by Katahdin Analytical Services, LLC (Scarborough, Maine). Cation exchange capacity was analyzed by assessing the exchangeable sodium cations by ALS Environmental (Houston, Texas). PFAS soil concentrations were analyzed via USEPA Draft Method 1633 by SGS AXYS Analytical Services, Ltd (British Columbia, Canada). PFAS porewater concentrations were analyzed by liquid chromatography high resolution mass spectrometry (LC-HRMS) for both quantifiable (i.e., target) and semi-quantifiable (i.e., HRMS suspect) analytes at the Colorado School of Mines using previously published methodologies (Hao et al., 2022; Nickerson et al., 2020; Murray et al., 2019). Additional details of the PFAS analyses and reporting limits are provided in **Appendix B** (PFAS Analytical).

The acronyms and molecular formulas for the quantifiable and semi-quantifiable PFAS identified in this study are also provided in **Appendix B**.

5.5 ESTIMATION OF AIR-WATER INTERFACIAL AREA

To quantify the changes in the air-water interfacial area per unit volume ($a_{aw,}$) upon wetting, the grain size distribution for each site soil was considered. The grain size distributions for soils from the 5 sites are shown in **Figures 4-1 through 4-5**. The comparatively small grain size fractions associated with Sites C and E are readily apparent, and are consistent with their clay contents shown in **Table 4-2**. Assuming small pores associated with small soil particles are wetted in the soil, the light (yellow) shading in **Figures 4-1 through 4-5** prepresent (approximately) the pore space wetted under field conditions, while the dark (red) shading represents additional wetting in the homogenized soil (from the collected soil core) used for the lysimeter micro-sampling.

For the three sites where the soils were wetted prior to the laboratory porewater sampling (Sites A, B, and C) using the collected soil, the loss of air-water interfacial area upon wetting can be estimated. The air-water interfacial area per volume of porous media is estimated based on the correlation developed by Brusseau (2023):

$$a_{aw} = [-2.85S + 3.6]\,[3.9d^{-1.2}(1 - S)] \qquad \text{Eq. 3}$$

where d is the average particle diameter, S is the water saturation (volume water/volume pore space), and a_{aw} is air-water interfacial area defined in units of cm^{-1}.

Using the grain size distributions shown in **Figures 4-1 through 4-5**, and a soil bulk density of 1.6 g cm^{-3} that is saturated at approximately 19% moisture content, the parameters in Eq. 3 can be estimated under both the comparatively dry field conditions and for the wetted conditions associated with the laboratory-collected (soil core) porewater sampling.

6.0 PERFORMANCE ASSESSMENT

6.1 SITES A THROUGH E

6.1.1 PFAS Soil Concentrations

Quantifiable PFAS soil concentrations for each site are provided in **Appendix C**. It is noted that these results represent the sum of PFAS mass adsorbed to the soil, adsorbed at the air-water interface, and dissolved in the aqueous phase. Conventional environmental sampling refers to such measurements as soil concentrations, so this convention is retained herein. A more detailed mass balance assessment is provided in Section 6.1.3.

In all cases, PFOS exhibited the most elevated PFAS concentration measured in the collected soil samples. The perfluorinated sulfonate relative concentration versus depth profiles for Sites A and B show clear chromatographic separation (**Figure 6-1**). The least hydrophobic compound (PFBS) has the deepest concentration maximum, while the PFOS concentration maximum is near the soil surface. In contrast, for Sites C and E, the relative concentration profiles are similar for each perfluorinated sulfonate, and no chromatographic separation was observed (Figure 6-1). Site D is omitted from Figure 6-1 due to the large number of perfluorinated sulfonate results that were below the analytical detection limit. Similar results with respect to the vertical concentration profiles were observed for the perfluorinated carboxylates (**Appendix C**). The reason for the differences between Sites A and B, and Sites C and E, are unclear, as they could be due to the nature of AFFF releases, rainfall, and/or other soil properties.

Semi-quantified PFAS in soil were analyzed at a single depth, corresponding to the approximate field lysimeter depth, for each site. Results are summarized in **Appendix D**. Estimated PFAS concentrations via semi-quantified analysis for suspect precursors should be interpreted with caution, as uncertainties remain as to the concentrations of compounds for which analytical standards are currently unavailable (Nickerson et al., 2020b; Pickard et al., 2022). For the depths examined herein, quantified PFAS (predominantly PFOS) were the primary PFAS identified in the unsaturated soil samples. These findings are generally consistent with those obtained by Adamson et al. (2020), who showed that precursors only accounted for approximately 15% of the PFAS soil mass within the permeable sandy regions of the shallow saturated zone.

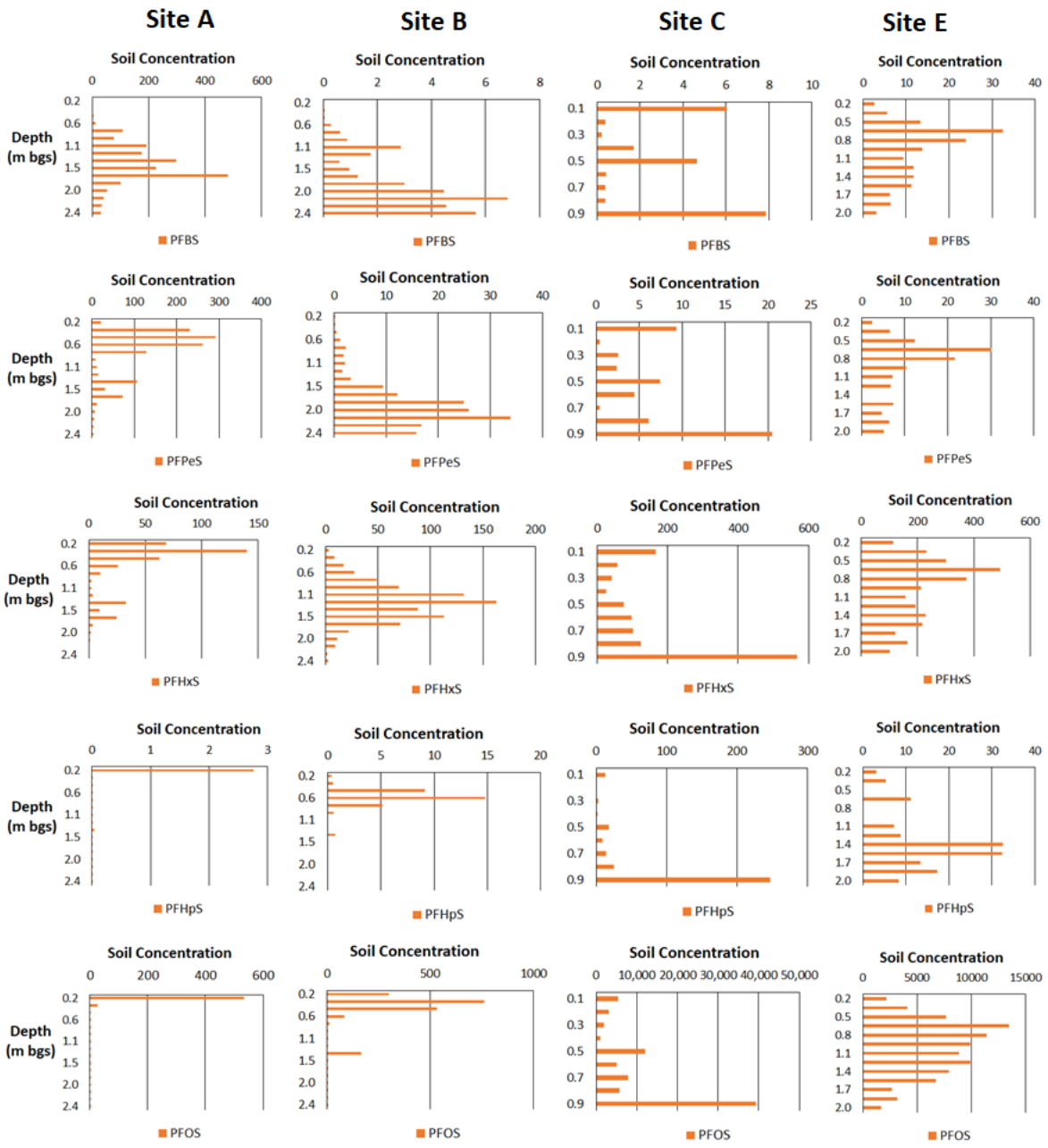

Figure 6-1. Perfluorinated Sulfonate Soil Concentrations (µg/kg) Measured as a Function of Depth in the Unsaturated Zone for Sites A. B, C, and E.

Non-detect results are plotted as 10% of the reporting limit. PFBS =perfluorobutanesulfonate, PFPeS=perfluoropentanesulfonate, PFHxS = perfluorohexanesulfonate, PFHpS= perfluoroheptanesulfonate, and PFOS = perfluorooctanesulfonate.

6.1.2 PFAS Porewater Composition Using Field Lysimeters

PFAS porewater results for each site are summarized in Appendix E. A clear increasing trend in PFAS concentration with cumulative lysimeter sample volume was observed for some PFAS (i.e., increasing PFAS concentrations with increasing round number for a given lysimeter).

This increasing trend was attributed to dilution of the porewater with slurry water added during lysimeter installation. The measured bromide concentration in the collected water from the lysimeters was used to calculate an appropriate dilution factor. Details of the dilution factor corrections are provided in the **Appendix F**. Dilution factors greater than approximately two were only relevant for Sites A and B (**Appendix E**). The limited number of porewater samples (n=3) for Site B was due the difficulty in extracting porewater at this site; one lysimeter at Site B did not yield any porewater. Target (quantified) PFAS concentrations for each site, corrected for the appropriate dilution factor, are summarized in **Figure 6-2**.

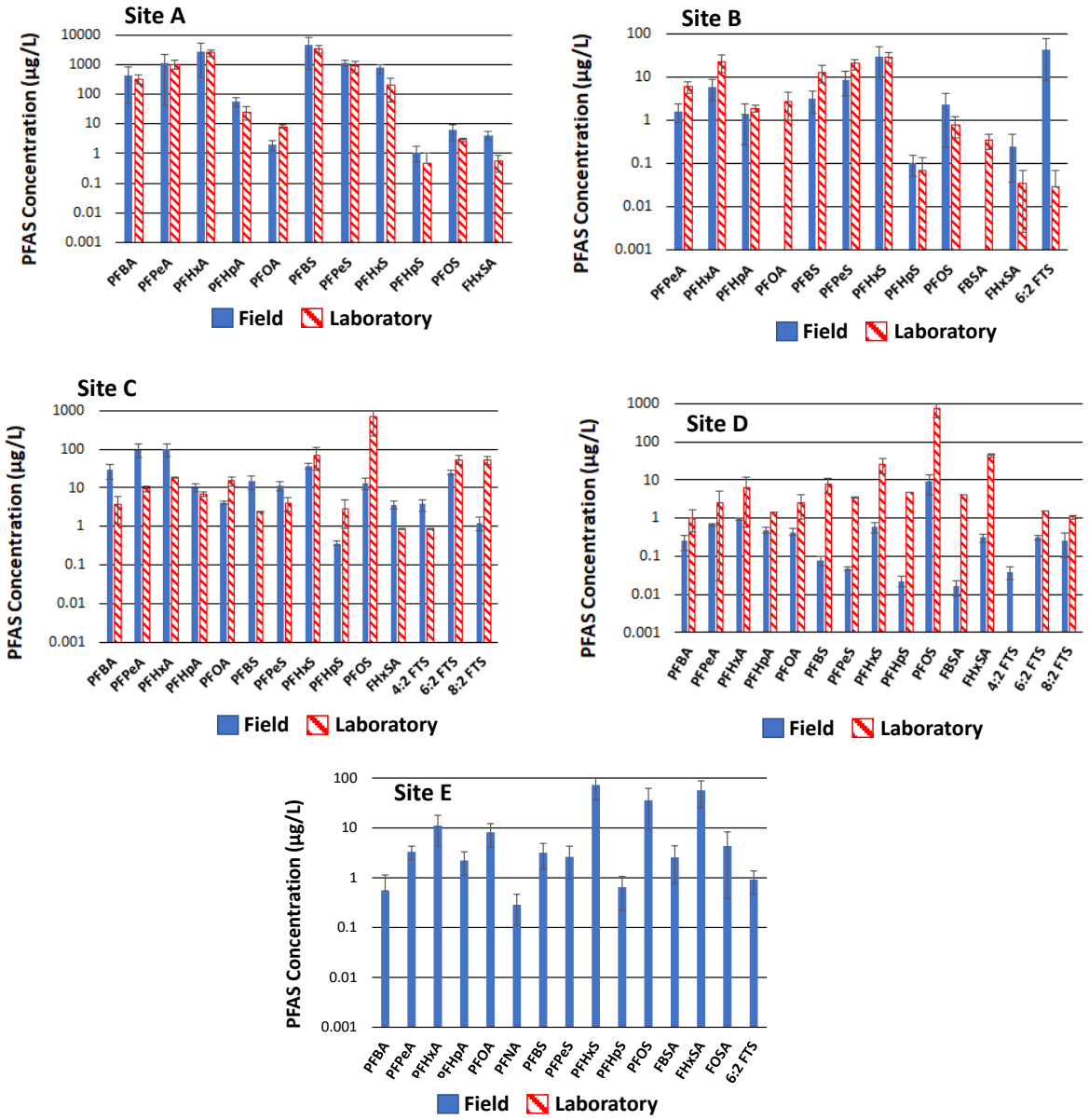

Figure 6-2. PFAS Porewater Concentrations for Quantifiable Analytes from Both the Field-Deployed Lysimeters and in the Laboratory Using Porewater from the Collected Soil Cores.

Error bars represent 95% confidence intervals. For Site E, laboratory-based porewater samples could not be collected

Sites B and E show that, despite more than a decade since the last known AFFF release, substantial (> 50 µg/L) levels of PFAS are migrating as either quantified (target) or suspect (semi-quantified) precursors in the porewater; again, semi-quantified analysis of suspect precursors should be interpreted with caution. Target precursors accounted for up to 70% of the quantifiable PFAS fluorine mass for Site B. This observed persistence of precursors in the unsaturated zone porewater is consistent with previous studies that showed the persistence of precursors in shallow source area groundwater (Adamson et al. 2020; Ruyle et al. 2023). Overall, these results highlight the importance of improved understanding of precursor transformation in source areas to better evaluate the PFAS source function and mass discharge to groundwater. It is currently unclear as to why identified precursors were dominant in porewater for Sites B and E, but not for the other investigated sites; it is possible that the apparent lack of semi-quantified precursors at the other sites was due to lack of detection using the current analytical technique.

At Site A, porewater PFAAs were largely dominated by shorter-chained (≤6 perfluorinated carbons) compounds (**Figure 6-2** and **Appendix E**). These porewater results are consistent with the corresponding soil data (Appendices C and D) collected at the lysimeter installation depth of 1.5 m below ground surface. For Site B, 4:2 FTS accounted for the majority of the identified PFAS mass in the porewater, although 4:2 FTS was only observed in one of the two water-producing lysimeters and was not observed in any soil samples. Besides this detection of 4:2 FTS, similar to Site A, porewater at Site B also was dominated by shorter-chained PFAS.

PFOS and/or PFHxS were the predominant PFAAs for Sites D and E. These results for Sites D and E are consistent with the soil data, and may reflect the greater migration of PFOS and PFHxS at these sites due to increased rainfall and shallower lysimeter placement compared to Sites A and B. In contrast to Sites D and E, the porewater data for Site C was not indicative of the soil concentrations, as PFPeA and PFHxA were the predominant porewater PFAAs despite the fact that PFOS was by far the predominant PFAA in the soil. This apparent discrepancy is likely due to the elevated affinity of PFOS to the soil compared to PFPeA and PFHxA, and/or the relative affinity of PFOS to the air-water interface (as discussed in Section 6.1.3). It is also possible the predominance of PFPeA and PFHxA in Site C porewater was due to biotransformation of precursors present in Site C soil.

Sulfonamides (FBSA, FHxSA, and/or PFOSA) were detected in porewater at all sites, as were (with the exception of Site A) 4:2 FTS and/or 6:2 FTS. These PFAS are able to biotically transform to PFAAs (Avendaño and Liu, 2015; Zhang et al., 2016; Ruyle et al., 2023b). The presence of the sulfonamides in porewater, since they are not typically present at high levels in AFFF formulations (Backe et al., 2013), suggests transformation of other AFFF precursors to these sulfonamides has occurred or is occurring. Sites C and E, which both had a substantial fraction of the PFAS-related fluorine in porewater associated with FBSA, FHxSA, and/or PFOSA, showed elevated levels (compared to the other sites) of MeFOSA, MeFOSAA, and AmPr-FHxSA in the soil; Site C also had Ampr-FPeSA and AmPr-FOSA in the soil. The AmPr-sulfonamides have been shown to biotically transform to perfluorinated sulfonamides and perfluorinated sulfonates (Cook et al., 2022), and thus may serve as the source of these dissolved perfluorinated sulfonamides observed in the porewater.

The semi-quantified suspect analytes identified in Site E porewater (**Appendix E**) were dominated by the cationic sulfonamide-based compound TAmPr-N-MeFBSA, although other zwitterionic sulfonamide-based suspect precursors (with 6 perfluorinated carbons) also were present in the porewater.

For Site C, a large number of suspect analytes were identified in the porewater (**Appendix E**). The majority of the suspect precursors at Site C were zwitterionic compounds with 6 or fewer perfluorinated compounds that were identified in ESI+ mode. The two most abundant suspect analytes for Site C, SPrAmPr-FHxSA and SPrAmPr-FHxSAA, are sulfonamide-based compounds. Barzen-Hanson et al. (2017) reported that TAmPr-N-MeFBSA and SPrAmPr-FHxSA were present in 3M AFFF formulations, so the findings herein indicate persistence of these released precursors at this AFFF-impacted site.

Many of the precursors in the porewater samples measured for the study described herein have been noted in previous investigations, but hitherto not directly measured via in situ porewater sampling in the unsaturated zone. The presence of FHxSA and 6:2 FTS were sporadically (likely due to detection limit issues) identified in a previous field porewater study at an AFFF-impacted site (Schaefer et al., 2022). Nickerson et al. (2020), Ruyle et al (2023), and the multi-site study of Adamson et al. (2022) also identified these precursors in shallow groundwater at AFFF-impacted sites. With respect to the semi-quantified precursors observed herein, Adamson et al. (2022) and Ruyle et al. (2023) identified several sulfonamide-based precursors in shallow groundwater.

6.1.3 Bench-Scale Porewater Samples

A comparison of the quantified PFAS porewater concentrations measured in the field lysimeters to those measured in the laboratory from the collected soil cores for each site, with the exception of Site E (field data only), is provided in **Figure 6-2**. As noted in **Table 4-1**, the small soil grain size for Site E precluded extraction of porewater in the laboratory from the collected soil core at the bench-scale. For Sites A and B, PFAS concentrations measured in the field-collected porewater and in laboratory-collected porewater are typically within a factor of 2 to 5. Given the potential pore-scale variability among field-collected porewater and collected soil samples, such order of magnitude agreement is considered reasonable. Notable exceptions for Sites A and B are PFOA and 6:2 FTS. For PFOA, the limit of quantification (LOQ) for the field-collected porewater sample was 0.57 µg/L, which is just over 4-times less than that PFOA concentration measured in the laboratory-collected porewater. The large (3 orders of magnitude) discrepancy for 6:2 FTS in Site B is not readily explained, but may be due to the variability of 6:2 FTS measured between lysimeters in the field (greater than 50 µg/L in one lysimeter, but below the LOQ of 0.11 µg/L at the other lysimeter; **Appendix E**).

For Site C, comparison between the field-collected porewater and laboratory-collected porewater are similar to that observed for Sites A and B. However, the concentrations for the long-chained compounds PFOS and 8:2 FTS are nearly 100-times greater in the laboratory-collected porewater sample than in the field-collected porewater sample. PFOS and 8:2 FTS are the most surface-active PFAS evaluated in this comparison (Lyu et al., 2018; Brusseau et al., 2019), and the wetting (**Table 4-1**) needed for the laboratory-collected porewater sample likely caused a substantial decrease in air-water interfacial area and subsequent release of PFAS into the aqueous phase (Schaefer et al., 2000; Schaefer et al., 2023).

Based on the data in **Table 4-1** and **Figures 4-1 through 4-5**, **Table 6-1** summarizes the parameters used in Eq. 3 and the calculated a_{aw} values for each site. The change in a_{aw} upon wetting (based on the difference in moisture content before and after wetting listed in **Table 4-1**) for Sites A and B are 250 cm^{-1} and 491 cm^{-1}, respectively. For Site C, the change in a_{aw} upon wetting

is 688 cm^{-1}, which is reflective of the increased fraction of small pores and increased wetting associated with this soil. For Site D, no wetting of the soil was needed (intact cores was used), so there was no change in a_{aw} between the field and laboratory.

Table 6-1. Parameters Used in Eq. 3 to Determine a_{aw}. d is the Average Grain Diameter and S is the Water Saturation.

"Field" values refer to the in situ conditions, while "Lab" values refer to conditions after wetting for the bench-scale. soil core porewater extractions.

Site	d (cm)	S (Field)	S (Lab)	Field a_{aw} (cm^{-1})	Lab a_{aw} (cm^{-1})
A	0.030	0.18	0.37	675	425
B	0.0019	0.28	0.54	921	430
C	0.025	0.21	0.80	774	86
D*	0.067	0.68	0.68	279	279
E**	0.0050	0.67	-	1260	-

* intact core at field moisture was used for bench-scale testing, so "field" and "lab" parameters were identical

** porewater could not be extracted from the bench-scale lysimeter

The impacts of these changes in a_{aw} on the measured PFAS concentrations in the field-collected and laboratory-collected porewater were evaluated via mass balance for the field, laboratory core, and soil slurry systems (PFAS Mass Balance Evaluation is presented in **Appendix G**). A key component of this model was determination of the PFAS interfacial sorption coefficient (K_i). Values for K_i (**Appendix G**) were estimated using quantitative structure-property relationships (QSPRs) developed by Stults et al. (2023), which (in addition to perfluorinated chain length and molar volume) accounts for both the PFAS porewater concentration and porewater ionic strength.

For Sites A and B, both the predicted and measured PFOS porewater concentrations in the wetted laboratory soil cores were approximately equal to those measured in the field shown in **Table 6-2**.

Table 6-2. For Sites A, B, and C, Comparisons of PFAS Porewater Concentrations Measured in the Field Lysimeters (C_1) and in the Wetted Soil Cores (C_2) to the Model-Predicted Wetted Soil Core Values.

± values indicate 95% confidence intervals. K_i values used for the model predicted porewater concentrations are provided in Appendix G. 8:2 FTS and PFHpS comparison for Sites A and B are not provided because these compounds were not detected in the porewater and/or in the soil (at the depth of the lysimeters) at these two sites.

	Measured Porewater Concentration In Situ (C_1) (µg/L)	Measured Porewater Concentration in Wetted Laboratory Cores (C_2) (µg/L)	Predicted Porewater Concentration (C_2) (µg/L)
Site A			
PFOS	6.2 ± 3.4	3.0 ± 0.37	6.6 ± 3.3
Site B			
PFOS	2.2 ± 2.0	0.78 ± 0.38	2.8 ± 2.0
Site C			
PFOS	13 ± 4.1	680 ± 460	164 ± 75
8:2 FTS	1.2 ± 0.46	52 ± 13	16 ± 6.0
PFHpS	0.36 ± 0.051	2.9 ± 2.0	5.9 ± 3.4

Thus, the results observed in **Figure 6-2** for even the most surface active PFAS examined in this study (PFOS) are in agreement with the mass balance model predictions. Interestingly, to satisfy the mass balance (described in **Appendix G**), the PFOS K_i values were 2 to 3 orders of magnitude less than the QSPR predicted values, suggesting that PFOS accumulation at the air-water interfaces at Sites A and B was substantially less than anticipated. These large discrepancies between the experimental and QSPR-predicted K_i values for Sites A and B cannot be explained based on the selection of the Freundlich- isotherm utilized in the QSPR model by Stults et al. (2023), as K_i values employing a Langmuir-based modeling approach are only up to approximately 10-times less than the Freundlich-based QSPR values estimated using the Stults et al. QSPR model (Stults et al., 2022, 2023). These low K_i values are 2 to 3 orders of magnitude below the predicted K_i values and greatly inconsistent with experimental data generated by several different bench-scale studies (as summarized in Stults et al. 2023). One potential explanation for the seemingly low PFOS K_i values is competitive sorption at the air-water interface. Prior studies have shown that competitive PFAS sorption at air-water interfaces can occur (Abraham et al., 2022; Huang et al., 2022; Guo et al. 2023), but such competitive effects typically occur at PFAS concentrations that are orders of magnitude greater than observed at these two sites. However, given the potential for yet unidentified compounds (e.g., hydrocarbon surfactants associated with AFFF) within the porewater matrix along with the relatively (compared to Site C) low PFOS porewater concentrations, competitive effects cannot be ruled out.

Air-water interfacial sorption from non-PFAS organic carbon (including natural organic carbon) also has been shown to inhibit PFOS accumulation at the air-water interface (Schaefer et al., 2022c). To further examine the potential for such inhibition in Site A and B porewaters, the previously described film technique (Schaefer et al., 2019) was used for Sites A and B to measure total organic carbon (TOC) accumulation at the air-water interface. This methodology is described in **Appendix H**.

Results of this testing showed that substantial TOC sorption occurred at the air-water interface, with TOC interfacial adsorption coefficients ($K_{i,TOC}$) of 1.3 cm and 0.38 cm for Sites A and B, respectively. With TOC concentrations of approximately 1 mg/L in the tested waters, the TOC air-water interfacial mass exceeds that of the PFAS interfacial mass by several orders of magnitude. Thus, it is plausible that TOC interfacial accumulation is inhibiting PFAS accumulation at the air-water interface for Sites A and B.

In contrast, for Site C, PFOS and 8:2 FTS concentrations in the laboratory-measured porewater (after wetting) is nearly 100-times greater than the field-measured porewater concentrations (**Table 6-2**). The model-predicted PFOS values were reasonably (approximately a factor of 4) close to the measured values in the laboratory-collected porewater. Similarly, **Table 6-1** shows that the predicted porewater concentrations for 8:2 FTS and PFHpS reasonably described (within a factor of approximately 2 to 3) the increases in porewater concentrations observed upon wetting. As expected, the impact of wetting on the porewater PFAS concentrations increased with increasing PFAS surface activity (PFOS > 8:2 FTS > PFHpS). Of note, and discussed in the PFAS Mass Balance in **Appendix G**, is that the PFOS K_i values at Site C (determined using the QSPR model) were 2 to 3 orders of magnitude greater than those determined via mass balance for Sites A and B; these elevated K_i values for Site C are largely responsible for the observed impacts of wetting (and subsequent loss of air-water interfacial area) on PFOS and 8:2 FTS porewater concentrations shown in **Table 6-2** and **Figure 6-2**. For PFAS that are less surface active than PFHpS (i.e., shorter-chained PFAS), the modeled increases in porewater concentrations upon wetting were comparatively small (less than a factor of 2), which is again generally consistent with the porewater data shown in **Figure 6-2**.

It is noted that the addition of the 5 mM $CaCl_2$ solution to the Site C porewater could have resulted in up to a 50% dilution in the porewater ionic strength, though re-equilibration of this added solution with the soil would likely have mitigated this dilution effect. Cai et al. (2022), who examined soils with organic carbon levels similar to that observed for Site C, showed that such small changes in ionic strength caused small (<50%) increases in the K_d values for PFOS. Similarly, the modest changes in ionic strength in the bench-scale experiments are expected to cause a minimal (~20%) change in adsorption to the air-water interface (Stults et al., 2023). Thus, the differences observed between the field- and bench-scale porewater concentrations in Table 6-2 are likely not due to changes in porewater ionic strength.

Importantly, for Sites A, B, and C, the equilibrium mass balance model was consistent with the porewater data shown in **Figure 6-2**, assuming soil moisture and air-water interfacial area were considered. Thus, invoking a local equilibrium assumption for these sites under the conditions tested within this study is reasonable, and consistent with prior work (Schaefer et al., 2022). These results also confirm the ability, at least for the conditions of this study, of bench-scale soil testing to inform on PFAS porewater and leaching behavior in the field. However, it is noted that transient variability due to high precipitation events or other subsurface heterogeneities (e.g., preferential flow in well-structured soils) could invalidate this local equilibrium assumption.

For Site D, PFAS concentrations measured in the field-collected porewater were generally 5- to 100-times less than those measured in the laboratory-collected porewater; Site D soils were not wetted prior to the laboratory-scale sampling (intact core was used). Thus, unlike Sites A, B, and C, the local equilibrium assumption does not appear to be valid for Site D.

The cause of this discrepancy was initially thought to be due to field conditions during lysimeter sampling, as rainstorms were occurring during sample collection that might have caused rapid infiltration and dilution of PFAS porewater concentrations. Sampling was repeated at this same Site D location several months later in absence of any rainfall (sampling included triplicate lysimeters and 3 rounds of porewater sample collection as before); PFAS porewater concentrations did not show any increasing/decreasing trend with sample round and PFAS porewater concentrations generally were within approximately a factor of two of those previously measured (data not shown). Thus, the orders of magnitude discrepancy between PFAS porewater concentrations measured in the field-collected and the laboratory-collected porewater could not be explained by rainfall and dilution effects.

While a conclusive explanation for the discrepancy between the field-collected and laboratory-collected PFAS porewater concentrations for Site D is not resolved for this study, it is noted that the backfilled material in Site D was quite heterogeneous. Specifically, core logging noted what appeared to be polyethylene plastic sheeting and cm-sized pieces of concrete/rubble intermittently dispersed within the soil cores. In addition, ground penetrating radar (GPR) surveying performed prior to lysimeter installation showed several anomalies throughout (**Appendix I**), indicating discontinuities throughout the interrogated zone and suggesting the presence of voids or other debris. Such discontinuities could result in preferential or non-uniform flow that could bias PFAS concentrations in the lysimeters. The applicability of porous cup suction lysimeters in this type of media warrants further study.

6.1.4 Batch Slurry Desorption

To further evaluate the role of air-water interfaces in soils for Sites A, B, and C, PFAS desorption in the batch slurry systems were evaluated. Desorption kinetics are provided in **Appendix J**. The absence of increasing PFAS concentrations over time suggests that any precursor biotransformation to the compounds shown in **Appendix J** is slow relative to the timescale of the laboratory porewater and batch experiments performed herein. As a final evaluation of the impacts of wetting and air-water interface collapse on PFAS porewater concentrations, PFAS concentrations in the batch experiments were compared to those measured in the field lysimeters for Sites A, B, and C (**Figure 6-3**). For Sites A and B, PFAS concentrations in the batch experiments are much less than those measured in the field-collected porewater. This is due to PFAS desorption and dilution in the comparatively high liquid:solid ratio of the batch slurries compared to the unsaturated field soils. However, for Site C, long-chained PFAS (i.e., PFOS, 8:2 FTS, PFHpS, and PFOA) concentrations in the batch slurry systems are greater than those in the unsaturated field-collected porewater. This is due to the collapse of all air-water interfaces in soil from Site C, the elevated air-water interfacial area under unsaturated field conditions, and elevated values of K_i (**Table 6-2** and as discussed in Section 6.1.3). Results for the shorter-chained and less surface-active PFAS in Site C soil do not show an increase in concentration in the batch slurries relative to unsaturated field conditions, which is consistent with air-water interfacial collapse being responsible for the observed concentration increases for the longer-chained PFAS. Results observed in Figure 6-3 are consistent with those observed in **Figure 6-2** and **Table 6-2**. Thus, both sets of bench-scale testing (microlysimeter sampling and batch slurry desorption) are qualitatively consistent with each other, and inform on field behavior.

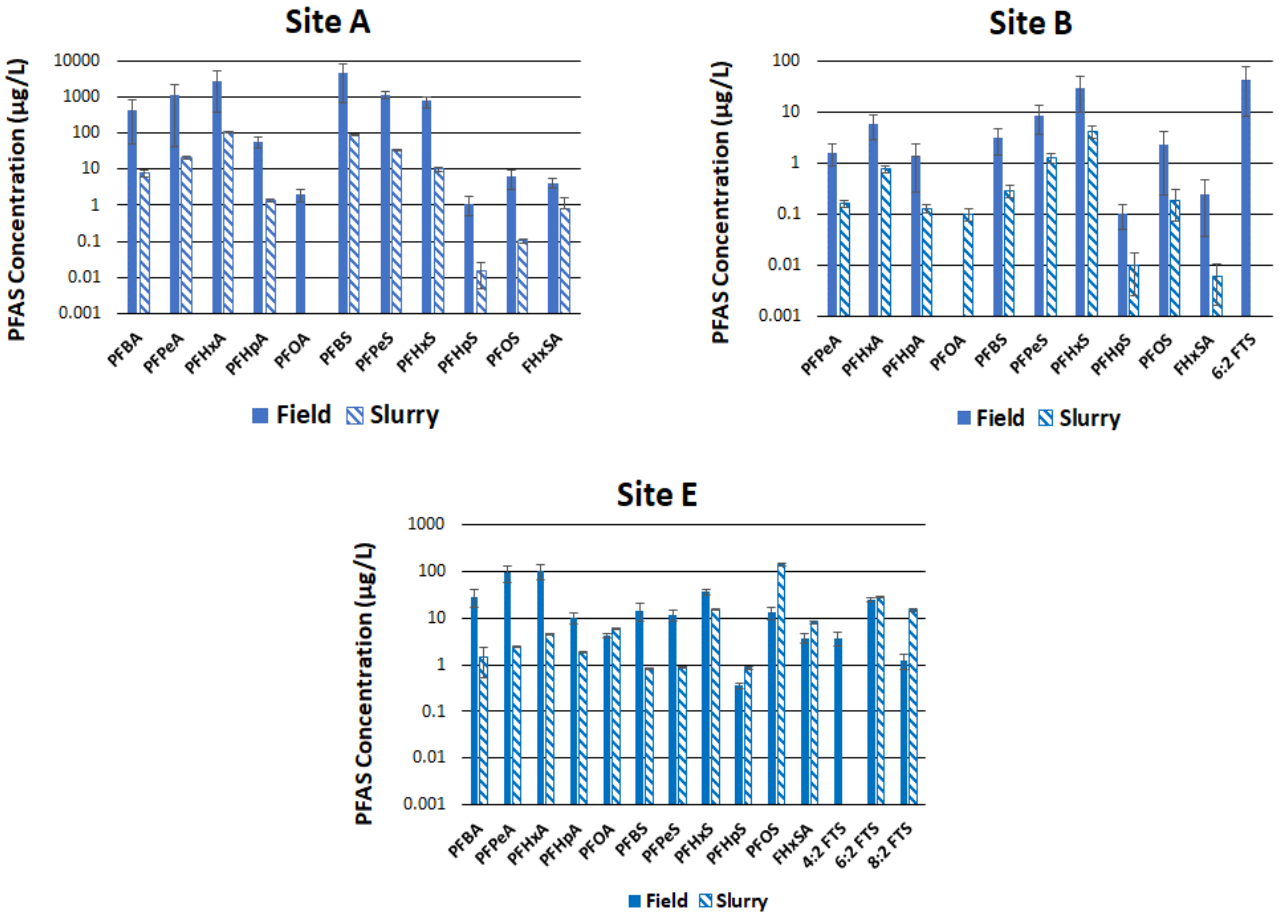

Figure 6-3. Comparisons between PFAS Porewater Concentrations Measured in the Field Lysimeters to those Measured in the Laboratory Batch Slurries for Sites A, B, and C.

Error bars indicate 95% confidence intervals.

6.2 SITE G

Water table elevations (Figure 6-4) and soil moisture/precipitation (Figure 6-5) are shown for JBCA (Site G). Sampling dates, applied vacuums, and collected porewater volumes are provided in Table 5-2. The first three porewater sampling events occurred before the water table increased such that the lysimeters were below the water table. While the final porewater sampling event occurred after the water table was again below the level of the lysimeters, it is unclear how PFAS contamination at these locations was impacted by PFAS mass migrating through the transiently saturated soil.

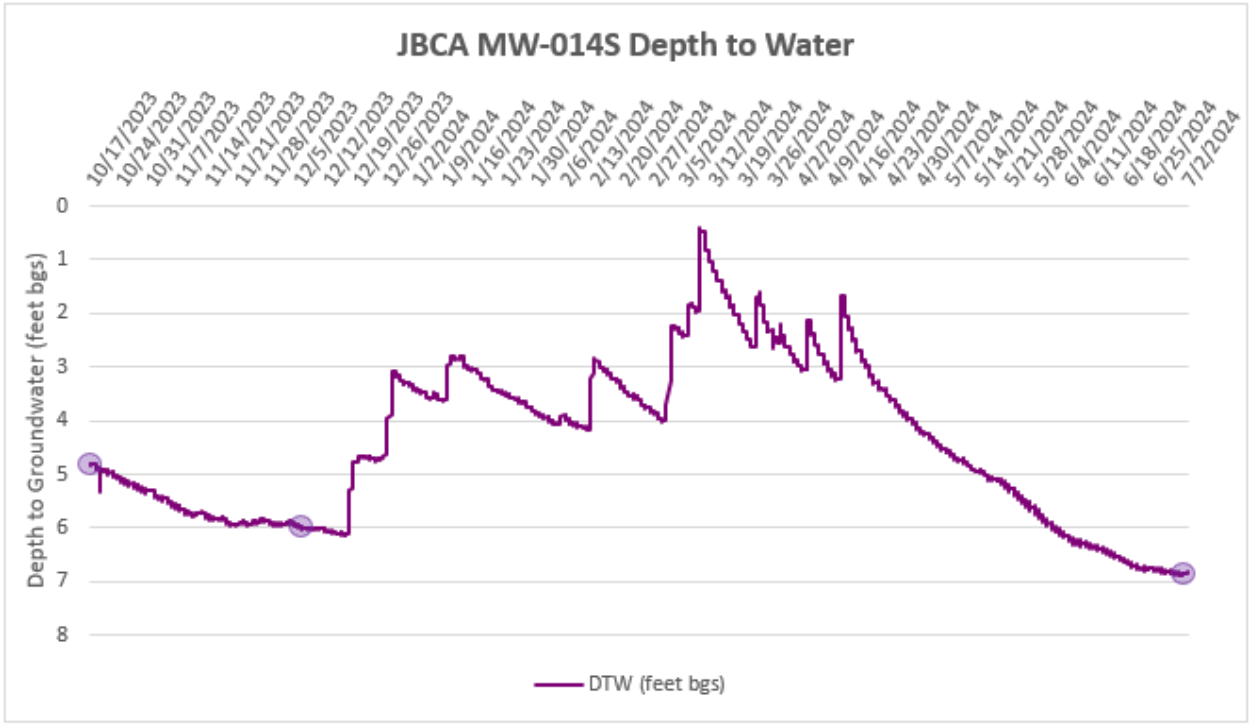

Note: Datalogger not installed until October 17, 2023.

- Sampling date

Figure 6-4. Site G Depth to Water for Monitoring Well Located Near Field Lysimeters.

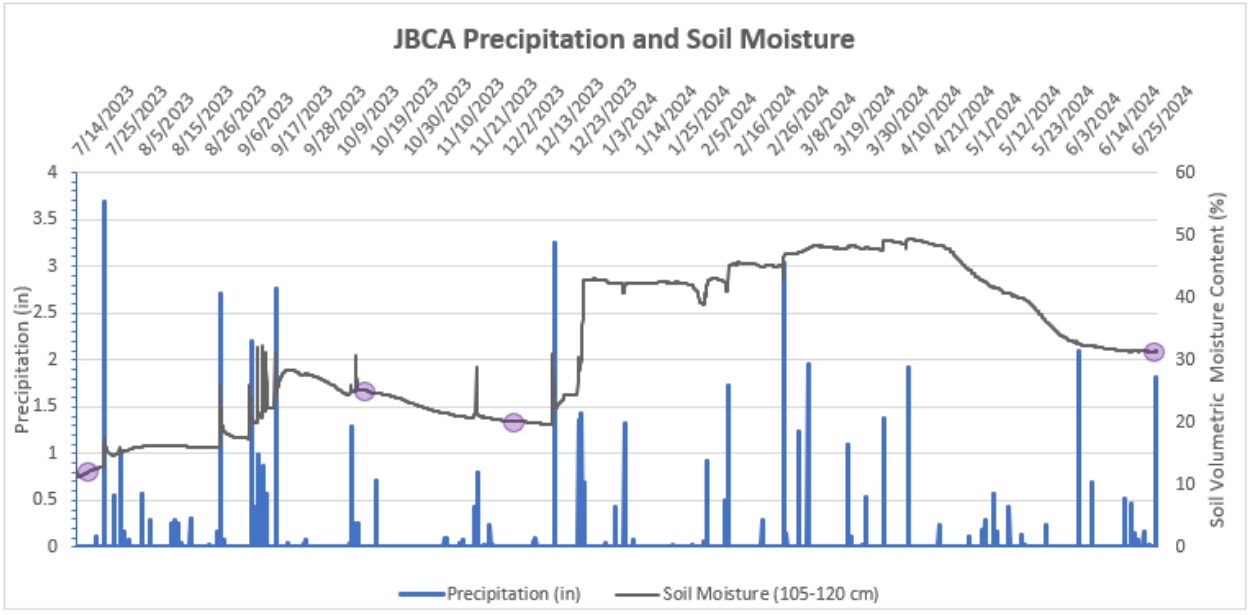

- Sampling date

Figure 6-5. Site G Precipitation and Soil Moisture Content.

Porewater results for the five most abundant PFAS in porewater are provided in **Figure 6-6**. The following observations are made:

- Consistent with our previous results (Schaefer et al., 2022, 2024), variation at a given lysimeter was typically within approximately a factor of two.

- With the exception of PFOS, PFAS concentrations at L29 for the July 2024 sampling event were approximately one order magnitude less than that measured during previous sampling rounds. Sampling at L29 at the July 2024 event only yielded 4 mL of porewater, which was approximately 4-times less than what was collected at the other lysimeters for this sampling event. It is possible that such low sample volumes were the cause for this apparent discrepancy.

- PFAS concentrations, at least for highly surface-active compounds like PFOS, are expected to increase with increasing moisture content as air-water interfaces collapse. Considering the first three sampling events (prior to the rapid rise in water table and submersion of the lysimeters), there is generally no correlation between the PFAS porewater concentrations and soil moisture content, with p values ranging from 0.54 to 0.71. The possible exception is PFOS, (the most surface active PFAS examined) which has a p value of 0.21. The low significance of this correlation for PFOS is likely attributable to the effect of interfacial area collapse being masked my other factors such as desorption mass transfer and flow heterogeneity. **Figure 6-7** shows that the impact of moisture content on PFOS concentration appears very clear in one lysimeter (L24), but less clear at the other two lysimeters.

- While not the focus of this investigation, the difference in PFAS concentrations among the three lysimeters suggest that PFAS concentrations in soil/porewater within an AFFF source area can vary substantially. Work as part of our ongoing AFCEC BAA 2108 project, which is evaluating the source area and PFAS distribution more holistically at this site, suggests that the differences observed among these three lysimeters was primarily due to variations in PFAS soil concentrations.

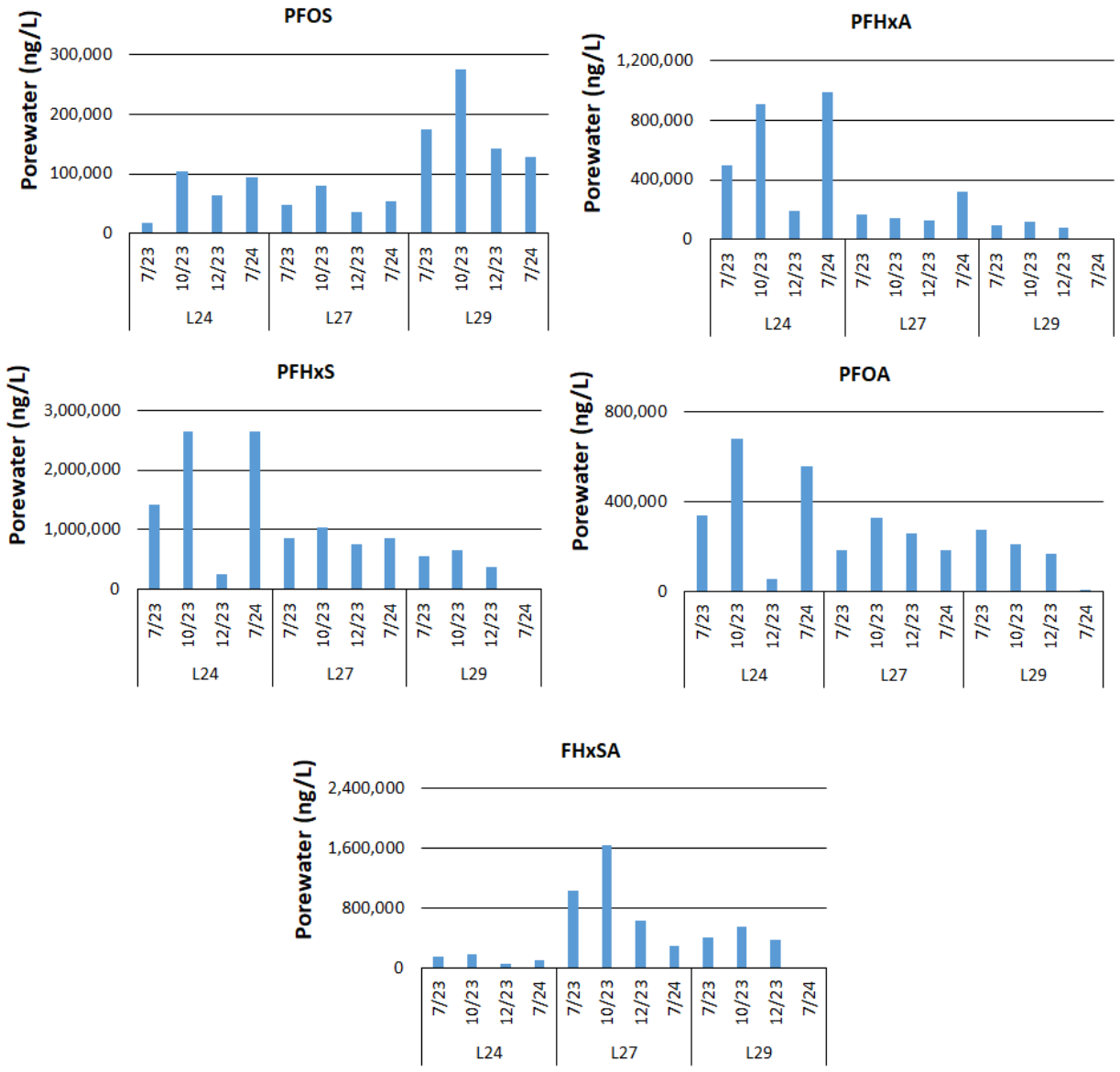

Figure 6-6. PFAS Porewater Concentrations Measured in Lysimeters L24, L27, and L29 at JBCA for the Four Sampling Dates Over a 13-month Time Period.

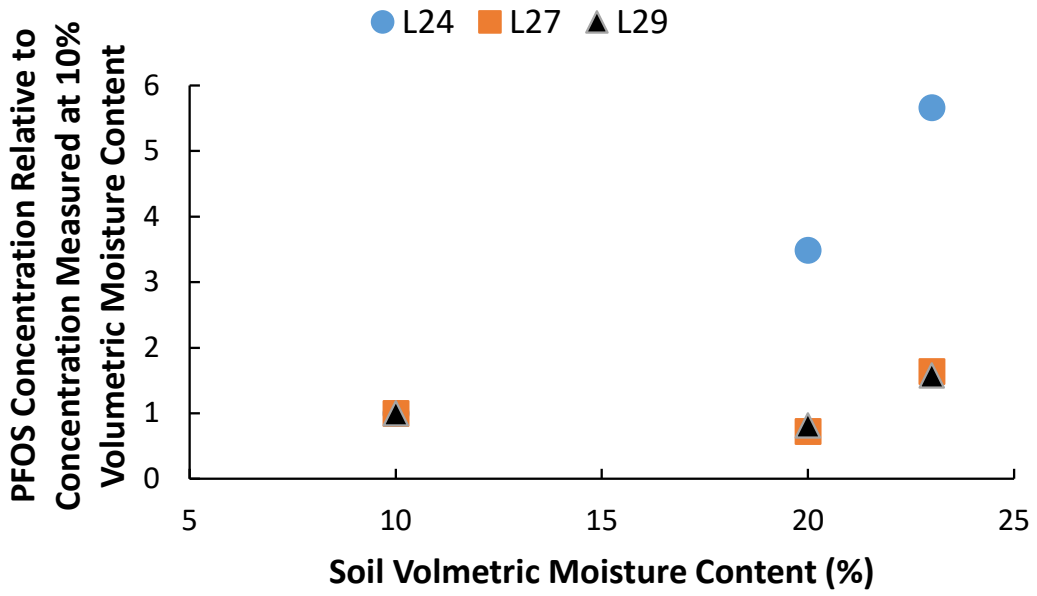

Figure 6-7. Relative Changes in PFOS Porewater Concentrations with Soil Moisture for each of the Three Lysimeters.

At a soil volumetric moisture content of 10%, the y-axis value for all three lysimeters is 1.

Overall, these results suggest that seasonal/temporal variability with respect to PFAS porewater concentrations was limited (generally within a factor of two). Also, for the conditions examined, soil moisture did not have a dominant effect on porewater concentration, even for PFOS. It is likely that a more robust data set would be needed to more appropriately evaluate the impacts of moisture content on PFAS porewater concentrations.

6.3 CONCLUSIONS AND ENVIRONMENTAL IMPLICATIONS

Results of this study highlight the contribution of precursors in unsaturated zone leachate from historically impacted AFFF source areas. Precursors constituted a substantial fraction of the total PFAS mass in the porewater at several of the tested locations, many of which were semi-quantified compounds that would not be detected via EPA Method 1633. Thus, appropriate accounting of the total PFAS-related fluorine mass balance in leachate and the subsequent mass discharge to underlying groundwater necessitates that appropriate analytical tools are employed for porewater analyses.

In addition, the presence of these precursors necessitates improved understanding regarding the long-term mass discharge and potential transformation of these compounds, and their impact on site conceptual models. The extent to which these persistent precursors at historic AFFF-impacted sites are transforming in the unsaturated zone or (for those only identified in soils) remain effectively sequestered to the soils remains unknown; this unknown remains a critical research question for the DoD. The ultimate fate of precursors that reach the water table also is poorly understood, largely due to uncertainties in both their naturally occurring transformation rates and their ultimate transformation products.

PFAS soil concentrations in the unsaturated zone remained elevated, even after several years to decades since the last reported AFFF reelase at each site. PFOS was the most abundant PFAS quantified in soil at each site, with maximum concentrations ranging from approximately 500 μg/kg to 40,000 μg/kg. For the two sites located in a semi-arid climate, a clear chromatographic separation was observed in the PFAS soil concentration depth profile, where PFAS migration was inversely proportional to PFAS chain length. For the sites located in more humid climates, PFAS concentration depth profiles were similar among PFAS, with no observable differences among compounds with differing chain lengths. While a much larger number of sites and more detailed history of AFFF release applications are needed to appropriately interpret these differences among sites, results herein suggest that further investigation into the role of climate on long-term PFAS migration and distribution in soil is warranted.

Porous cup suction lysimeters (PCSLs) were shown to be a useful tool for determining PFAS concentrations in unsaturated zone porewater, where the sites examined had total target PFAS concentrations ranging from approximately 10 to 10,000 μg/L. Repeatability for measured PFAS concentrations was typically within a factor of two, demonstrating the use of PCSLs for estimating PFAS leaching. Repeatability within a factor of two for porewater concentrations as measured by the bench-scale microlysimeters also was observed. Importantly, with the exception of one site, measurements of PFAS porewater concentration using the field-deployed PCSLs compared to the bench-scale microlysimeters were reasonably (typically within a factor of 3 and/or within the 95% confidence interval of the field measurements) when changes in moisture were properly taken into consideration. This finding further validates the local apparent equilibrium assumption, suggests that the field-deployed PCSLs are collecting a representative porewater sample, and that both PCSLs and microlysimeters may serve as useful tools for estimating PFAS porewater concentrations. The one site that was a notable exception to these finding was a site where the soil had been previously removed, thermally treated, and then backfilled; ground penetrating radar revealed many anomalies in this soil. Thus, it is unclear if PCSLs were able to collect a truly representative porewater sample at this site.

Furthermore, results herein highlight the potential importance of PFAS accumulation at air-water interfaces in unsaturated soils, and how moisture content can impact these concentrations due to the collapse of air-water interfaces and the subsequent release of PFAS. Thus, soil moisture content should be considered when interpreting field lysimeter data, as changes in moisture content due to precipitation can have a substantial impact on measured PFAS porewater concentrations (especially for fine-grained soils). For example, the porewater PFOS concentration for soil C increased approximately 4-fold as the soil moisture content increased from 4.8% to 15%. Careful examination of soil moisture and texture, similar to that performed herein, may serve useful in future studies. However, PFAS accumulation at air-water interfaces in AFFF-impacted soils may, in some cases, be substantially less than expected. Competitive processes among PFAS and other porewater constituents (e.g., natural organic matter, hydrocarbon surfactants) could potentially diminish PFAS accumulation at the air-water interface. Further research in such complex systems may be required to for improved predictions of PFAS accumulation at the air-water interface, and ultimately PFAS leaching.

Finally, for the sites and conditions examined herein, bench-scale testing using collected soils were shown to inform on field-scale behavior with respect to PFAS porewater concentrations. While results herein clearly showed that sole reliance of bench-scale testing performed under saturated conditions could lead to substantial (order of magnitude) overestimates of PFAS concentrations in unsaturated porewater, batch soil slurry data were useful in determining PFAS-soil partitioning.

Such readily-implementable bench-scale testing thus provides value with respect to predicting field-scale porewater concentrations if PFAS accumulation at the air-water interface is considered in the overall PFAS mass balance. Also, as previously noted, collected soil cores coupled with bench-scale porewater extractions also serve as a useful tool for confirming field-scale porewater data. Such complimentary bench-scale testing provides critical lines of evidence for both validating and properly interpreting field lysimeter data.

7.0 COST ASSESSMENT

A cost assessment is presented in **Table 7-1** to estimate the resources needed to provide bench-scale validation/evaluation of PFAS concentrations measured in situ using porous cup suction lysimeters. Specifically, costs associated with the micro-lysimeter porewater sampling of collected soil sample (**Figure 5-1**) is determined. For the micro-lysimeter sampling, the estimate cost (including PFAS analysis) for evaluation within a typical fire-training is $7,750. This cost is largely driven by the PFAS analysis ($450/sample x 12 samples assumed). Key assumptions in deriving this cost are provided in the table below.

Table 7-1. Cost Assessment

Task	Units	Estimated Cost per Unit	Quantity	Total Cost
Soil Core Sample Collection and Lysimeter Installation	Hour	$125	2	$250
Sample Shipping Cost	Cooler	$500	1	$500
Lab Technician	Hour	$125	8	$1,000
Lab Materials	Lump Sump	$600	1	$600
PFAS Analysis	Sample	$450	12	$5,400
Total Estimated Cost for a Typical Fire-Training Area				**$7,750**

Notes:

Assumes sufficient soil data (including depth resolution) such that PFAS concentration as a function of depth is known.

Assumes two soil core locations per Fire-Training Area

Assumes two 10 cm depth intervals within each of the two collected soil cores for microlysimeter porewater sampling, and 3 porewater extraction points within each 10 cm interval.

8.0 IMPLEMENTATION ISSUES

The field-scale and bench-scale porewater sampling employed in this study were generally readily implementable. Specific challenges are noted as follows:

- Dry soil conditions. Sufficient soil moisture is needed to extract field porewater samples. Herein, porewater collection was challenging in the two driest soils (3.5% and 4.3% moisture content). Although a sufficient volume and number of porewater samples were collected for quantitative analyses, the targeted number of lysimeter samples was not obtained. Results of this study suggest that a soil moisture content of approximately 5% is needed for routine porewater collection use PCSLs (although this value also is dependent upon the soil grain size and texture). At many semi-arid or arid sites, this may necessitate timing lysimeter sampling events with rainfall events. Another option would be to apply vacuum for a longer period of time than what was used herein (typically 8 to 12 hours). Such extended vacuum application would require additional labor efforts, or the use of a vacuum manifold system. For the microlysimeters, a soil moisture content of approximately 7% was needed to effectively extract porewater; this higher moisture content is due to the fact that the maximum vacuum that could be applied on the microlysimeters was less than that which could be applied to the field-deployed lysimeters.

- Low permeability soils. It is well-known that low permeability soils can prevent the effective collection of porewater when using PCSLs. Sites E and G had clay contents of 14% and 15%, respectively. Despite elevated moisture contents (9.6% and 13% for sites E and G, respectively), collecting porewater was challenging. For Site E, sufficient porewater was collected for quantitative analyses, but not all lysimeters produced water and no porewater was collected for some of the sampling rounds; site G yielded insufficient porewater to include in the study. Porewater collection results for site G, given the elevated moisture and average grain size of 0.2 mm, were particularly surprising. One possibility is that local heterogeneity in the clay distribution may have contributed to the difficulties in collecting porewater at site G. Overall, results of this study suggest that elevated clay levels could result in challenges when attempting to collect porewater using PCSLs.

- Applied vacuum. Another issue that occurred was that the lysimeters would occasionally not hold vacuum, and therefore porewater collection was limited. In most cases, this was due to improperly securing either the lysimeter cap, or improperly securing/crimping the vacuum tubing. Thus, proper attention should be given to these details. Another challenge (observed herein and in other lysimeter studies in which the project investigators are involved) the lysimeter caps appeared to be tampered with by wildlife. Thus, proper securing and protecting of the lysimeter caps is recommended.

- Site heterogeneity. For this project, lysimeters were installed at a single depth, and within a single stratigraphic zone. For sites where the soil data suggest that the geology and PFAS distribution are likely not uniform throughout the unsaturated zone, installing lysimeters at multiple depths should be considered to better inform on overall PFAS leaching and mass discharge to underlying groundwater. While such evaluation was beyond the scope of this current study, it is important to recognize that the spatially limited lysimeter investigation performed herein would need to be expanded to provide appropriate site characterization.

- Comparison of lab vs field Collected porewater. While reasonable agreement (typically within a factor of 3 and/or within the 95% confidence interval of the field measurements) was observed between field-collected porewater and porewater extracted in the laboratory from soil cores, two findings are noteworthy. First, in most cases, the soil needed to be wetted and re-packed to collected porewater in the laboratory. Second, if wetting caused a significant decrease in the air-water interfacial area, the impact on PFAS porewater concentrations due to release of PFAS at the air-water interface had to be accounted for (via mass balance) to properly compare the laboratory PFAS porewater concentrations to the field data.

9.0 REFERENCES

Abraham, J.E., Mumford, K.G., Patch, D.J. and Weber, K.P. 2022. Retention of PFOS and PFOA mixtures by trapped gas bubbles in porous media. *Environ. Sci. Technol*., 56, 15489-15498.

Adamson, D.T., Nickerson, A., Kulkarni, P.R., Higgins, C.P., Popovic, J., Field, J., Rodowa, A., Newell, C., DeBlanc, P. and Kornuc, J.J. 2020. Mass-based, field-scale demonstration of PFAS retention within AFFF-associated source areas. *Environ. Sci. Technol*., 54, 15768-15777.

Adamson, D.T., Kulkarni, P.R., Nickerson, A., Higgins, C.P., Field, J., Schwichtenberg, T., Newell, C. and Kornuc, J.J. 2022. Characterization of relevant site-specific PFAS fate and transport processes at multiple AFFF sites. *Environ. Advances*, 7, 100167.

Ahrens, L., Taniyasu, S., Yeung, L.W.Y., Yamashita, N., Lam, P.K.S., Ebinghaus, R. (2010). Distribution of polyfluoroalkyl compounds in water, suspended particulate matter and sediment from Tokyo Bay, Japan. *Chemosphere* 79, 266-272.

Anderson, R.H., Adamson, D.T. and Stroo, H.F., 2019. Partitioning of poly-and perfluoroalkyl substances from soil to groundwater within aqueous film-forming foam source zones. *J. Contam. Hydrol.,* 220, 59-65.

Avendaño, S.M. and Liu, J. 2015. Production of PFOS from aerobic soil biotransformation of two perfluoroalkyl sulfonamide derivatives. *Chemosphere*, 119, 1084-1090.

Backe, W.J., Day, T.C. and Field, J.A. 2013. Zwitterionic, cationic, and anionic fluorinated chemicals in aqueous film forming foam formulations and groundwater from US military bases by nonaqueous large-volume injection HPLC-MS/MS. *Environ. Sci. Technol*., *47*, 5226-5234.

Barzen-Hanson, K.A., Roberts, S.C., Choyke, S., Oetjen, K., McAlees, A., Riddell, N., McCrindle, R., Ferguson, P.L., Higgins, C.P. and Field, J.A., 2017. Discovery of 40 classes of per-and polyfluoroalkyl substances in historical aqueous film-forming foams (AFFFs) and AFFF-impacted groundwater. *Environ. Sci. Technol*., 51, 2047-2057.

Brusseau, M.L., 2018. Assessing the potential contributions of additional retention processes to PFAS retardation in the subsurface. *Sci. Total Environ.,* 613, 176-185.

Brusseau, M.L., Yan, N., Van Glubt, S., Wang, Y., Chen, W., Lyu, Y., Dungan, B., Carroll, K.C. and Holguin, F.O., 2019. Comprehensive retention model for PFAS transport in subsurface systems. *Water Research,* 148, 41-50.

Brusseau, M.L.. 2023. Determining air-water interfacial areas for the retention and transport of PFAS and other interfacially active solutes in unsaturated porous media. *Sci. Total Environ*., *884*, 163730.

Cai, W., Navarro, D.A., Du, J., Ying, G., Yang, B., McLaughlin, M.J. and Kookana, R.S. 2022. Increasing ionic strength and valency of cations enhance sorption through hydrophobic interactions of PFAS with soil surfaces. *Sci. Tot. Environ.*, 817, 152975.

Cheng, T. and Saiers, J.E. (2010). Colloid-facilitated transport of cesium in vadose-zone sediments: the importance of flow transients. *Environ. Sci. Technol.* 44, 7443-7449.

Choi, J-W., Tillman Jr., F.D., Smith, J.A. (2002). Relative importance of gas-phase diffusive and advective trichloroethene (TCE) fluxes in the unsaturated zone under natural conditions. *Environ. Sci. Technol.* 36, 3157-3164.

DiFilippo, E.L., Brusseau, M.L. (2008). Relationship between mass flux and source-zone mass removal: analysis of field data. *J. Contam. Hydrol.* 96, 22-35.

Enami, S., Fujii, T., Sakamoto, Y., Hama, T., Kajii, Y. (2016). Carboxylate ion availability at the air-water interface. *J. Phys. Chem. A.* 120, 9224-9234.

EPA (1996). Soil Screening Guidance: Technical Background Document. EPA/540/R95/128.

Falta, R.W., Basu, N., Rao, P.S. (2005). Assessing impacts of partial mass depletion in DNAPL source zones: II. Coupling source strength functions to plume evolution. *J. Contam. Hydrol*. 79, 45-66.

Flury, M., Flühler, H., Jury, W.A. and Leuenberger, J. (1994). Susceptibility of soils to preferential flow of water: A field study. *Water Resour. Res.,* 30, 1945-1954.

Guo, B., Saleem, H. and Brusseau, M.L. 2023. Predicting Interfacial Tension and Adsorption at Fluid–Fluid Interfaces for Mixtures of PFAS and/or Hydrocarbon Surfactants. *Environ. Sci. Technol*, 21, 8044-8052.

Hao, S., Choi, Y.J., Deeb, R.A., Strathmann, T.J. and Higgins, C.P. 2022. Application of hydrothermal alkaline treatment for destruction of per-and polyfluoroalkyl substances in contaminated groundwater and soil. *Environ. Sci. Technol.*, 56, 6647-6657.

Hendrickx, J.M. and Flury, M. (2001). Uniform and preferential flow mechanisms in the vadose zone. *Conceptual Models of flow and transport in the fractured vadose zone,* 149-187.

Høisæter, Å., Pfaff, A. and Breedveld, G.D. (2019). Leaching and transport of PFAS from aqueous film-forming foam (AFFF) in the unsaturated soil at a firefighting training facility under cold climatic conditions. *J. Contam. Hydrol.,* 222, 112-122.

Huang, D., Saleem, H., Guo, B. and Brusseau, M.L. 2022. The impact of multiple-component PFAS solutions on fluid-fluid interfacial adsorption and transport of PFOS in unsaturated porous media. *Sci. Total Environ.,* 806, 150595.

Jia, C., You, C., Pan, G. 2010. Effect of temperature on the sorption and desorption of perfluorooctane sulfonate on humic acid. *J. Environ. Sci.* 22, 355-361.

Lyu, Y., Brusseau, M.L., Chen, W., Yan, N., Fu, X. Lin, X. 2018. Adsorption of PFOA at the air–water interface during transport in unsaturated porous media. *Environ. Sci. Technol*., 52, 7745-7753.

Mobile, M.A., Widdowson, M.A., Gallagher, D.L. (2012). Multicomponent NAPL source dissolution: Evaluation of mass-transfer coefficients. Environ. Sci. Technol. 46, 10047-10054.

Murray, C. C.; Vatankhah, H.; McDonough, C. A.; Nickerson, A.; Hedtke, T. T.; Cath, T. Y.; Higgins, C. P.; Bellona, C. L. 2019. Removal of per- and polyfluoroalkyl substances using super-fine powder activated carbon and ceramic membrane filtration. *J. Hazard. Mater., 366*, 160−168.

Nickerson, A., Rodowa, A.E., Adamson, D.T., Field, J.A., Kulkarni, P.R., Kornuc, J.J. and Higgins, C.P. 2020. Spatial trends of anionic, zwitterionic, and cationic PFAS at an AFFF-impacted site. *Environ. Sci. Technol*., 55, 313-323.

Nickerson, A., Maizel, A.C., Kulkarni, P.R., Adamson, D.T., Kornuc, J.J. and Higgins, C.P. 2020b. Enhanced extraction of AFFF-associated PFAS from source zone soils. *Environ. Sci. Technol*., 54, 4952-4962.

Pickard, H.M., Ruyle, B.J., Thackray, C.P., Chovancova, A., Dassuncao, C., Becanova, J., Vojta, S., Lohmann, R. and Sunderland, E.M.. 2022. PFAS and precursor bioaccumulation in freshwater recreational fish: implications for fish advisories. *Environ. Sci. Technol*., 56, 15573-15583.

Psillakis, E., Cheng, J., Hoffmann, M.R., Colussi, A.J. (2009). Enrichment factors of perfluoroalkyl oxoanions at the air/water interface. *J. Phys. Chem. A*. 113, 8826-8829.

Rádi, J., Tóth, Z., Marton, A., Földényi, R. (2014). Equilibrium studies of binding of cationic surfactants to sodium humate. *Periodica Polytechnica* 58, 27-33.

Ruyle, B.J., Thackray, C.P., Butt, C.M., LeBlanc, D.R., Tokranov, A.K., Vecitis, C.D. and Sunderland, E.M., 2023. 2023. Centurial Persistence of Forever Chemicals at Military Fire Training Sites. *Environ. Sci. Technol.*, 57, 8096-8106.

Ruyle, B.J., Schultes, L., Akob, D.M., Harris, C.R., Lorah, M.M., Vojta, S., Becanova, J., McCann, S., Pickard, H.M., Pearson, A. and Lohmann, R.. 2023b. Nitrifying Microorganisms Linked to Biotransformation of Perfluoroalkyl Sulfonamido Precursors from Legacy Aqueous Film-Forming Foams. *Environ. Sci. Technol.*, 57, 5592-5602.

Ryan, J.N., Illangasekare, T.H., Litaor, M.I., Shannon, R. (1998). Particle and plutonium mobilization in macroporous soils during rainfall simulations. *Environ. Sci. Technol*. 32, 476-482.

Schaefer, C.E., DiCarlo, D.A., and Blunt, M.J. (2000). Experimental Measurement of Air-Water Interfacial Area during Gravity Drainage and Secondary Imbibition in Porous Media, *Water Resour. Res.* 36, 885-890.

Schaefer, C.E., Culina, V., Nguyen, D., Field, J. (2019). Uptake of poly- and perfluoroalkyl substances at the air-water interface, Environ. Sci. Technol. 53, 12442-12448, 2019.

Schaefer, C.E., Nguyen, D., Christie, E., Shea, S., Higgins, C.P. Field, J.A. (2021). Desorption of Poly-and Perfluoroalkyl Substances from Soil Historically Impacted with Aqueous Film-Forming Foam. *J. Environ. Engin.* 147, 06020006.

Schaefer, C.E.; Lavorgna, G.M.; Lippincott, D.R.; Nguyen, D.; Christie, E.; Shea, S.; O'Hare, S.; Lemes, M.C.; Higgins, C.P.; Field, J. 2022. A field study to assess the role of air-water interfacial sorption on PFAS leaching in an AFFF source area. *J. Contam. Hydrol*., *248*, 104001.

Schaefer, C.E., Lemes, M.C., Schwichtenberg, T. and Field, J.A. 2022c. Enrichment of poly-and perfluoroalkyl substances (PFAS) in the surface microlayer and foam in synthetic and natural waters. *J. Haz. Mat.,* 440, .129782.

Schaefer, C.E., Lavorgna, G.M., Lippincott, D.R., Nguyen, D., Schaum, A., Higgins, C.P. and Field, J.. 2023. Leaching of perfluoroalkyl acids during unsaturated zone flushing at a field site impacted with aqueous film forming foam. *Environ. Sci. Technol*., 57, 1940-1948.

Schaefer, C.E., Nguyen, D., Fang, Y., Gonda, N., Zhang, C., Shea, S. and Higgins, C.P., 2024. PFAS Porewater concentrations in unsaturated soil: Field and laboratory comparisons inform on PFAS accumulation at air-water interfaces. *Journal of Contaminant Hydrology*, *264*, p.104359.

Sirivithayapakorn, S., Keller, A. (2003). Transport of colloids in unsaturated porous media: A pore-scale observation of processes during the dissolution of air-water interface. *Water Resour. Res.* 39, 1-10.

Stahl, T., Riebe, R.A., Falk, S., Failing, K. and Brunn, H. (2013). Long-term lysimeter experiment to investigate the leaching of perfluoroalkyl substances (PFAS) and the carry-over from soil to plants: results of a pilot study. *J. Agricultural Food Chem*., 61, 1784-1793.

Stults, J.F., Choi, Y.J., Schaefer, C.E., Illangasekare, T.H. and Higgins, C.P., 2022. Estimation of transport parameters of perfluoroalkyl acids (PFAAs) in unsaturated porous media: critical experimental and modeling improvements. *Environmental Sci. Technol.*, 56, 7963-7975.

Stults, J.F., Choi, Y.J., Rockwell, C., Schaefer, C.E., Nguyen, D.D., Knappe, D.R., Illangasekare, T.H. and Higgins, C.P. 2023. Predicting Concentration-and Ionic-Strength-Dependent Air–Water Interfacial Partitioning Parameters of PFAS Using Quantitative Structure–Property Relationships (QSPRs). *Environmental Sci. Technol.*, 57, 5203-5215.

Wang, Q., Cameron, K., Buchan, G., Zhao, L., Zhang, E.H., Smith, N. and Carrick, S. (2012). Comparison of lysimeters and porous ceramic cups for measuring nitrate leaching in different soil types. *New Zealand J. Agricultural Res*. 55, 333-345.

Weihermüller, L., Kasteel, R. and Vereecken, H. (2006). Soil heterogeneity effects on solute breakthrough sampled with suction cups. *Vadose Zone J.* 5, 886-893.

Weihermüller, L., Siemens, J., Deurer, M., Knoblauch, S., Rupp, H., Göttlein, A. and Pütz, T. (2007). *In situ* soil water extraction: a review. *J. Environ. Qual.* 36, 1735-1748.

Zhang, S., Lu, X., Wang, N. and Buck, R.C. 2016. Biotransformation potential of 6: 2 fluorotelomer sulfonate (6: 2 FTSA) in aerobic and anaerobic sediment. *Chemosphere*, 154, 224-230.

Zotarelli, L., Scholberg, J.M., Dukes, M.D. and Munoz-Carpena, R. (2007). Monitoring of nitrate leaching in sandy soils. *J. Environ. Quality,* 36, 953-962.

APPENDIX A POINTS OF CONTACT

Point of Contact Name	Organization Name Address	Phone Email	Role in Project
Charles Schaefer, Ph. D.	CDM Smith 110 Fieldcrest Avenue, #8 6th Floor Edison, NJ 08837	732-590-4633 schaeferce@cdmsmith.com	Principal Investigator
Maxwell Hire, PG	CDM Smith 8080 Ward Parkway, Suite 100, Kansas City, MO 64114	816-412-3156 hirems@cdmsmith.com	Field Geologist
Teri Myers, Ph.D., PMP	CDM Smith 10306 Eaton Place Suite 220 Fairfax VA 22030 United States	240-409-7986 myersts@cdmsmith.com	Project Manager
Christopher Higgins, Ph. D.	Colorado School of Mines Department of Civil and Environmental Engineering 1500 Illinois St, Golden, CO 80401	303-384-2002 chiggins@mines.edu	Co-Principal Investigator
Stephanie Shea, Ph. D.	Colorado School of Mines Department of Civil and Environmental Engineering 1500 Illinois St, Golden, CO 80401	303-273-3427 sshea@mines.edu	PFAS Analytical Support

APPENDIX B PFAS ANALYTICAL

Aqueous sample preparation: each sample was diluted to ensure that concentrations fall between the PFAS calibration range (0.1 - 10000 ng·L-1). A 1.5 mL solution containing 59.3% of the total volume of sample, 15.6% methanol, 3% ammonium hydroxide in water, 8.6% isopropanol, 10% trifluoroethanol and 100 pg/1.5 mL IS was transferred to an HPLC vial for analysis.

Soil sample preparation: The soil samples were extracted according to methods described previously.[1] For LC/MS analysis, each sample was diluted to ensure that concentrations fell between the PFAS calibration range (0.2- 20000 ng/L). A 400 µL solution containing 20% water, 25% soil extract, 49.3% methanol, 0.6% ammonium hydroxide, and 5% of 15 ng/mL (300pg) of injection standard (M2PFOA, Wellington Laboratories).

Liquid chromatography-mass spectrometry (LC-MS) analysis for aqueous and soil samples: LC-MS analysis was performed using a SCIEX Exion LC high-pressure liquid chromatography (HPLC) system with a SCIEX X500R QToF-MS system (Framingham, MA) using negative electrospray ionization (ESI-) and positive electrospray ionization (ESI+) as previously described.1 Chromatographic separation was accomplished using a Gemini C18 analytical column (3 mm × 100 mm, 5 µm; Phenomenex, Torrance, CA) with one SecurityGuardTM C18 Guard Cartridge (4 mm × 2 mm I.D.; Phenomenex) and two Zorbax DIOL guard columns (4.6 mm × 12.5 mm, 6 µm; Agilent, Santa Clara, CA). The DIOL guard columns were removed when analyzing samples in ESI+ mode. The column oven temperature was set to 40 °C. One mL of each sample was injected for aqueous analysis and 100 uL of each sample was injected for soil analysis. The mobile phase included two eluents: (A) 20 mM ammonium acetate (Fisher Scientific, Hampton, NH) in Optima® HPLC-grade water, and (B) 100% Optima® HPLC-grade methanol. Eluent flow rate was 0.60 mL/min, and composition was linear from 90:10 A/B to 50:50 A/B over the first 0.5 min, to 1:99 A/B at 8 min, held constant at 1:99 A/B until 13 min, and ramped to 90:10 A/B at 13.5 min, followed by a post time at 90:10 A/B until 20 min for equilibration.

Compounds were ionized by operating in ESI negative mode with SWATH® Data-Independent Acquisition and the protonated molecular ion in ESI positive mode. Precursor ion data for m/z 100-1200 Da was collected for 1283 cycles with a total scan time of 842 ms and accumulation time of 20 ms. The ion spray voltage was set at -4500 V and temperature was set to 550 °C with an ion source gas pressure of 60 psi, a curtain gas pressure of 35 psi, and a collision (CAD) gas pressure of 10 psi. For QToF scanning, the collision energy was set to -5 V and the declustering potential was set to -20 V, both with a spread of 0 V. Product ion (MS/MS) scanning for m/z 50-1200 Da was conducted in the following mass m/z windows (Da): 100 − 150, 149 − 200, 199 − 250, 249 − 300, 349 − 400, 399 − 450, 449 − 550, 549 −650, 649 − 800, 799 − 1200. For each SWATH window, the accumulation time was 50 ms and collision energy was -35 V with spread of 30 V.

Qualitative suspect screening involved the comparison of identified mass spectral features against an in-house custom spectral library and a custom extracted ion chromatogram (XIC) list. Suspect screening method was adopted from our previous studies [1,2]. In brief, unknown PFAS were identified based on the molecular ion, isotopic pattern, and the library purity score. Samples were screened by searching for the deprotonated molecular ion $[M-H]^-$ for ESI- analysis and the protonated molecular ion $[M+H]^+$ in ESI+ analysis with parameters: XIC window = 0.01 Da, signal-to-noise threshold = 10:1, minimum peak intensity = 100, and baseline subtraction > 2 min.

An R script (R v 4.1.1) was used to process SCIEX OS data and to screen suspected hits including library and XIC list matches. Features matching <10 ppm mass error, <20% isotope ratio difference, and >70% spectral library match based on the Sciex OS algorithm were considered as library matches, which are equivalent to level 2b on the PFAS identification confidence scale proposed by Charbonnnet et al.[3] eatures matching <5 ppm mass error, <10% isotope ratio difference, and <70 spectral library match were considered as XIC matches. Both library and XIC matches were considered as suspected hits in this study. Semiquantitative analysis was performed as previously described.[1 2] Briefly, compounds identified as suspect matches were assigned a target calibrant and internal standard according to their functional group and perfluorinated chain length. The estimated concentration of the suspect compound was calculated as a function of the response factor of the assigned calibrant and internal standard, the molar masses of both the suspect compound and the calibrant, and the peak areas of the internal standard and suspect compound. All semiquantified concentrations are estimates, and may be over or under estimated from their true concentration in the sample. This may be particularly true for the concentrations measured in ESI+ mode due to the limited number of analytical standards and current lack of mass-labeled internal standards for ESI+ analysis. Further discussion of the accuracy of the semiquantitation method used can be found in Nickerson et al.[1]

References

(1) Nickerson, A.; Maizel, A. C.; Kulkarni, P. R.; Adamson, D. T.; Kornuc, J. J.; Higgins, C. P. Enhanced Extraction of AFFF-Associated PFAS from Source Zone Soils. *Environ. Sci. Technol.* **2020**, *54* (8), 4952–4962. https://doi.org/10.1021/acs.est.0c00792.

(2) Hao, S.; Choi, Y. J.; Deeb, R. A.; Strathmann, T. J.; Higgins, C. P. Application of Hydrothermal Alkaline Treatment for Destruction of Per- and Poly Fl Uoroalkyl Substances in Contaminated Groundwater and Soil. *Env. Sci Technol* **2022**, *56*, 6647–6657.

(3) Charbonnet, J. A.; McDonough, C. A.; Xiao, F.; Schwichtenberg, T.; Cao, D.; Kaserzon, S.; Thomas, K. V.; Dewapriya, P.; Place, B. J.; Schymanski, E. L.; Field, J. A.; Helbling, D. E.; Higgins, C. P. Communicating Confidence of Per- and Polyfluoroalkyl Substance Identification via High-Resolution Mass Spectrometry. *Environ. Sci. Technol. Lett.* **2022**, *9* (6), 473–481. https://doi.org/10.1021/acs.estlett.2c00206.

Appendix B – Table 1. Target (Quantifiable) Analytes.

PFPrS, PFBSA, PFHxSA, PFEtCHxS, and Cl-PFOS were only quantified in the aqueous phase analysis.

Chemical Name	Acronym	Molecular Formula
Perfluorobutanoic acid	PFBA	C4HO2F7
Perfluoropentanoic acid	PFPeA	C5HO2F9
Perfluorohexanoic acid	PFHxA	C6HO2F11
Perfluoroheptanoic acid	PFHpA	C7HO2F13
Perfluorooctanoic acid	PFOA	C8HO2F15
Perfluorononanoic acid	PFNA	C9HO2F17
Perfluoropropane sulfonate	PFPrS	C3HO3SF7
Perfluorobutane sulfonate	PFBS	C4HO3SF9
Perfluoropentane sulfonate	PFPeS	C5HO3SF11
Perfluorohexane sulfonate	PFHxS	C6HO3SF13
Perfluoroheptane sulfonate	PFHpS	C7HO3SF15
Perfluorooctane sulfonate	PFOS	C8HO3SF17
4:2 Fluorotelomer sulfonate	4:2 FTS	C6H5F9SO3
6:2 Fluorotelomer sulfonate	6:2 FTS	C8H5F13SO3
8:2 Fluorotelomer sulfonate	8:2 FTS	C10H5F17SO3
Perfluorobutane sulfonamide	PFBSA	C4H2F9NO2S
Perfluorohexane sulfonamide	PFHxSA	C6H2F13NO2S
Perfluorooctane sulfonamide	PFOSA	C8H2F17NO2S
Methylperfluorooctane sulfonamide	MeFOSA	C9H4F17NO2S
Methylperfluorooctane sulfonamido acetic acid	MeFOSAA	C11H6F17NO4S
Ethylperfluorooctane sulfonamido acetic acid	EtFOSAA	C12H8F17NO4S
Perfluoro(ethylcyclohexane)	PFEtCHxS	$C_8HF_{15}O_3S$
Chloro-perfluorooctane sulfonate	Cl-PFOS	C8HO3SF16Cl
Perfluoro-2-propoxypropanoate (Gen X)	HFPO-DA	C6HO3F11

Appendix B – Table 2. Suspect (Semi-quantifiable) Analytes in Porewater.

This analysis was performed on porewater samples only. (p. B-4 through B-5)

Chemical Name	Acronym	Molecular Formula
ESI Negative (ESI-)		
Perfluoropropanoic acid	PFPrA	C3HO2F5
Perfluoropropane sulfonamide	FPrSA	C3H2O2SNF7
Perfluoropentane sulfonamide	FPeSA	C5H2O2SNF11
Perfluoroheptane sulfonamide	FHpSA	C7H2O2SNF15
Perfluorohexane sulfinate	PFHxSi	C6HO2SF13
Perfluoropropane sulfonamido acetic acid	FPrSAA	C5H4O4SNF7
Perfluorohexane sulfonamido acetic acid	FHxSAA	C8H4O4SNF13
Perfluoroethane sulfonate	PFEtS	C2HO3SF5
Methylperfluorohexane sulfonamide	MeFHxSA	C7H4O2SNF13
Methylperfluoropropane sulfonamide acetic acid	MeFPrSAA	C6H6O4SNF7
Methylperfluoropentane sulfonamide acetic acid	MeFPeSAA	C8H6O4SNF11
Methylperfluorohexane sulfonamide acetic acid	MeFHxSAA	C9H6O4SNF13
N-methylperfluoromethane sulfonamido acetic acid	MeFMeSAA	C4H6O4SNF3
N-methylperfluoroethane sulfonamido acetic acid	MeFEtSAA	C5H6O4SNF5
Perfluoro methyl cyclopentane sulfonic acid	PFMeCPeS	C6HO3SF11
Perfluoro propyl cyclopentane sulfonic acid	PFPrCPeS	C8HO3SF15
N-sulfopropyl perfluorohexane sulfonamide	SPr-FHxSA	C9H8O5S2NF13
N-sulfo propyl dimethyl ammonio propyl perfluorohexane sulfonamide	SPrAmPr-FHxSA	C16H19O5S2N2F17
Perflourocyclohexane sulfonate	PFCHxS	C6HO3SF11
6:2 fluorotelomer sulfate	6:2 FTOS	C8H5O4SF13
6:2 unsaturated fluorotelomer sulfonate	6:2 UFTS	C8H4O3SF12
perfluorohexane sulfate	PFHx-OS	C6HO4SF13
Hydrido perfluorohexanoic acid	H-PFHxA	C6H2O2F10
Hydrido perfluorooctanoic acid	H-PFOA	C8H2O2F14
Keto-perfluoropentane sulfonate	K-PFPeS	C5HO4SF9
Keto-perfluorohexane sulfonate	K-PFHxS	C6HO4SF11
1-hydroxy-4:2 fluorotelomer sulfonate	1OH-4:2 FTS	C6H5O4SF9
1-hydroxy-6:2 fluorotelomer sulfonate	1OH-6:2 FTS	C8H5O4SF13
ESI Positive (ESI+)		
N-CarboxyMethyldimethylAmmonioPropyl Perfluoropropane Sulfonamide	CMeAmPr-FPrSA	C10H15O4SN2F7
N-CarboxyMethyldimethylAmmonioPropyl Perfluorobutane Sulfonamide	CMeAmPr-FBSA	C11H15O4SN2F9
N-CarboxyMethyldimethylAmmonioPropyl Perfluoropentane Sulfonamide	CMeAmPr-FPeSA	C12H15O4SN2F11

Appendix B – Table 2. Suspect (Semi-quantifiable) Analytes in Porewater (Continued)

Chemical Name	Acronym	Molecular Formula
N-CarboxyMethyldimethylAmmonioPropyl Perfluorohexane Sulfonamide	CMeAmPr-FHxSA	C13H15O4SN2F13
N-carboxy ethyl dimethyl ammonio propyl perfluoropropane sulfonamide	CEtAmPr-FPrSA	C11H17O4N2SF7
N-carboxy ethyl dimethyl ammonio propyl perfluorobutane sulfonamide	CEtAmPr-FBSA	C12H17O4N2SF9
N-carboxy ethyl dimethyl ammonio propyl perfluoropentane sulfonamide	CEtAmPr-FPeSA	C13H17O4N2SF11
N-Sulfo Propyl dimethyl Ammonio Propyl Perfluorobutane Sulfonamide	SPrAmPr-FBSA	C12H19O5S2N2F9
N-Sulfo Propyl dimethyl Ammonio Propyl Perfluoropentane Sulfonamide	SPrAmPr-FPeSA	C13H19O5S2N2F11
N-Sulfo Propyl dimethyl Ammonio Propyl Perfluorohexane Sulfonamide	SPrAmPr-FHxSA	C14H19O5S2N2F13
N-CarboxyMethyldimethylAmmonioPropyl Perfluorobutane Sulfonamide acetic acid	CMeAmPr-FBSAA	C13H17O6SN2F9
N-CarboxyMethyldimethylAmmonioPropyl Perfluoropentane Sulfonamide acetic acid	CMeAmPr-FPeSAA	C14H17O6SN2F11
N-CarboxyMethyldimethylAmmonioPropyl Perfluorohexane Sulfonamide acetic acid	CMeAmPr-FHxSAA	C15H17O6SN2F13
N-SulfoPropyldimethylAmmonioPropyl-Perfluoropropane Sulfonamido Acetic Acid	SPrAmPr-FPrSAA	C13H21O7S2N2F7
N-SulfoPropyldimethylAmmonioPropyl-Perfluorobutane Sulfonamido Acetic Acid	SPrAmPr-FBSAA	C14H21O7S2N2F9
N-SulfoPropyldimethylAmmonioPropyl-Perfluorohexane Sulfonamido Acetic Acid	SPrAmPr-FHxSAA	C16H21O7S2N2F13
N-SulfoPropyldimethylAmmonioPropyl Perfluoropropane SulfonAmido PropylSulfonate	SPrAmPr-FPrSAPrS	C14H25O8S3N2F7
N-SulfoPropyldimethylAmmonioPropyl Perfluorobutane SulfonAmido PropylSulfonate	SPrAmPr-FBSAPrS	C15H25O8S3N2F9
N-TrimethylAmmonioPropyl Perfluorobutane SulfonAmido Propanoic acid	TAmPr-FBSAPrA	C13H19O4SN2F9
N-TrimethylAmmonioPropyl N-Methyl Perfluorobutane Sulfonamide	TAmPr-N-MeFBSA	C11H17O2SN2F9
6:3 2-hydroxy fluorotelomer trimethylammonium	6:3 OH-FT-Tam	C12H14ONF13
4:2 fluorotelomer sulfonyl ethano amido propyl trimethyl ammonium	4:2 FTSO2-EtAdPrTAm	C14H21O3SN2F9

Appendix B – Table 3. Suspect (semi-quantifiable) Analytes Identified in Soil

(p. B-6 through B-11)

Compound Name	Acronym	Chemical Formula
ESI Negative (ESI-)		
1-hydroxy-6:2 fluorotelomer sulfonate	1OH-6:2 FTS	C8H5O4SF13
1-hydroxy-7:2 fluorotelomer sulfonate	1OH-7:2 FTS	C9H5O4SF15
1-hydroxy-8:2 fluorotelomer sulfonate	1OH-8:2 FTS	C10H5O4SF17
perfluoro cyclohexane sulfonate	PFCHxS	C6HO3SF11
perfluoro ethyl cyclohexane sulfonate	PFEtCHxS	C8HO3SF15
perfluoro butyl cyclohexane sulfonate	PFBCHxS	C10HO3SF19
perfluoro ethyl cyclohexane sulfonate	PFPeCHxS	C11HO3SF21
perfluoro hexyl cyclohexane sulfonate	PFHxCHxS	C12HO3SF23
Chloro-perfluorohexane sulfonate	Cl-PFHxS	C6HO3SClF12
N-dihydroxybutyl dimethylammoniopropyl perfluorobutane sulfonamide	diOHBAmPr-FBSA	C13H21O4SN2F9
N-dihydroxybutyl dimethylammoniopropyl perfluoropentane sulfonamide	diOHBAmPr-FPeSA	C14H21O4SN2F11
N-dihydroxybutyl dimethylammoniopropyl perfluorohexane sulfonamide	diOHBAmPr-FHxSA	C15H21O4SN2F13
N-dihydroxybutyl dimethylammoniopropyl perfluorooctane sulfonamide	diOHBAmPr-FOSA	C17H21O4SN2F17
N-dihydroxy propyl dimethyl ammonio hydroxymethyl propyl-perfluorohexanesulfonamide	diOHPrAm-MeOHPr-FHxSA	C15H21O5SN2F13
N-dihydroxy propyldimethyl ammoniohydroxymethyl propyl-perfluorohexane sulfonamido propyl sulfonate	diOHPrAm-MeOHPr-FHxSAPrS	C18H27O8S2N2F13
N-dihydroxy propyldimethyl ammoniohydroxymethyl propyl-perfluorooctane sulfonamido propyl sulfonate	diOHPrAm-MeOHPr-FOSAPrS	C20H27O8S2N2F17
N-ethylperfluorohexane sulfonamido acetic acid	EtFHxSA	C8H6O2SNF13
N-ethylperfluorohexane sulfonamido acetic acid	EtFHxSAA	C10H8O4SNF13
PentaFluoroSulfide PerFluorooctanoic Acid	F5S-PFOA	C8HO2SF19
PentaFluoroSulfide PerFluorononanoic Acid	F5S-PFNA	C9HO2SF21
PentaFluoroSulfide perfluorohexane sulfonate	F5S-PFHxS	C6HO3S2F17
PentaFluoroSulfide perfluoroheptane sulfonate	F5S-PFHpS	C7HO3S2F19
PentaFluoroSulfide perfluorooctane sulfonate	F5S-PFOS	C9HO3S2F23
PentaFluoroSulfide perfluorononane sulfonate	F5S-PFNS	C10HO3S2F25
PentaFluoroSulfide perfluorodecane sulfonate	F5S-PFDS	C10HO3S2F25
perfluoroethane sulfonamide	FEtSA	C2H2O2SNF5
perfluoropropane sulfonamide	FPrSA	C3H2O2SNF7
perfluoropentane sulfonamide	FPeSA	C5H2O2SNF11
perfluoroheptane sulfonamide	FHpSA	C7H2O2SNF15

Appendix B – Table 3. Suspect (semi-quantifiable) Analytes Identified in Soil (Continued)

Compound Name	Acronym	Chemical Formula
perfluorononane sulfonamide	FNSA	C9H2O2SNF19
perfluorodecane sulfonamide	FDSA	C10H2O2SNF21
Perfluoroethane sulfonamido acetic acid	FEtSAA	C4H4O4SNF5
Perfluoropropane sulfonamido acetic acid	FPrSAA	C5H4O4SNF7
Perfluorobutane sulfonamido acetic acid	FBSAA	C6H4O4SNF9
Perfluorohexane sulfonamido acetic acid	FHxSAA	C8H4O4SNF13
Perfluorotridecane sulfonamido acetic acid	FTrDSAA	C15H4O4SNF27
Hydrogen-substituted perfluoropentanoic acid	H-PFPeA	C5H2O2F8
Hydrogen-substituted perfluorohexanoic acid	H-PFHxA	C6H2O2F10
Hydrogen-substituted PerFluoroPropane Sulfonate	H-PFPrS	C3H2O3SF6
Hydrogen-substituted PerFluoroButane Sulfonate	H-PFBS	C4H2O3SF8
Hydrogen-substituted PerFluoroPentane Sulfonate	H-PFPeS	C5H2O3SF10
Hydrogen-substituted PerFluoroHexane Sulfonate	H-PFHxS	C6H2O3SF12
Hydrogen-substituted PerFluoroOctane Sulfonate	H-PFOS	C8H2O3SF16
Hydrogen-substituted PerFluoroNonane Sulfonate	H-PFNS	C9H2O3SF18
Hydrogen-substituted PerFluoroDecane Sulfonate	H-PFDS	C10H2O3SF20
Hydrogen-substituted Unsaturated PerFluoroOctane Sulfonate	H-UPFOS	C8H2O3SF14
Hydrogen-substituted Unsaturated PerFluoroDecane Sulfonate	H-UPFDS	C10H2O3SF18
Hydrogen-substituted Unsaturated PerFluoroPentadecane Sulfonate	H-UPFPeDS	C15H2O3SF28
Keto-perfluorohexane sulfonate	K-PFHxS	C6HO4SF11
Keto-perfluoroheptane sulfonate	K-PFHpS	C7HO4SF13
Keto-perfluorooctane sulfonate	K-PFOS	C8HO4SF15
Keto-perfluorononane sulfonate	K-PFNS	C9HO4SF17
N-methyl perfluoro-1-propane sulfonamide	MeFPrSA	C4H4O2SNF7
N-methyl perfluoro-1-butane sulfonamide	MeFBSA	C5H4O2SNF9
N-methyl perfluoro-1-pentane sulfonamide	MeFPeSA	C6H4O2SNF11
N-methyl perfluoro-1-hexane sulfonamide	MeFHxSA	C7H4O2SNF13
N-methyl perfluoro-1-heptane sulfonamide	MeFHpSA	C8H4O2SNF15
N-methylperfluoropropane sulfonamido acetic acid	MeFPrAA	C6H6O4SNF7
N-methylperfluoromethane sulfonamido acetic acid	MeFMeSAA	C4H6O4SNF3
perfluoropropane sulfate	PFPr-OS	C3HO4SF7
perfluorobutane sulfate	PFB-OS	C4HO4SF9
perfluoroheptane sulfate	PFHp-OS	C7HO4SF15
perfluorooctane sulfate	PFO-OS	C8HO4SF17
perfluorononane sulfate	PFN-OS	C9HO4SF19

Appendix B – Table 3. Suspect (semi-quantifiable) Analytes Identified in Soil (Continued)

Compound Name	Acronym	Chemical Formula
perfluorodecane sulfate	PFD-OS	C10HO4SF21
perfluoroundecane sulfate	PFUd-OS	C11HO4SF23
perfluorododecane sulfate	PFDo-OS	C12HO4SF25
perfluorotridecane sulfate	PFTrD-OS	C13HO4SF27
perfluorotetradacane sulfate	PFTeD-OS	C14HO4SF29
perfluoro-n-tridecanoic acid	PFTrDA	C13HO2F25
perfluoro-n-tetradacanoic acid	PFTeDA	C14HO2F27
perfluoro cyclopentane carboxylic acid	PFCPeCA	C6HO2F9
perfluoroundecane sulfonate	PFUdS	C11HO3SF23
perfluorotridecane sulfonate	PFTrDS	C13HO3SF27
perfluorotetradacane sulfonate	PFTeDS	C14HO3SF29
perfluoropentadecane sulfonate	PFPeDS	C15HO3SF31
perfluorohexadecane sulfonate	PFHxDS	C16HO3SF33
perfluoropentane sulfinate	PFPeSi	C5HO2SF11
perfluorohexane sulfinate	PFHxSi	C6HO2SF13
perfluorooctane sulfinate	PFOSi	C8HO2SF17
N-sulfo propyl perfluorobutane sulfonamide	SPr-FBSA	C7H8O5S2NF9
N-sulfo propyl perfluorohexane sulfonamide	SPr-FHxSA	C9H8O5S2NF13
N-sulfo propyl perfluorooctane sulfonamide	SPr-FOSA	C11H8O5S2NF17
Unsaturated perfluorododecane sulfonate	UPFDoS	C12HO3SF23
Unsaturated perfluorotridecane sulfonate	UPFTrDS	C13HO3SF25
Unsaturated perfluorotetradecane sulfonate	UPFTeDS	C14HO3SF27
7:1 perfluorooctane sulfonate	7:1 PFOS	C8H3O3SF15
6:2 fluorotelomer sulfate	6:2 FTOS	C8H5O4SF13
8:2 fluorotelomer sulfate	8:2 FTOS	C10H5O4SF17
12:2 fluorotelomer sulfonate	12:2 FTS	C14H5O3SF25
6:2 fluorotelomer sulfonamide	6:2 FTSA	C8H6O2SNF13
8:2 fluorotelomer sulfonamide	8:2 FTSA	C10H6O2SNF17
8:2 fluorotelomersulfonyl propanoic acid	8:2 FTSO2PrA	C13H9O4SF17
5:3 keto-fluorotelomer thia keto 2-hydroxy propanoic acid	5:3 K-FTTh-K-OH-PrA	C11H7O5SF11
ESI Positive (ESI+)		
Class 38 (Cn+9H22O2SN2F2n+1)	Class 38-C12	C12H21O2SN2F7
Class 38 (Cn+9H22O2SN2F2n+1)	Class 38-C13	C13H21O2SN2F9
Class 38 (Cn+9H22O2SN2F2n+1)	Class 38-C14	C14H21O2SN2F11
Class 38 (Cn+9H22O2SN2F2n+1)	Class 38-C15	C15H21O2SN2F13
Class 38 (Cn+9H22O2SN2F2n+1)	Class 38-C16	C16H21O2SN2F15

Appendix B – Table 3. Suspect (semi-quantifiable) Analytes Identified in Soil (Continued)

Compound Name	Acronym	Chemical Formula
Class 38 (Cn+9H22O2SN2F2n+1)	Class 38-C17	C17H21O2SN2F17
N-betaine propyl perfluoropentane amide	BPr-FPeAd	C12H15O3N2F9
N-carboxyethyl dimethyl ammonio propyl perfluorobutane sulfonamide	CEtAmPr-FBSA	C12H17O4N2SF9
N-carboxyethyl dimethyl ammonio propyl perfluoropentane sulfonamide	CEtAmPr-FPeSA	C13H17O4N2SF11
N-carboxyethyl dimethyl ammonio propyl perfluorohexane sulfonamide	CEtAmPr-FHxSA	C14H17O4N2SF13
N-carboxyethyl dimethyl ammonio propyl perfluoroheptane sulfonamide	CEtAmPr-FHpSA	C15H17O4N2SF15
N-carboxyethyl dimethyl ammonio propyl perfluoropentane sulfonamido propanoic acid	CEtAmPr-FPeSA-PrA	C16H21O6N2SF11
N-carboxyethyl dimethyl ammonio propyl perfluorohexane sulfonamido propanoic acid	CEtAmPr-FHxSA-PrA	C17H21O6N2SF13
N-Carboxymethyldimethylammoniopropyl-perfluorobutanesulfonamide	CMeAmPr-FBSA	C11H15O4SN2F9
N-Carboxymethyldimethylammoniopropyl-perfluoropentanesulfonamide	CMeAmPr-FPeSA	C12H15O4SN2F11
N-Carboxymethyldimethylammoniopropyl-perfluorohexanesulfonamide	CMeAmPr-FHxSA	C13H15O4SN2F13
N-carboxymethyl dimethylammoniopropyl-perfluoropentane sulfonamido acetic acid	CMeAmPr-FPeSAA	C14H17O6SN2F11
N-carboxymethyl dimethylammoniopropyl-perfluorohexane sulfonamido acetic acid	CMeAmPr-FHxSAA	C15H17O6SN2F13
N-carboxymethyldimethyl ammoniopropyl-perfluorobutane sulfonamido propanoic acid	CMeAmPr-FBSAPrA	C14H19O6SN2F9
N-carboxymethyldimethyl ammoniopropyl-perfluoropentane sulfonamido propanoic acid	CMeAmPr-FPeSAPrA	C15H19O6SN2F11
N-carboxymethyldimethyl ammoniopropyl-perfluorohexane sulfonamido propanoic acid	CMeAmPr-FHxSAPrA	C16H19O6SN2F13
N-dimethyl ammonio propyl perfluoropentane sulfonamide	AmPr-FPeSA	C10H13O2N2SF11
N-dimethyl ammonio propyl perfluorohexane sulfonamide	AmPr-FHxSA	C11H13O2N2SF13
N-dimethyl ammonio propyl perfluorooctane sulfonamide	AmPr-FOSA	C13H13O2N2SF17
N-dimethylammoniocarboxypropyl-perfluoropentane sulfonamide	Am-CPr-FPeSA	C11H13O4SN2F11
N-dimethylammoniocarboxypropyl-perfluorohexane sulfonamide	Am-CPr-FHxSA	C12H13O4SN2F13
N-dimethylammoniocarboxypropyl-perfluorooctane sulfonamide	Am-CPr-FOSA	C14H13O4SN2F17

Appendix B – Table 3. Suspect (semi-quantifiable) Analytes Identified in Soil (Continued)

Compound Name	Acronym	Chemical Formula
N-ethyl dimethyl ammonio propyl perfluorohexane N-ethyl sulfonamide	EtAmPr-FHx-N-EtSA	C15H21O2SN2F13
N-ethyl dimethyl ammonio propyl perfluoroheptane N-ethyl sulfonamide	EtAmPr-FHp-N-EtSA	C16H21O2SN2F15
N-ethyl dimethyl ammonio propyl perfluorooctane N-ethyl sulfonamide	EtAmPr-FO-N-EtSA	C17H21O2SN2F17
N-hydroxyethyldimethylammoniopropyl perfluoropentanesulfonamidoethanol	EtOH-AmPr-FPeSA-EtOH	C14H21O4SN2F11
N-hydroxyethyldimethylammoniopropyl perfluorohexanesulfonamidoethanol	EtOH-AmPr-FHxSA-EtOH	C15H21O4SN2F13
N-hydroxyethyldimethylammoniopropyl perfluorooctanesulfonamidoethanol	EtOH-AmPr-FOSA-EtOH	C17H21O4SN2F17
N-hydroxyethyl dimethylammoniopropyl perfluorohexane sulfonamido propylsulfonate	EtOH-AmPr-FHxSAPrS	C16H23O6S2N2F13
N-hydroxyethyl dimethylammoniopropyl perfluorohexane sulfonamido propylsulfonate	EtOH-AmPr-FPeSA	C12H17O3SN2F11
N-hydroxyethyl dimethylammoniopropyl perfluorohexane sulfonamido propylsulfonate	EtOH-AmPr-FHxSA	C13H17O3SN2F13
N-hydroxyethyl dimethylammoniopropyl perfluorohexane sulfonamido propylsulfonate	EtOH-AmPr-FOSA	C15H17O3SN2F17
N-hydroxyethyl dimethylammoniopropyl perfluorohexane sulfonamido propylsulfonate	EtOH-AmPr-FDSA	C17H17O3SN2F21
N-sulfo propyl dimethyl ammonio propyl perfluorobutane sulfonamide	SPrAmPr-FBSA	C12H19O5S2N2F9
N-sulfo propyl dimethyl ammonio propyl perfluoropentane sulfonamide	SPrAmPr-FPeSA	C13H19O5S2N2F11
N-sulfo propyl dimethyl ammonio propyl perfluorohexane sulfonamide	SPrAmPr-FHxSA	C14H19O5S2N2F13
N-sulfo propyl dimethyl ammonio propyl perfluoroheptane sulfonamide	SPrAmPr-FHpSA	C15H19O5S2N2F15
N-sulfo propyl dimethyl ammonio propyl perfluorooctane sulfonamide	SPrAmPr-FOSA	C16H19O5S2N2F17
N-sulfopropyldimethylammoniopropyl N-methyl perfuorobutanesulfonamide	SPrAmPr-N-Me-FBSA	C13H21O5S2N2F9
N-sulfopropyldimethylammoniopropyl N-methyl perfuorohexanesulfonamide	SPrAmPr-N-Me-FHxSA	C15H21O5S2N2F13
N-sulfopropyl dimethylammoniopropyl perfluorohexane sulfonamido propyl sulfonate	SPrAmPr-FHxSAPrS	C17H25O8S3N2F13
N-sulfopropyldimethylammoniopropyl-perfluorohexane sulfonamido acetic acid	SPrAmPr-FHxSAA	C16H21O7S2N2F13
N-trimethylammoniopropyl N-methylperfluorobutanesulfonamide	TAmPr-N-MeFBSA	C11H17O2SN2F9

Appendix B – Table 3. Suspect (semi-quantifiable) Analytes Identified in Soil (Continued)

Compound Name	Acronym	Chemical Formula
N-trimethylammoniopropyl N-methylperfluoropentanesulfonamide	TAmPr-N-MeFPeSA	C12H17O2SN2F11
N-trimethylammoniopropyl N-methylperfluorohexanesulfonamide	TAmPr-N-MeFHxSA	C13H17O2SN2F13
N-trimethylammoniopropyl N-methylperfluoroheptanesulfonamide	TAmPr-N-MeFHpSA	C14H17O2SN2F15
N-trimethylammoniopropyl N-methylperfluorooctanesulfonamide	TAmPr-N-MeFOSA	C15H17O2SN2F17
N-Trimethylammoniopropyl perfluorohexane sulfonamide	TAmPr-FHxSA	C12H15O2SN2F13
N-Trimethylammoniopropyl perfluorooctane sulfonamide	TAmPr-FOSA	C14H15O2SN2F17
N-trimethylammoniopropyl perfluoropropane sulfonamido propanoic acid	TAmPr-FPrSAPrA	C12H19O4SN2F7
N-trimethylammoniopropyl perfluorobutane sulfonamido propanoic acid	TAmPr-FBSAPrA	C13H19O4SN2F9
N-trimethylammoniopropyl perfluorohexane sulfonamido propanoic acid	TAmPr-FHxSAPrA	C15H19O4SN2F13
N-trimethylammoniopropyl perfluoroheptane sulfonamido propanoic acid	TAmPr-FHpSAPrA	C16H19O4SN2F15
4:2 fluorotelomer sulfonamido propyl betaine	4:2 FTSA-PrB	C13H19O4N2SF9
6:2 fluorotelomer sulfonamido propyl dimethyl amine	6:2 FTSAPr-DiMeAn	C13H17O2N2SF13
8:2 fluorotelomer sulfonamido propyl dimethyl amine	8:2 FTSAPr-DiMeAn	C15H17O2N2SF17
8:2 fluorotelomer sulfonamido propyl methyl amine	8:2 FTSA-Pr-MeAn	C14H15O2N2SF17
4:2 fluorotelomer sulfonamido propyl methyl amino acetic acid	4:2 FTSA-Pr-MeAA	C12H17O4N2SF9
6:2 fluorotelomer sulfonamido propyl methyl amino acetic acid	6:2 FTSA-Pr-MeAA	C14H17O4N2SF13
6:2 fluorotelomer sulfonyl propanoamido-dimethylethyl sulfonate	6:2 FTSO2PrAd-DiMeEtS	C15H18O6NS2F13
8:2 fluorotelomer sulfonyl propanoamido-dimethylethyl sulfonate	8:2 FTSO2PrAd-DiMeEtS	C17H18O6NS2F17

APPENDIX C QUANTIFIABLE PFAS SOIL CONCENTRATIONS

Appendix C. Quantifiable PFAS soil concentrations as a function of depth for each site. PFAS concentrations are in µg/kg.

Site A																	
Depth (m bgs)	PFOSA	4:2 FTS	6:2 FTS	8:2 FTS	MeFOSA	MeFOSAA	PFBA	PFPeA	PFHxA	PFHpA	PFOA	PFNA	PFBS	PFPeS	PFHxS	PFHpS	PFOS
0.15	8.1	<0.784	<0.706	<0.784	<.2	<.2	1.77	0.743	2.34	2.91	3.43	<0.196	1.2	21.1	68.7	2.76	533
0.30	<.191	<0.805	<0.725	<0.805	<.2	<.2	<0.805	<0.402	14.5	32.2	0.423	<0.201	2.32	231	140	<0.201	25.8
0.46	<.189	<0.772	<0.696	<0.772	<.2	<.2	<0.772	<0.386	33	19	<0.193	<0.193	4.95	292	62.5	<0.193	0.518
0.61	<.098	<0.691	<0.623	<0.691	<.2	<.2	<0.691	0.411	86.9	7.17	<0.173	<0.173	11	261	25.7	<0.173	0.254
0.76	<.0395	<0.749	<0.675	<0.749	<.2	<.2	4.9	13.2	375	1.52	<0.187	<0.187	108	128	10.2	<0.187	<0.187
0.91	<.0396	<0.269	<0.242	<0.269	<.2	<.2	11.1	29.3	38	0.225	<0.0672	<0.0672	75.7	9.36	2.06	<0.0672	0.2
1.07	<.0391	<0.762	<0.687	<0.762	<.2	<.2	29.8	60.5	107	0.292	<0.19	<0.19	192	11.3	2.13	<0.19	<0.19
1.22	<.0396	<0.74	<0.667	<0.74	<.2	<.2	15.2	50.6	58.3	0.345	<0.185	<0.185	175	15.3	3.73	<0.185	<0.185
1.37	0.434	<1.33	<1.2	<1.33	<.2	<.2	20.1	53.8	431	4.3	<0.334	<0.334	297	106	32.8	<0.334	0.482
1.52	<.019	<0.764	<0.689	<0.764	<.2	<.2	51.2	95.9	132	1.08	<0.191	<0.191	226	30.4	9.41	<0.191	0.221
1.68	<.017	<0.756	<0.682	<0.756	<.2	<.2	19.4	118	267	2.44	<0.189	<0.189	480	71.9	24.3	<0.189	<0.189
1.83	<.187	<0.393	<0.354	<0.393	<.2	<.2	9.18	30.4	39.2	0.462	<0.0983	<0.0983	100	11.2	3.52	<0.0983	<0.0983
1.98	<.672	<0.158	<0.142	<0.158	<.2	<.2	5.39	17.4	22.3	0.189	<0.0395	<0.0395	53.2	7.6	1.84	<0.0395	0.046
2.13	<.19	<0.158	<0.143	<0.158	<.2	<.2	3.95	14.6	19.6	0.147	<0.0396	<0.0396	40.5	5.57	1.2	<0.0396	<0.0396
2.29	<.185	<0.156	<0.141	<0.156	<.2	<.2	2.45	10.1	13.3	0.096	<0.0391	<0.0391	32.9	4.49	0.827	<0.0391	<0.0391
2.44	<.334	<0.158	<0.143	<0.158	<.2	<.2	1.72	7.92	12.1	0.068	<0.0396	<0.0396	31.7	3.17	0.673	<0.0396	<0.99
Site B																	
Depth (m bgs)	PFOSA	4:2 FTS	6:2 FTS	8:2 FTS	MeFOSA	MeFOSAA	PFBA	PFPeA	PFHxA	PFHpA	PFOA	PFNA	PFBS	PFPeS	PFHxS	PFHpS	PFOS
0.15	0.324	<0.793	<0.715	<0.793	<.4	<.4	<0.793	<0.397	0.475	<0.0198	0.386	0.273	<0.198	<0.199	3.12	0.39	300
0.30	<.38	<1.53	<1.38	<1.53	<.4	<.4	1.7	<0.764	0.474	<0.0382	<0.0382	0.636	<0.382	<0.384	8.57	0.523	763
0.46	<.34	<1.36	<1.23	<1.36	<.4	<.4	1.65	<0.68	0.673	<0.034	0.899	1.08	<0.34	0.527	17.3	9.14	532
0.61	0.07	<0.256	<0.23	<0.256	<.4	<.4	0.998	0.623	1.65	0.109	5.16	0.328	0.282	1.19	27.4	14.8	82.6
0.76	<.0495	<0.198	<0.178	<0.198	<.4	<.4	1.34	0.968	2.04	0.094	10.2	0.052	0.628	2.18	48.9	5.15	9.9
0.91	<.0642	<0.257	<0.231	<0.257	<.4	<.4	1.25	0.827	2.44	0.134	7.27	<0.0642	0.892	1.86	69.9	0.555	1.91
1.07	<.1	<0.405	<0.365	<0.405	<.4	<.4	1.56	1.15	3.09	0.213	5.61	<0.101	2.87	2.08	132	<0.101	0.898
1.22	<.19	<0.759	<0.684	<0.759	<.4	<.4	0.986	0.47	1.1	0.511	3.93	<0.19	1.73	1.54	163	<0.19	0.666
1.37	<.178	<0.714	<0.643	<0.714	<.4	<.4	0.753	0.434	1.07	1.41	1.03	0.194	0.593	3.16	88.2	0.737	164
1.52	<.099	<0.397	<0.358	<0.397	<.4	<.4	0.523	0.419	2.1	2.76	0.629	<0.0993	0.967	9.41	113	<0.0993	5.04
1.68	<.067	<0.266	<0.24	<0.266	<.4	<.4	0.377	0.497	1.98	2.73	0.263	<0.0666	1.27	12.1	70.9	<0.0666	0.812
1.83	<.04	<0.157	<0.142	<0.157	<.4	<.4	0.298	0.491	5.01	1.84	0.086	<0.0393	3	24.9	22.1	<0.0393	0.194
1.98	<.04	<0.151	<0.136	<0.151	<.4	<.4	0.321	0.538	7.82	1.06	0.052	<0.0377	4.47	25.8	10.7	<0.0377	0.177
2.13	<.04	<0.156	<0.141	<0.156	<.4	<.4	0.374	0.608	10.7	0.974	0.043	<0.039	6.82	33.9	8.7	<0.039	0.175
2.29	<.04	<0.159	<0.143	<0.159	<.4	<.4	0.302	0.4	8.39	0.181	<0.00398	<0.0398	4.55	16.7	1.52	<0.0398	0.067
2.44	<.04	<0.159	<0.144	<0.159	<.4	<.4	0.392	0.427	7.48	0.204	<0.00398	<0.0398	5.65	15.8	1.98	<0.0398	0.105

Site C

Depth (m bgs)	PFOSA	4:2 FTS	6:2 FTS	8:2 FTS	MeFOSA	MeFOSAA	PFBA	PFPeA	PFHxA	PFHpA	PFOA	PFNA	PFBS	PFPeS	PFHxS	PFHpS	PFOS
0.10	884	<15	359	1320	13.1	12.4	<16	32.8	40.2	23.4	80.1	93.6	6.05	9.33	166	12.6	5500
0.20	339	<16	135	832	4.77	<3.9	<16	16.9	19.1	9.91	35.2	44.4	<3.9	<3.9	58.3	<3.9	3090
0.30	109	<8.3	127	411	2.25	<3.9	<8.3	15.3	13.1	6.26	21	18.6	<2.1	2.58	42	2.59	1940
0.41	10.6	<1.7	98.1	136	<0.418	<0.418	3.13	11.9	14.6	5.27	12.3	6.64	1.72	2.38	25.6	1.67	1010
0.51	17.5	<16	305	812	<4.0	<4.0	<16	17.5	32.9	12.5	45.1	28.4	4.64	7.45	74.9	18.3	12000
0.61	17	<16	328	515	<4.1	<4.1	<16	<8.1	17.1	9.56	34.2	8.71	<4.1	4.42	98.2	9.5	5050
0.71	13.8	<16	446	904	<4.0	<4.0	<16	10.4	17.3	7.29	64.9	20	<4.0	<4.0	103	13.9	7830
0.81	33.1	<16	301	560	<4.1	<4.0	<16	13.2	20.5	9.93	53.3	15.5	<4.0	6.13	125	25.6	5750
0.91	114	<26	1190	3040	<6.4	<6.4	<26	43.9	61.5	27.3	299	67.3	7.86	20.5	567	247	39400

Site D

Depth (m bgs)	PFOSA	4:2 FTS	6:2 FTS	8:2 FTS	MeFOSA	MeFOSAA	PFBA	PFPeA	PFHxA	PFHpA	PFOA	PFNA	PFBS	PFPeS	PFHxS	PFHpS	PFOS
0.15	0.13	<0.165	<0.149	0.221	<.2	<.2	<0.165	0.156	0.312	0.148	0.383	0.23	<0.0413	<0.0415	0.394	<0.0413	11.4
0.30	0.152	<0.332	<0.299	0.826	<.2	<.2	<0.332	<0.166	0.247	0.241	0.572	1.42	<0.0831	<0.0835	0.708	<0.0831	124
0.46	0.795	<0.57	<0.514	5.94	<.2	<.2	<0.57	<0.285	0.168	<0.143	0.617	1.74	<0.143	<0.143	0.448	<0.143	171
0.61	0.901	<0.559	<0.504	7.07	<.2	<.2	<0.559	<0.28	0.198	0.175	0.51	1.47	<0.14	<0.14	0.421	<0.14	159
0.76	0.81	<0.558	<0.503	10	<.2	<.2	<0.558	<0.279	0.162	0.189	0.608	1.59	<0.14	<0.14	0.455	<0.14	194
0.91	1.29	<0.574	<0.517	25.3	<.2	<.2	<0.574	<0.287	0.208	0.194	0.778	2.54	<0.143	<0.144	0.597	<0.143	273
1.07	1.95	<0.611	<0.551	28.7	<.2	<.2	<0.611	<0.305	0.191	0.193	0.725	2.05	<0.153	<0.154	0.459	<0.153	242

Site E

Depth (m bgs)	PFOSA	4:2 FTS	6:2 FTS	8:2 FTS	MeFOSA	MeFOSAA	PFBA	PFPeA	PFHxA	PFHpA	PFOA	PFNA	PFBS	PFPeS	PFHxS	PFHpS	PFOS
0.15	728	< 8.65	< 7.79	< 8.65	10.3	24.7	< 8.67	5.18	12	5.43	40.9	2.72	2.56	2.51	113	3.18	2170
0.30	1190	< 17.1	< 15.4	< 17.1	15.2	33.3	< 17.1	< 8.55	20.2	10	68.5	5.01	5.58	6.57	232	5.37	4140
0.46	998	< 25.4	< 22.9	< 25.4	< 6.35	35.9	< 25.5	< 12.7	37.8	15.4	92.5	9.55	13.3	12.4	301	< 6.35	7650
0.61	1330	< 41.2	< 37.2	101	11.1	46	51.9	37.1	108	25.7	156	13.3	32.4	30.1	493	11.2	13500
0.76	701	< 35.6	< 32	67.1	< 8.89	27.9	< 35.6	26.5	97.3	17.5	99.6	10.5	23.8	21.6	372	< 8.89	11400
0.91	499	< 38.5	< 34.7	< 38.5	< 9.62	28	< 38.6	< 19.2	58	12.5	71.7	10.5	13.7	10.3	212	< 9.62	9930
1.07	321	< 25.8	< 23.3	29.6	< 6.45	15.3	< 25.9	< 12.9	41	11	60	8.44	9.41	7.15	156	7.2	8890
1.22	326	< 26.1	< 23.5	< 26.1	< 6.51	16.4	< 26.1	< 13	46.3	10.3	59.6	8.75	11.8	6.72	193	8.81	9930
1.37	208	< 30.1	< 27.1	< 30.1	< 7.52	10.7	< 30.2	18.5	51.5	9	79.4	11	11.7	< 7.56	228	32.6	7920
1.52	206	< 28.5	< 25.7	< 28.5	< 7.12	8.42	< 28.5	17	63.7	10.8	72.2	8.51	11.2	7.26	216	32.3	6740
1.68	69.8	< 8.44	< 7.61	< 8.44	< 2.11	2.56	< 8.46	6.37	31.8	5.14	29.7	3.35	6.25	4.69	120	13.3	2710
1.83	63.9	< 8.66	< 7.8	< 8.66	< 2.16	< 2.49	< 8.68	4.99	37.9	8.19	41.1	4.81	6.38	6.37	163	17.3	3200
1.98	28.1	< 8.08	< 7.28	< 8.08	< 2.02	< 2.32	< 8.1	< 4.04	28.4	6.93	24.4	3.46	3.13	5.19	102	8.38	1710

APPENDIX D SEMI-QUANTIFIED PFAS CONCENTRATIONS IN SOIL

The soil sample was collected at the approximate depth of the lysimeter, as listed in Exhibit S1. An EXCEL version of this table is also included.

Site A	
PFAS	**µg/kg**
5:3 K-FTTh-K-OH-PrA	32.16
FPrSA	23.99
FPrSAA	0.50
MeFPrAA	1.34
H-PFHxA	1.52
H-PFPeA	1.98
PFCPeCA	1.34
EtOH-AmPr-FPeSA-EtOH	0.20
Site B	
PFAS	**µg/kg**
EtOH-AmPr-FPeSA-EtOH	0.341605

Site C				
PFAS	**µg/kg**		**PFAS**	**µg/kg**
1OH-6:2 FTS	1.75		4:2 FTSA-Pr-MeAA	3.09
1OH-7:2 FTS	1.11		6:2 FTSA-Pr-MeAA	9.60
1OH-8:2 FTS	12.69		CEtAmPr-FPeSA-PrA	2.78
PFBCHxS	9.70		CEtAmPr-FHxSA-PrA	25.45
PFPeCHxS	4.76		CMeAmPr-FBSA	5.36
PFHxCHxS	3.15		CMeAmPr-FPeSA	62.05
diOHBAmPr-FHxSA	3.58		CMeAmPr-FHxSA	455.82
diOHBAmPr-FOSA	0.14		CMeAmPr-FPeSAA	8.33
diOHPrAm-MeOHPr-FHxSA	0.24		CMeAmPr-FHxSAA	240.68
diOHPrAm-MeOHPr-FHxSAPrS	2.69		CMeAmPr-FBSAPrA	11.47
F5S-PFNA	0.27		CMeAmPr-FPeSAPrA	4.00
F5S-PFHpS	4.86		CMeAmPr-FHxSAPrA	96.77
F5S-PFOS	22.95		AmPr-FPeSA	4.88
F5S-PFNS	12.85		AmPr-FHxSA	124.98
F5S-PFDS	0.40		AmPr-FOSA	0.94
FPrSA	0.53		Am-CPr-FPeSA	0.45
FNSA	0.42		Am-CPr-FHxSA	12.75
FDSA	0.50		Am-CPr-FOSA	18.25
H-PFNS	0.21		EtOH-AmPr-FOSA-EtOH	0.82
H-PFDS	0.94		EtOH-AmPr-FHxSA	8.51
H-UPFOS	7.55		EtOH-AmPr-FDSA	19.95
H-UPFDS	8.60		SPrAmPr-FBSA	1.58
H-UPFPeDS	0.96		SPrAmPr-FPeSA	11.22
K-PFHxS	0.14		SPrAmPr-FHxSA	763.05
K-PFOS	0.87		SPrAmPr-FOSA	2.88
MeFBSA	0.11		SPrAmPr-N-Me-FBSA	1.46
MeFHxSA	5.78		SPrAmPr-N-Me-FHxSA	16.04
PFHp-OS	0.24		SPrAmPr-FHxSAA	58.56
PFO-OS	10.57		TAmPr-N-MeFBSA	4.20
PFN-OS	15.53		TAmPr-N-MeFPeSA	7.07
PFD-OS	0.88		TAmPr-N-MeFHxSA	130.05
PFUd-OS	0.78		TAmPr-N-MeFOSA	7.85
PFTrDS	5.49		TAmPr-FHxSA	13.06
PFTeDS	3.98		TAmPr-FOSA	4.42
PFPeDS	1.40		TAmPr-FHxSAPrA	6.39
PFHxDS	2.24		4:2 FTSA-PrB	1.27
PFPeSi	0.09		8:2 FTSO2PrAd-DiMeEtS	38.84
PFHxSi	2.35			
SPr-FHxSA	7.83			
SPr-FOSA	1.62			
6:2 FTSA	2.76			
8:2 FTSA	0.53			
8:2 FTSO2PrA	41.54			

Site D	
PFAS	**µg/kg**
PFUdS	0.8
diOHBAmPr-FHxSA	4.6
6:2 FTSAPr-DiMeAn	136.5
8:2 FTSA-Pr-MeAn	7.8
EtAmPr-FHx-N-EtSA	37.8
EtOH-AmPr-FHxSA	3.8
TAmPr-FOSA	8.5
TAmPr-N-MeFHxSA	148.6

Site E				
PFAS	**µg/kg**		**PFAS**	**µg/kg**
12:2 FTS	1.43		diOHBAmPr-FBSA	0.44
PFTrDS	52.16		diOHBAmPr-FPeSA	1.25
PFTeDS	53.03		diOHBAmPr-FHxSA	49.12
PFPeDS	29.63		diOHPrAm-MeOHPr-FHxSA	1.69
UPFTeDS	21.99		FPrSA	28.34
UPFTrDS	21.41		FPeSA	11.99
H-PFPrS	0.70		FHpSA	28.27
H-PFBS	1.18		FNSA	4.05
H-PFPeS	0.58		SPr-FBSA	0.16
H-PFHxS	1.58		SPr-FHxSA	36.52
H-PFOS	13.53		FHxSAA	15.98
H-PFNS	6.43		MeFBSA	1.52
K-PFHxS	0.98		MeFPeSA	1.25
K-PFHpS	0.27		MeFHxSA	40.36
K-PFNS	6.90		MeFHpSA	1.76
K-PFOS	19.13		MeFPrAA	1.19
F5S-PFHxS	7.18		EtFHxSA	1.71
F5S-PFHpS	11.57		BPr-FPeAd	3.83
F5S-PFOS	72.83		AmPr-FHxSA	9.18
F5S-PFDS	8.90		CMeAmPr-FPeSA	6.72
PFTrDA	3.48		CMeAmPr-FHxSA	546.91
PFTeDA	2.45		CEtAmPr-FPeSA	2.03
H-PFHxA	2.08		CEtAmPr-FHpSA	11.46
F5S-PFOA	4.84		CEtAmPr-FHxSA-PrA	5.63
F5S-PFNA	164.88		EtOH-AmPr-FHxSA	28.34
PFCHxS	1.56		EtOH-AmPr-FHxSAPrS	3.15
PFEtCHxS	12.35		SPrAmPr-FHxSA	371.68
PFBCHxS	22.94		SPrAmPr-FHpSA	10.72
PFPeCHxS	17.20		SPrAmPr-N-Me-FHxSA	35.63
PFHxSi	3.22		SPrAmPr-FHxSAA	77.7
PFOSi	3.55		SPrAmPr-FHxSAPrS	23.37
6:2 FTOS	1.57		TAmPr-FBSAPrA	3.55
8:2 FTOS	8.48		TAmPr-FHpSAPrA	32.1
7:1 PFOS	1.41		TAmPr-FHxSA	32.19
PFB-OS	0.46		TAmPr-FOSA	25.36
PFHp-OS	5.59		TAmPr-N-MeFBSA	16.75
PFO-OS	31.79		TAmPr-N-MeFPeSA	38.14
PFN-OS	39.63		TAmPr-N-MeFHxSA	1435.12
PFD-OS	6.67		TAmPr-N-MeFHpSA	5.19
PFUd-OS	6.53		Class 38-C12	5.34
PFDo-OS	10.29		Class 38-C13	16.67
PFTrD-OS	6.97		Class 38-C14	26.02
PFTeD-OS	20.17		Class 38-C15	1440.08
			Class 38-C17	57.46

APPENDIX E PFAS POREWATER CONCENTRATIONS (µG/L)

For Site C, only semi-quantified PFAS accounting for at least 1% of the semi-quantified PFAS mass are included. L1 through L3 are the lysimeters. Concentrations presented in this table are the directly measured values (not corrected for the bromide-based dilution factors). <LOQ means below quantification level.

Soil A	L1	L2		L3		
	Round 2	Round 1	Round 2	Round 1	Round 2	Round 3
PFBA	5.15	81.92	175.28	6.12	14.91	31.44
PFPeA	23.45	217.66	408.23	6.83	13.99	28.77
PFHxA	99.04	521.92	662.75	39.59	70.48	122.49
PFHpA	1.52	3.23	3.99	7.43	11.37	15.04
PFOA	1.26	2.88	3.53	1.88	1.24	1.06
PFNA	<LOQ	<LOQ	<LOQ	<LOQ	<LOQ	<LOQ
PFBS	125.43	820.30	1368.30	65.95	116.28	215.83
PFPeS	42.43	106.57	168.27	93.89	143.55	209.01
PFHxS	32.61	43.88	47.96	98.35	119.18	133.98
PFHpS	0.82	1.76	2.20	1.35	0.60	< LOQ
PFOS	4.06	3.56	4.99	15.18	6.63	2.57
FBSA	7.7	61.90	113.42	8.76	12.44	21.27
FHxSA	6.7	4.68	5.04	5.13	2.31	1.52
4:2 FTS	<LOQ	<LOQ	<LOQ	<LOQ	<LOQ	<LOQ
6:2 FTS	<LOQ	<LOQ	<LOQ	<LOQ	<LOQ	<LOQ
8:2 FTS	<LOQ	<LOQ	<LOQ	<LOQ	<LOQ	<LOQ
Semi-quantified						
FBSAA	0.63	2.29	3.86	<LOQ	<LOQ	<LOQ
FEtSAA	< LOQ	3.09	4.90	<LOQ	<LOQ	<LOQ
FPeSA	2.83	5.19	6.46	2.68	2.60	3.18
FPrSA	15.41	109.92	<LOQ	9.64	15.51	29.86
FPrSAA	1.13	34.70	<LOQ	0.43	0.55	0.65
H-PFHxA	<LOQ	3.43	5.47	<LOQ	<LOQ	<LOQ
H-PFHxS	<LOQ	<LOQ	0.58	<LOQ	<LOQ	<LOQ
H-PFPeS	<LOQ	<LOQ	0.82	<LOQ	<LOQ	<LOQ
K-PFHxS	<LOQ	<LOQ	0.81	0.82	1.30	1.91
K-PFPeS	<LOQ	6.06	12.68	<LOQ	<LOQ	<LOQ
MeFMeSAA	2.64	18.40	<LOQ	<LOQ	<LOQ	3.98
PFEtS	1.01	9.84	20.22	<LOQ	0.92	2.66
PFMeCPeS	<LOQ	2.54	4.52	<LOQ	1.00	1.48
PFPrA	<LOQ	12.93	38.54	<LOQ	<LOQ	5.39
PFPrCPeS	<LOQ	0.58	0.80	<LOQ	<LOQ	< LOQ
SPr-FBSA	<LOQ	<LOQ	0.47	<LOQ	<LOQ	<LOQ
CEtAmPr-FBSA	<LOQ	<LOQ	<LOQ	0.27	<LOQ	<LOQ
CEtAmPr-FPeSA	<LOQ	<LOQ	<LOQ	0.38	0.31	<LOQ
CEtAmPr-FPrSA	<LOQ	0.71	1.08	< LOQ	<LOQ	<LOQ
CMeAmPr-FHxSA	0.59	<LOQ	<LOQ	<LOQ	<LOQ	<LOQ
SPrAmPr-FBSA	<LOQ	0.31	0.33	0.42	0.47	<LOQ
SPrAmPr-FBSAA	0.25	0.34	0.47	0.27	0.44	<LOQ
SPrAmPr-FBSAPrS	<LOQ	<LOQ	<LOQ	0.58	1.23	<LOQ
SPrAmPr-FHxSAPrS	0.31	<LOQ	0.39	0.46	0.00	<LOQ
SPrAmPr-FPeSAPrS	<LOQ	<LOQ	<LOQ	0.46	0.78	<LOQ
SPrAmPr-FPrSA	<LOQ	<LOQ	0.53	<LOQ	<LOQ	<LOQ
SPrAmPr-FPrSAA	<LOQ	1.32	3.04	<LOQ	<LOQ	<LOQ
SPrAmPr-FPrSAPrS	<LOQ	0.68	1.48	<LOQ	<LOQ	<LOQ
TAmPr-FBSAPrA	0.60	1.40	2.39	1.18	1.66	<LOQ
dilution factor	***31***	***17***	***4.6***	***13***	***7***	***3.9***

Soil B	L1		L3	
	Round 1	Round 2	Round 1	Round 2
PFBA	< LOQ	< LOQ	< LOQ	< LOQ
PFPeA	< LOQ	0.59	0.41	0.50
PFHxA	0.80	1.74	1.53	1.83
PFHpA	< LOQ	< LOQ	0.41	0.49
PFOA	< LOQ	< LOQ	< LOQ	< LOQ
PFNA	< LOQ	< LOQ	< LOQ	< LOQ
PFBS	0.35	1.14	0.62	1.19
PFPeS	0.96	2.61	1.82	3.22
PFHxS	3.31	4.59	9.83	9.13
PFHpS	< LOQ	0.05	0.16	0.09
PFOS	< LOQ	0.19	4.44	1.99
FBSA	< LOQ	< LOQ	0.07	0.11
FHxSA	0.02	0.03	0.49	0.22
4:2 FTS	< LOQ	< LOQ	< LOQ	< LOQ
6:2 FTS	< LOQ	< LOQ	72.97	57.12
8:2 FTS	< LOQ	< LOQ	< LOQ	< LOQ
Semi-quantified				
6:2 FTOS	< LOQ	0.00	0.50	0.43
6:2 UFTS	< LOQ	0.00	0.21	0.18
FHxSAA	< LOQ	0.00	0.04	0.03
FPeSA	< LOQ	0.00	0.06	0.05
FPrSA	0.06	0.16	0.10	0.21
MeFBSAA	< LOQ	0.00	0.00	0.36
MeFHxSAA	< LOQ	0.00	1.10	0.56
MeFPeSAA	< LOQ	0.00	0.29	0.24
MeFPrSAA	< LOQ	0.00	0.16	0.14
PFMeCPeS	< LOQ	0.04	0.00	0.00
PFMeCPeS	< LOQ	0.04	0.00	0.00
6:3 OH-FT-TAm	1.22	1.27	1.35	1.26
SPrAmPr-FHxSA	< LOQ	0.00	0.36	0.00
dilution factor		***1.2***	***4.7***	*4.2*

Grayed boxes are not used for further evaluation, but are presented in this table for comparative purposes

Soil C	L1			L2		L3	
	Round 1	Round 2	Round 3	Round 2	Round 3	Round 2	Round 3
PFBA	4.24	11.00	14.42	17.28	21.56	12.83	19.82
PFPeA	12.06	34.23	47.88	49.48	73.56	48.42	78.96
PFHxA	15.99	33.99	56.18	48.30	75.44	49.63	88.55
PFHpA	2.98	3.74	6.82	3.86	5.04	5.14	10.02
PFOA	4.36	3.14	4.81	4.60	3.82	3.94	4.89
PFNA	< LOQ	< LOQ	< LOQ	< LOQ	< LOQ	< LOQ	< LOQ
PFBS	1.79	4.36	7.15	6.79	10.99	7.09	12.59
PFPeS	2.49	4.42	9.00	3.97	6.49	5.78	11.25
PFHxS	15.97	17.47	35.25	13.55	14.71	15.49	24.78
PFHpS	0.48	0.32	0.43	0.39	0.31	0.29	0.30
PFOS	15.44	13.53	18.86	6.47	18.61	3.48	15.22
FBSA	1.86	2.72	4.33	3.05	3.35	5.22	8.51
FHxSA	4.24	3.12	2.71	2.72	2.39	5.47	5.18
4:2 FTS	0.59	1.35	2.31	1.65	2.61	1.74	3.33
6:2 FTS	25.35	19.12	27.42	22.19	19.65	27.36	31.74
8:2 FTS	0.55	1.07	1.95	0.14	0.56	0.22	0.82
Semi-quantified							
1OH-3:2 FTS	<LOQ	0.04	0.05	0.05	0.07	<LOQ	0.07
1OH-4:2 FTS	0.20	0.54	0.83	0.81	1.33	0.86	1.64
1OH-5:2 FTS	0.09	0.19	0.34	0.27	0.39	0.29	0.64
1OH-6:2 FTS	0.47	0.46	0.84	0.54	0.49	0.55	0.89
1OH-7:2 FTS	0.04	<LOQ	<LOQ	0.07	0.06	<LOQ	<LOQ
1OH-8:2 FTS	0.12	0.12	0.10	0.06	0.14	0.05	0.11
PFCHxS	0.04	0.08	0.16	0.09	0.14	0.12	0.21
FEtSA	<LOQ	0.11	0.12	0.13	0.15	0.12	0.16
FPrSA	0.93	1.81	2.64	2.70	3.12	3.17	4.66
FPeSA	0.84	0.57	1.00	0.79	0.68	1.53	1.96
FPrSAA	0.02	0.02	0.03	0.03	0.04	0.01	0.01
FBSAA	0.12	0.16	0.25	0.12	0.15	0.05	0.10
FPeSAA	0.10	0.10	0.18	0.08	0.08	0.04	0.11
FHxSAA	0.31	0.29	0.49	0.50	0.36	0.15	0.29
H-PFOA	0.00	0.48	0.80	0.57	0.82	0.49	0.77
H-PFEtS	0.13	0.19	0.25	0.12	0.16	<LOQ	<LOQ
H-PFPrS	0.01	0.02	0.02	0.02	0.02	0.02	0.03
H-PFBS	<LOQ	<LOQ	<LOQ	<LOQ	0.04	<LOQ	0.05
H-PFPeS	0.00	0.01	0.02	0.02	0.03	0.02	0.04
H-PFHxS	0.07	0.17	0.33	0.16	0.23	0.17	0.40
H-UPFOS	0.02	0.02	0.03	0.02	0.01	0.01	0.02
K-PFPeS	<LOQ	<LOQ	0.05	0.00	0.07	0.04	0.09
K-PFHxS	0.05	0.08	0.16	0.06	0.10	0.09	0.18
K-PFOS	0.03	0.02	0.03	0.03	0.02	0.02	0.03

	MeFMeSAA	0.18	0.00	0.51	0.54	0.73	0.49	0.69
	MeFEtSAA	2.61	2.48	2.92	2.82	3.21	2.49	3.13
	MeFPrAA	0.12	<LOQ	<LOQ	<LOQ	0.19	0.18	0.32
	MeFBSAA	0.28	0.19	0.26	0.26	<LOQ	0.21	0.25
	MeFHxSAA	2.29	2.32	2.29	2.39	2.34	2.10	2.20
	PeH-FHpOS	0.04	0.09	0.15	0.13	0.16	0.10	0.18
	PFPe-OS	0.01	0.01	0.03	0.01	0.02	0.02	0.04
	PFPrCPeS	0.16	0.15	0.29	0.11	0.09	0.10	0.15
	PFEtS	0.04	0.06	0.10	0.10	0.14	0.11	0.16
	PFPeSi	<LOQ	0.02	0.03	0.02	0.04	0.03	0.07
	PFHxSi	<LOQ	<LOQ	0.12	0.09	0.10	<LOQ	0.09
	SPr-FBSA	<LOQ	<LOQ	0.21	0.16	0.24	0.33	0.34
	SPr-FPeSA	<LOQ	<LOQ	0.19	<LOQ	<LOQ	0.26	0.22
	SPr-FHxSA	1.83	1.42	1.41	1.19	1.21	2.31	1.30
	7:1 PFOS	0.02	0.01	0.00	0.01	<LOQ	<LOQ	0.01
	8:2 FTOS	0.12	0.12	0.10	0.06	0.14	0.05	0.11
	4:2 FTSi	0.04	0.04	0.06	0.07	0.06	0.06	0.07
	6:2 FTSi	0.10	0.16	0.24	0.17	0.23	0.17	0.18
	8:2 FTSi	0.02	0.02	0.02	0.02	0.02	0.01	0.02
	6:2 FTSO2PrAd-DiMeEt	1.36	0.71	0.52	1.06	0.86	0.42	0.33
	6:2 UFTS	0.10	0.06	0.10	0.08	0.07	0.10	0.12
	4:3 FTS	<LOQ	<LOQ	<LOQ	<LOQ	<LOQ	0.04	0.07
	6:3 K-FTTh-K-OH-PrA	0.25	<LOQ	<LOQ	<LOQ	0.13	0.14	<LOQ
	CEtAmPr-N-EtFPrSA	0.41	0.29	0.00	0.56	<LOQ	0.41	0.49
	CMeAmPr-FPrSA	<LOQ	<LOQ	<LOQ	1.38	<LOQ	1.56	2.48
	CMeAmPr-FBSA	3.44	2.39	2.58	3.24	2.42	5.19	4.67
	CMeAmPr-FPeSA	1.36	1.32	1.17	2.79	1.80	4.04	3.75
	CMeAmPr-FHxSA	0.75	1.91	1.93	1.11	2.92	2.20	2.60
	CMeAmPr-FPrSAA	0.35	0.70	0.87	0.73	0.90	0.56	0.87
	CMeAmPr-FBSAA	2.01	2.12	2.57	2.20	2.20	1.76	2.55
	CMeAmPr-FPeSAA	1.89	1.35	1.57	2.12	1.85	2.20	2.15
	CMeAmPr-FHxSAA	1.60	1.87	0.53	1.39	5.71	1.14	1.14
	AmPr-FPeAd	<LOQ	0.06	<LOQ	<LOQ	<LOQ	<LOQ	<LOQ
	Am-CPr-FHxSA	0.11	0.09	0.10	0.09	<LOQ	0.10	0.11
	Am-CPr-FHpSA	0.11	0.11	<LOQ	0.12	<LOQ	0.28	0.24
	Am-CPr-FOSA	0.16	0.42	0.44	0.20	0.46	0.43	0.53
	SPrAmPr-FPrSA	<LOQ	<LOQ	<LOQ	1.13	<LOQ	1.04	1.73
	SPrAmPr-FBSA	3.06	2.18	2.43	2.47	2.06	2.69	2.67
	SPrAmPr-FPeSA	2.72	2.55	1.92	2.94	1.79	7.80	6.22
	SPrAmPr-FHxSA	3.48	9.52	11.22	3.01	11.66	11.19	13.27
	S-OHPrAmPr-FBSA	0.31	0.25	0.32	0.29	0.30	0.27	0.30
	S-OHPrAmPr-FHxSAA	1.39	1.04	<LOQ	0.67	0.58	0.81	0.73
	S-OHPrAmPr-FHpSAA	0.54	0.65	0.61	0.43	0.51	1.09	0.89
	S-OHPrAmPr-FHxSA-OH	0.46	<LOQ	0.42	<LOQ	<LOQ	<LOQ	<LOQ
	SPrAmPr-FPrSAPrS	0.00	0.38	0.47	0.40	0.53	0.34	0.61
	SPrAmPr-FBSAPrS	0.92	1.07	1.43	0.88	1.02	0.74	1.32
	SPrAmPr-FPeSAPrS	0.55	0.43	0.52	0.37	0.31	0.32	0.37
	SPrAmPr-FHxSAPrS	4.20	4.50	4.09	3.00	3.66	8.74	6.77
	SPrAmPr-FPrSAA	<LOQ	0.55	<LOQ	0.68	0.97	0.68	0.76
	SPrAmPr-FBSAA	1.20	1.66	2.21	1.78	2.30	1.62	2.80
	SPrAmPr-FPeSAA	1.14	0.69	1.19	0.79	0.69	0.61	0.86
	SPrAmPr-FHxSAA	8.54	7.55	7.06	7.72	7.57	11.60	9.82
	TAmPr-N-MeFPeSA	0.14	0.06	<LOQ	0.21	0.06	0.22	0.45
	TAmPr-FHpSAPrA	<LOQ	<LOQ	<LOQ	<LOQ	0.11	0.26	0.16
	6:2 FTSO2PrAd-DiMeEt	0.17	0.11	<LOQ	0.14	0.13	<LOQ	<LOQ
	dilution factor	***2.4***	***1.5***	***1.2***	***3.3***	***2.0***	***2.4***	***1.5***

Soil D	L1			L2			L3	
	Round 1	Round 2	Round 3	Round 1	Round 2	Round 3	Purge	Round 1
PFBA	0.31	0.26	0.47	0.3	< LOQ	< LOQ	0.24	0.4
PFPeA	0.72	0.73	0.76	0.62	0.58	0.65	0.61	0.64
PFHxA	0.96	1.04	1.16	0.81	0.95	1	0.84	0.76
PFHpA	0.48	0.56	0.64	0.45	0.49	0.6	0.28	0.32
PFOA	0.38	0.48	0.59	0.43	0.5	0.59	0.21	0.26
PFNA	0.09	0.13	0.18	0.16	0.21	0.27	0.05	0.05
PFBS	0.09	0.06	0.07	0.05	0.07	0.05	0.09	0.14
PFPeS	0.05	0.06	0.06	0.04	0.04	0.05	0.04	0.04
PFHxS	0.69	0.82	0.98	0.48	0.57	0.67	0.23	0.24
PFHpS	0.02	0.03	0.04	0.02	0.02	0.03	0.01	0.01
PFOS	3.66	9.31	15.23	7.99	12.16	22.04	0.8	0.91
FBSA	0.02	0.02	0.03	0.02	0.02	0.02	< LOQ	< LOQ
FHxSA	0.25	0.26	0.3	0.4	0.41	0.46	0.17	0.2
4:2 FTS	0.03	< LOQ	0.02	0.03	< LOQ	0.02	0.06	0.07
6:2 FTS	0.21	0.26	0.33	0.31	0.35	0.45	0.23	0.31
8:2 FTS	0.05	0.22	0.47	0.13	0.4	0.67	0.02	0.03
Semi-quantified								
FPeSA	0.02	0.00	0.03	0.02	0.00	0.00	0.00	0.02
CMeAmPr-FHxSA	0.06	0.08	0.00	0.00	0.00	0.00	0.00	0.00
TAmPr-FHxSA	0.00	0.00	0.00	0.00	0.16	0.00	0.00	0.00

Soil E	L2		L3		
	Round 1	Round 2	Round 1	Round 2	Round 3
PFBA	1.35	0.00	1.39	< LOQ	< LOQ
PFPeA	4.87	4.35	3.08	2.24	1.98
PFHxA	22.65	17.78	7.82	3.68	3.6
PFHpA	4.27	3.04	1.68	1.13	1
PFOA	10.13	15.45	1.58	7.07	6.46
PFNA	<LOQ	0.52	0.1	0.44	0.38
PFBS	5.94	4.81	2.85	1.23	1.08
PFPeS	5.76	3.75	2.08	0.81	0.71
PFHxS	138.62	104.42	35.99	43.55	41.28
PFHpS	0.00	1.29	0.18	0.87	0.89
PFOS	0.21	81.74	5.04	46.24	45.78
FBSA	5.30	4.73	1.51	0.67	0.6
FHxSA	99.88	99.44	29.65	26.62	26.78
4:2 FTS	< LOQ	< LOQ	< LOQ	< LOQ	< LOQ
6:2 FTS	0.81	1.84	0.24	0.8	0.9
8:2 FTS	< LOQ	< LOQ	< LOQ	< LOQ	< LOQ
Semi-quantified					
FHxSAA	0.44	0.63	0.12	0.20	0.22
FPeSA	3.93	2.68	1.05	0.32	0.34
FPrSA	1.82	1.76	1.06	0.57	0.53
K-PFHxS	0.18	0.11	0.06	<LOQ	<LOQ
PFCHxS	0.20	0.14	0.07	<LOQ	0.03
PFHx-OS	0.06	0.08	<LOQ	<LOQ	<LOQ
PFHxSi	0.25	0.24	0.14	0.13	0.09
SPr-FHxSA	0.50	1.42	0.00	0.71	0.66
SPrAmPr-FHxSA	0.12	0.76	0.49	0.87	0.84
FPrSAA	0.06	0.07	0.05	0.04	0.04
MeFHxSA	0.14	0.24	<LOQ	0.77	0.50
diOHBAmPr-FPeSA	<LOQ	1.23	<LOQ	<LOQ	<LOQ
FHpSA	<LOQ	1.36	0.09	0.81	0.79
diOHBAmPr-FHxSA	<LOQ	<LOQ	0.15	1.94	0.68
SPrAmPr-FHxSAPrS	<LOQ	<LOQ	<LOQ	<LOQ	0.22
4:2 FTSO2-EtAdPrTAm	<LOQ	25.00	16.34	21.02	0.00
Am-CPr-FOSA	<LOQ	<LOQ	<LOQ	<LOQ	3.36
CMeAmPr-FHxSA	<LOQ	21.48	10.66	48.15	52.46
CMeAmPr-FHxSAA	<LOQ	<LOQ	<LOQ	8.40	<LOQ
SPrAmPr-FHxSA	8.43	36.80	22.97	63.65	61.50
SPrAmPr-FHxSAA	<LOQ	<LOQ	<LOQ	6.59	<LOQ
TAmPr-FHpSAPrA	<LOQ	<LOQ	<LOQ	<LOQ	16.20
TAmPr-N-MeFBSA	273.79	392.62	36.07	19.32	20.11

Site G		L24				L27				L29			
		Round 1	Round 2	Round 3	Round 4	Round 1	Round 2	Round 3	Round 4	Round 1	Round 2	Round 3	Round 4
PFHxA	µg/L	498.12	909.01	193.18	986.64	165.65	143.74	124.51	321.28	92.70	117.59	77.27	4.09
PFOA	µg/L	337.52	679.56	56.25	559.18	185.25	329.32	257.87	186.91	272.90	211.11	167.44	8.83
FHxSA	µg/L	153.29	180.06	57.35	102.00	1037.73	1644.99	1342.95	640.99	407.90	558.93	372.35	12.71
PFHxS	µg/L	1427.84	2642.04	250.84	2641.76	858.64	1049.05	750.15	861.81	557.68	651.60	381.30	27.70
PFOS	µg/L	18.40	104.18	64.16	94.01	48.19	79.08	34.98	53.47	173.89	274.08	142.05	127.37

APPENDIX F POREWATER DILUTION FACTORS

PFAS concentrations (µg/L) measured in the field-deployed lysimeters for the multiple rounds of porewater samples that were collected (see Exhibit S3) are provided in Exhibit S10. The grayed-column for Site B represents porewater concentrations that were not used for evaluation (this sample was an initial lysimeter purge sample), but are shown in Exhibit S10 for reference only due to the limited amount of samples collected at Site B.

Sites A, B, and C showed increasing trends in PFAS concentrations as a function of cumulative lysimeter sample volume for short-chain (≤7 perfluorinated carbons) PFAS and 8:2 FTS. Such trends were likely due to mixing/dilution with water within the silica flour slurry used for lysimeter installation. Dilution factors based on the bromide concentration measured in each porewater sample were calculated for these soils and are listed in Exhibit S10. The dilution factor (DF) was calculated as follows:

$$DF = \frac{C_0}{C_0 - C_{Br}} \qquad \text{Eq. S1}$$

where C_0 is the bromide concentration initially in the slurry and C_{Br} is the bromide concentration measured in the porewater sample. **Exhibit S11** shows how the dilution factor approximately corrected for this dilution effect and reduced the variability across the sampling rounds for the shorter-chained PFAS. Thus, for Sites A, B, and C, dilution factors were used in all subsequent evaluations of short-chained PFAS. These dilution factors were also used for the semi-quantified compounds at these sites.

Dilution and increasing PFAS concentrations with cumulative lysimeter volume were not issues for the long-chained PFAS (i.e., PFOS, PFHpS, and PFOA) and 6:2 FTS, suggesting concentrations measured in the lysimeters were representative of the surrounding porewater and weren't impacted by dilution. Thus, DF corrections were not applied to these PFAS. One possible explanation for this observation is that shorter chain PFAS (with lower K_d values) were more readily depleted/diluted at the slurry-soil interface within the borehole, whereas longer chain PFAS (with larger K_d values) were far less impacted by depletion/dilution effects. It is noted that if the bromide-based dilution factors listed in Exhibit S10 for Site A were applied to PFOS, the PFOS mass in the porewater would exceed that in the soil aggregate (soil, water, and interfacial phases) nearly 10-fold. In addition, it is noted that the dilution factors are only substantial (greater than approximately a factor of 2) for Sites A and B.

For Site E, increases in PFAS concentrations were not observed across the three sampling rounds for lysimeter 3, so no dilution factor correction was applied. Based on the bromide concentrations measured in the Site E lysimeters, dilution factor corrections would have been less than 2, so any calculated dilution effects would have been relatively minor. For Site D, bromide-based dilution factors were less than 1.2, and thus were not applied; due to the rainfall, it is not possible to ascribe any trends or variability due to the dilution factor.

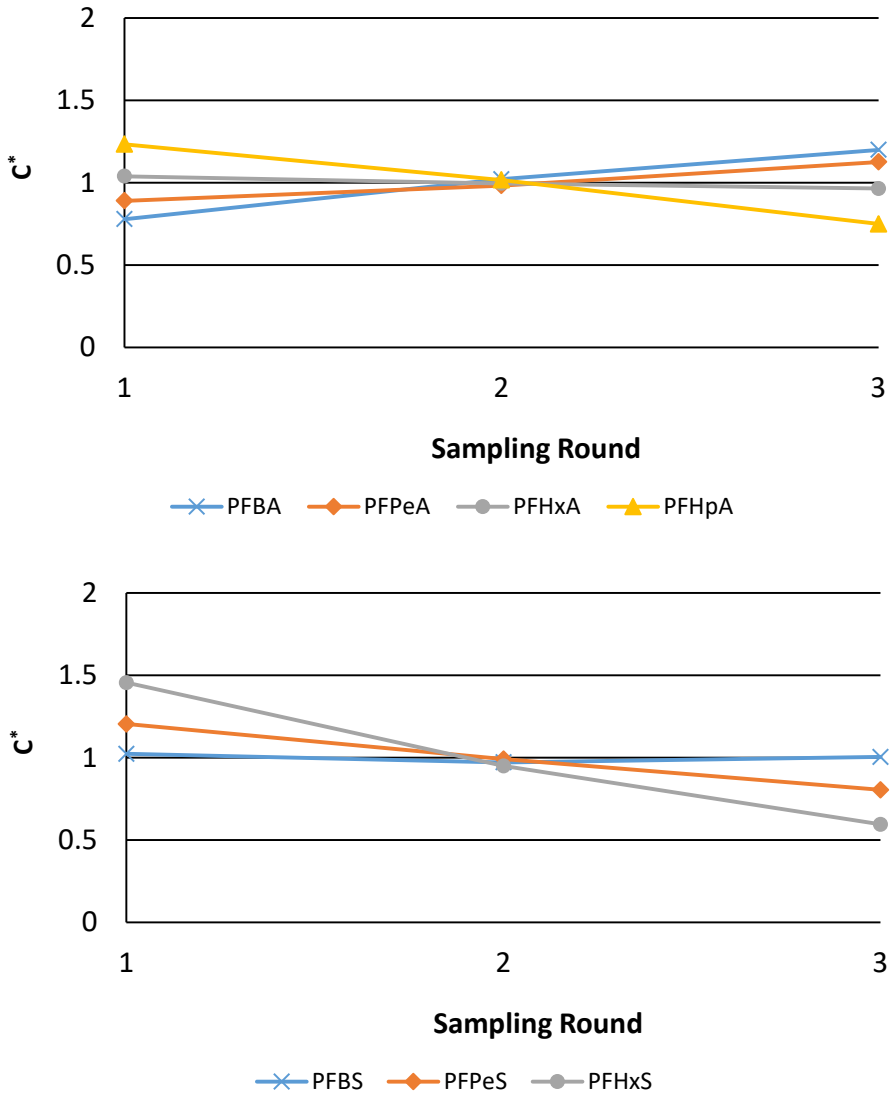

Appendix F – Figure 1. Dilution Factor (DF) Normalized PFAS Concentrations for Site A, Which had the Greatest DF values.

Perfluorinated carboxylates are shown in the top figure, and perfluorinated sulfonates are shown in the bottom figure. Values are shown for lysimeter 3. The DF-based normalized concentrations plotted on the y-axis (C^*) are calculated as follows:

$$C^* = \frac{C_{ri}\, DF_i}{average(C_{r1}DF_1 + C_{r2}DF_2 + C_{r3}DF_3)} \qquad \text{Eq. S2}$$

where C is the measured PFAS porewater concentration, i refers to the sampling round (1, 2, or 3), and the numerical subscripts refer to the sampling round. Applying the bromide-based dilution factors generally eliminated or substantially reduced the observed increasing PFAS concentration trends with cumulative sample volume (rounds 1 through 3). Thus, the DF correction was appropriate for these short-chained PFAS.

APPENDIX G PFAS MASS BALANCE EVALUATION

Individual PFAS mass balances per unit soil mass are as follows:

$$M_{T1} = M_{s1} + M_{w1} + M_{i1} \quad \text{Eq. S3}$$

$$M_{T2} = M_{s2} + M_{w2} + M_{i2} \quad \text{Eq. S4}$$

$$M_{T3} = M_{s3} + M_{w3} \quad \text{Eq. S5}$$

where M is PFAS mass (per unit soil mass) directly measured in this study (Exhibit S8), and the subscripts T, s, w, and i refer to total (soil, water, and , interfacial, which is what is measured in collected "soil" samples), soil, water, and air-water interface, respectively. The subscripts 1, 2 and 3 refer to the field, collected soil core, and batch soil slurry, respectively. Since soil from the adjacent locations and depths were used for the field and laboratory testing, M_{T1} is assumed to be equal to M_{T2} and M_{T3}; soil samples collected in adjacent cores at the lysimeters installation depths confirmed this assumption.

Values of M_{w1} were determined from the field lysimeter data, M_{w2} was determined from the bench-scale soil porewater collection, and M_{w3} was determined from the batch desorption test (based on direct PFAS measurements of the aqueous phase and measured water volumes). We note that previous field and laboratory experiments (Schaefer et al., 2023; Lyu et al., 2018) show that percolating porewater extracted from unsaturated soils generally does not include PFAS retained at the air-water interface. Because the batch slurries were performed under saturated conditions, no PFAS mass is assumed to reside at the air-water interface in the slurry systems (Eq. S5). Assuming the PFAS interfacial sorption coefficient (K_i, defined as the PFAS mass per unit area divided by the bulk porewater concentration) describes the relationship between PFAS accumulated at the air-water interface and PFAS in the bulk aqueous phase, the following equations are used:

$$\frac{M_{i1}}{Va_{aw1}C_1} = K_{i1} \quad \text{Eq. S6a}$$

$$\frac{M_{i2}}{Va_{aw2}C_2} = K_{i2} \quad \text{Eq. S6b}$$

where V is the unit soil volume and C_1 and C_2 are the measured PFAS concentrations in field porewater and laboratory core porewater, respectively. Values of the air-water interfacial area (a_{aw}) are provided in Table 2. PFAS K_i values are estimated based on the quantitative structure-property relationship (QSPR) model developed by Stults et al. (2023), and are dependent upon the PFAS concentration and ionic strength of the porewater. Values are provided in Exhibit S12. It is assumed, for the PFAS concentrations examined herein, the K_i values calculated for single solute PFAS are appropriate in the mixed PFAS system (Schaefer et al., 2019).

It is noted that Eqs. S6a and S6b are subject to the mass balance constraints in Eqs. S3 and S4. Thus, if the predicted value of K_i causes an exceedance of the measured total mass of the system, it is assumed that the predicted K_i value is too large. In such cases, the QSPR-predicted K_i value is reduced in the model until the mass balance is satisfied.

K_{i1} (field) and K_{i2} (lab core) values used for PFOS, 8:2 FTS, and PFHpS for Sites A. B, and C are provided in Exhibit S12.; K_i values are based on measured porewater ionic strengths of 16, 13, and 45 mM in Sites A, B, and C, respectively.

Finally, linear desorption behavior is assumed (Chen et al., 2016; Schaefer et al., 2022), and is expressed as:

$$\frac{M_{S1}}{mC_1} - \frac{M_{S2}}{mC_2} = \frac{M_{S2}}{mC_2} - \frac{M_{S3}}{mC_3} \qquad \text{Eq. S7}$$

where m is the unit soil mass. It is noted that Eq. S7 assumes linear desorption behavior (linear slope) for the PFAS concentration range examined, but is not constrained to a zero y-intercept. Using the estimated K_i values, Equations S3 through S7 can be solved for C_2, thereby determining the change in PFAS porewater concentrations when wetting the collected core (i.e., the increase in PFAS porewater concentrations from the comparatively dry field conditions).

In terms of model sensitivity for predicting C_2, sensitivity analysis showed that the key parameter for Site C is M_T. By conservatively assuming the PFAS soil concentrations for Site C has a 95% confidence interval that is 2-times the measured value (see Exhibit S8), the 95% confidence interval on the prediction of C_2 is determined and is shown in Table 3. For Sites A and B, the sensitivity in the predicted value of C_2 is proportional to the confidence in the measured value of C_1.

References

Chen, H., M. Reinhard, V. T. Nguyen, and K. Y. H. Gin. 2016. Reversible and irreversible sorption of perfluorinated compounds (PFCs) by sediments of an urban reservoir. *Chemosphere* 144: 1747–1753.

Schaefer, C.E.; Culina, V.; Nguyen, D.; Field, J. Uptake of Poly-and perfluoroalkyl substances at the air–water interface. *Environ. Sci. Technol*. 2019, 53, 12442–12448.

Schaefer, C.E., Nguyen, D., Christie, E., Shea, S., Higgins, C.P. and Field, J., 2022. Desorption isotherms for poly-and perfluoroalkyl substances in soil collected from an aqueous film-forming foam source area. *J. Environ. Engineering* 148, 04021074.

Stults, J.F., Choi, Y.J., Rockwell, C., Schaefer, C.E., Nguyen, D.D., Knappe, D.R., Illangasekare, T.H. and Higgins, C.P., 2023. Predicting Concentration-and Ionic-Strength-Dependent Air–Water Interfacial Partitioning Parameters of PFAS Using Quantitative Structure–Property Relationships (QSPRs). *Environ. Sci. Technol.* 57, 5203-5215.

Appendix G – Table 1. K_i Values Used in the Mass Balance Model.

K_{i1} is the for the field values, and K_{i2} is for the laboratory (microlysimeter sampling) value. The ratio K_{i1}/K_{i2} also is shown.

	Site A		Site B		Site C	
PFAS	**K_{i1} (cm)**	**K_{i2} (cm)**	**K_{i1} (cm)**	**K_{i2} (cm)**	**K_{i1} (cm)**	**K_{i2} (cm)**
PFOS[1]	0.00019	0.00023	0.00057	0.00083	0.16	0.039
	K_{i1}/K_{i2} = 0.82		K_{i1}/K_{i2} = 0.69		K_{i1}/K_{i2} = 4.1	
8:2 FTS[2]	*Not quantified in porewater at Sites A and B*				0.22	0.060
					K_{i1}/K_{i2} = 3.7	
PFHpS[3]	*Not quantified in soil at Sites A and B*				0.046	0.023
					K_{i1}/K_{i2} = 2.0	

[1] The K_i values for PFOS predicted by the QSPR model were 850-times and 350-times greater than those shown in the table above for Sites A and B, respectively. However, mass balance constraints limited the maximum permissible K_i values to those shown in the table.

[2] Stults et al. (2023) showed 6:2 FTS overpredicted experimental data) by a factor of 3, so the QSPR predicted 8:2 FTS K_i values used herein were decreased by a factor of 3.

[3] The K_i values for PFHpS predicted by the QSPR model were 3.5-times greater than those shown in the table above. However, mass balance constraints limited the maximum permissible K_i values to those shown in the table.

APPENDIX H FILM EXPERIMENTS TO DETERMINE TOC ACCUMULATION AT THE AIR-WATER INTERFACE

Details of the film experiments for measuring PFAS accumulation at the air-water interface has been previously described in detail (Schaefer et al., 2019). Herein, we apply this same technique for measuring TOC uptake at the air-water interface for Sites A and B. The HDPE cylindrical vessel used for the film testing had a 25 cm diameter and was 4 cm deep. With a valve in the bottom face for drainage. Approximately 2.2 L of porewater was initially placed in the vessel. Because collection of such a large quantity of porewater was not practical for Sites A and B, a soil:water slurry was prepared with an approximate 2:1 liquid to solid ratio (5 mM $CaCl_2$ was used as the aqueous solution). The solution was gently mixed for approximately 1 week before it was allowed to settle and subsequently used in the film experiment.

Once this water was placed in the HDPE vessel, the vessel was covered with aluminum foil to limit evaporation. After 3 days, the water was drained so that only a film remained (approximately 0.5 cm in depth and 300 mL volume). The TOC concentration in the drained water and in the 300 mL film sample were subsequently measured using combustion ion chromatography, Experiments were performed in triplicate for both the Site A and Site B soils.

The mass of TOC sorbed at the air − water interface per unit volume (Γ) was determined by mass balance as follows:

$$\Gamma = \frac{M_{TOC} - C_{TOC} V_f}{A} \qquad \text{Eq. S8}$$

where M_{TOC} is the TOC in the water film, C_{TOC} is the concentration in the bulk (drained) water, V_f is the volume of the film, and A is the air-water interfacial area. The TOC air-water interfacial adsorption coefficient ($K_{i,TOC}$) is then calculated for Sites A and B as follows:

$$K_{i,TOC} = \frac{\Gamma}{C_{TOC}} \qquad \text{Eq. S9}$$

APPENDIX I SITE D GPR IMAGE

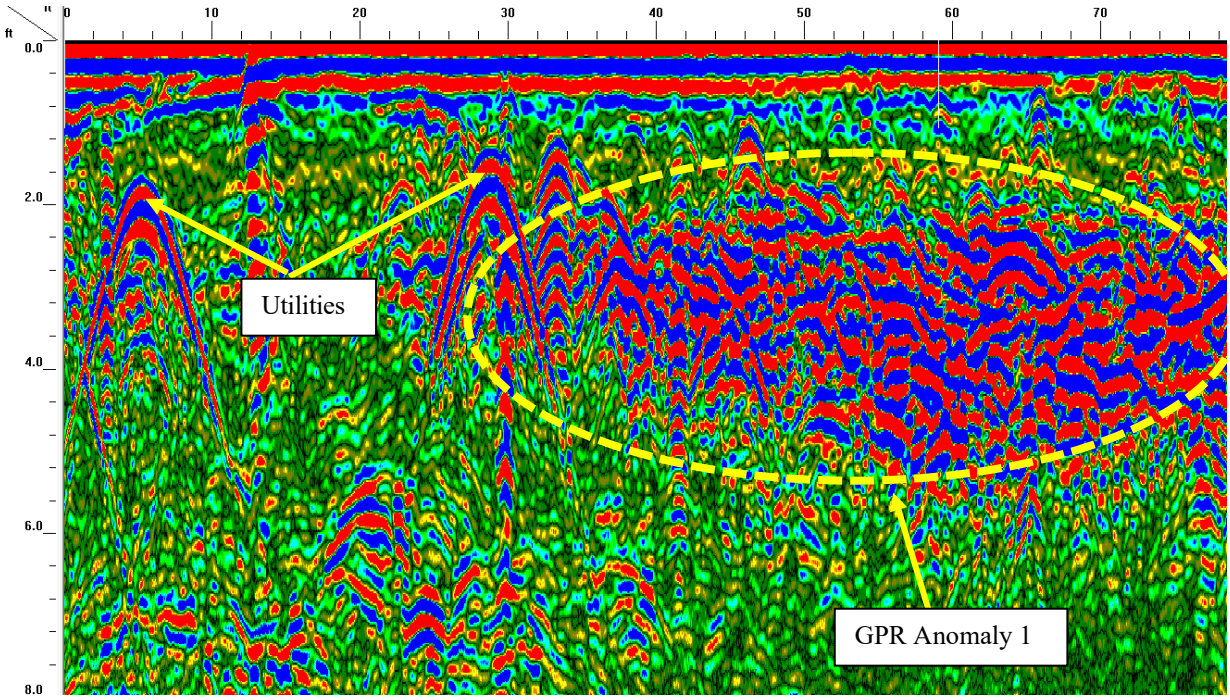

Appendix I – Figure 1. Ground Penetrating Radar (GPR) Image from Utility Survey, Where the Circled Region (GPR Anomaly 1) Is Where the Lysimeters for Site D Were Installed.

GPR surveying was performed by GeoView, Inc. using a GSSI radar system utilizing a 350-megahertz antenna. The axis scales are in feet (8 feet of total depth and 80 feet x-axis distance). The multiple hyperbolas in the circled zone indicate anomalies. Materials with large changes in dielectric properties show up in red, which are scaled to fade to blue as these changes in dielectric properties diminish.

APPENDIX J PFAS DESORPTION KINETICS FROM SITE SOILS

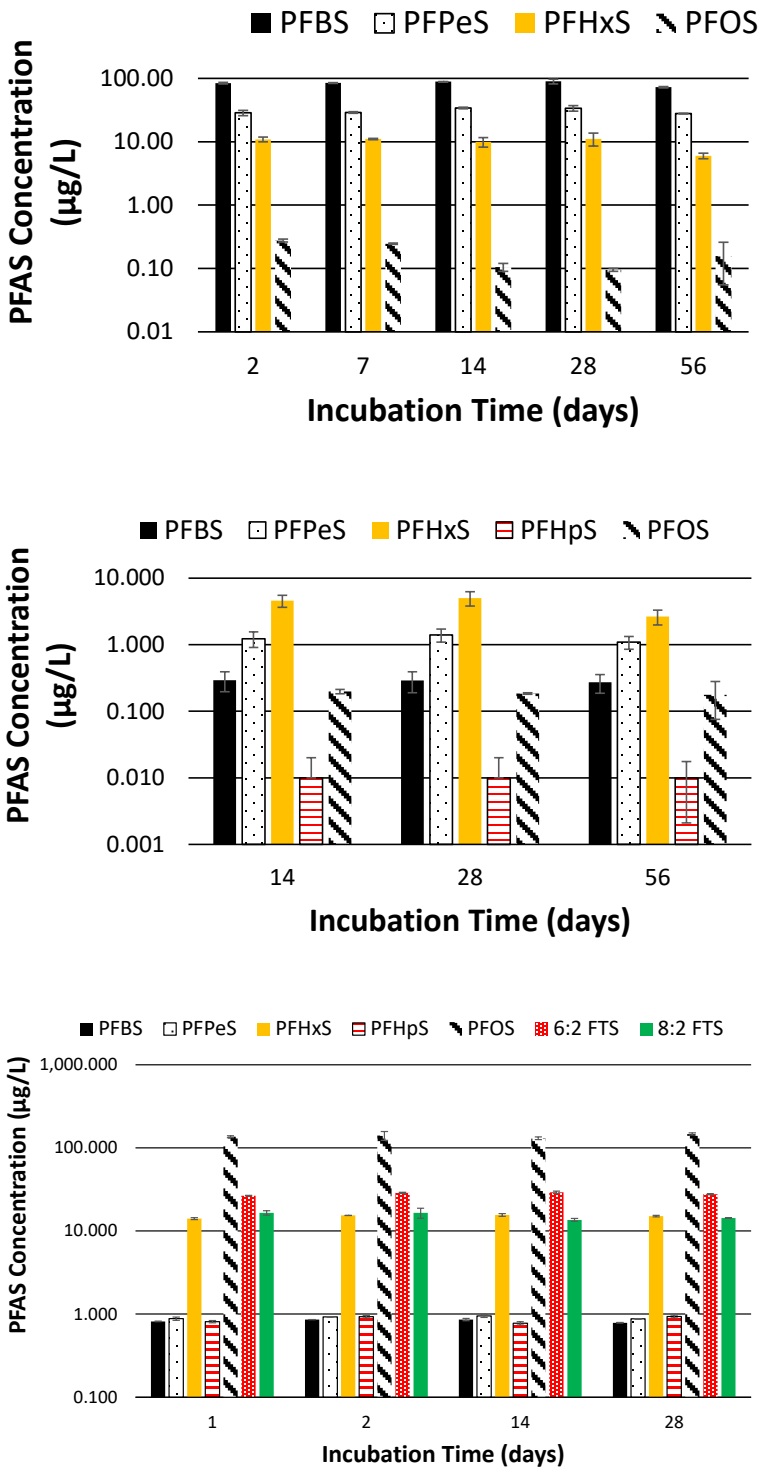

Appendix J – Figure 1. PFAS Desorption Kinetics from Site Soils A (Top), B (Middle), and C (Bottom) in Batch Slurry Experiments.